

Copyright
by
Whitney Franklin
2019

**The Dissertation Committee for Whitney Franklin Certifies that this is the
approved version of the following dissertation:**

**Onset of Insulin Resistance in Hippocampal Synapses After
Traumatic Brain Injury:
Relevance to Alzheimer's disease and Therapeutic Implications**

Committee:

Giulio Taglialatela, Ph.D., Mentor, Chair

Balaji Krishnan, Ph.D.

Rakez Kayed, Ph.D.

Nicola Abate, M.D.

Lee Shapiro, Ph.D.

**Onset of Insulin Resistance in Hippocampal Synapses After
Traumatic Brain Injury:
Relevance to Alzheimer's disease and Therapeutic Implications**

by

Whitney Franklin

Dissertation

Presented to the Faculty of the Graduate School of
The University of Texas Medical Branch
in Partial Fulfillment
of the Requirements
for the Degree of

Doctor of Philosophy

The University of Texas Medical Branch

April, 2019

Acknowledgements

I would like to thank my mentor, Dr. Tagliatela, for all of his guidance and support over the years, both professionally and personally. I would like to thank both past and present members of Dr. Tagliatela's lab- Dr. Olga Zolochovska, Dr. Claudia Marino, Dr. Salvo Saieva, Dr. David Briley, Wen Ru Zhang, Dr. Michele Comerota, and Dr. Anna Fracassi for their technical and emotional support throughout my time in the lab. An additional thank you to Dr. Balaji Krishnan for his assistance and advice to accomplish all of the electrophysiology experiments.

Guidance and advice for my project from my committee members: Drs. Rakez Kayed, Lee Shapiro, Nicola Abate, Balaji Krishnan, and Giulio Tagliatela.

The UTMB dean Dr. David Niesel, NGP program director Dr. Owen Hamill, and past NGP program coordinator Aurora Galvan.

Most importantly, to my family, to whom I owe everything. To my parents, Pam and Darrell, who gave me everything I could ever need, made sacrifices to provide me with the best, helped me to explore and guide me throughout my professional endeavors, and their unfailing emotional support through my life and throughout graduate school- I would be lost without you both, and I will never be able to express how grateful and lucky I am to be your daughter. To my devoted husband Jimmy, whose incredible support allows me to follow my dreams without any worries, you crack the whip to keep me focused but you also lighten my life so much with your love and humor. You keep me sane and make even the hardest days' worth it to come home to you. I love you.

**Onset of Insulin Resistance in Hippocampal Synapses After
Traumatic Brain Injury:
Relevance to Alzheimer's disease and Therapeutic Implications**

Publication No. _____

Whitney Franklin, Ph.D.

The University of Texas Medical Branch, 2019

Supervisor: Giulio Tagliatela

Traumatic brain injury (TBI) is a risk factor for the later development of Alzheimer's disease (AD), although the mechanisms contributing to this increased risk are unknown. Insulin resistance is an additional risk factor for AD whereby decreased insulin signaling increases synaptic sensitivity to amyloid beta ($A\beta$) and tau, thus contributing to the cognitive decline that characterizes this neurodegenerative disorder. Considering this, I used male Sprague-Dawley rats that underwent a lateral fluid percussion injury (FPI) at acute (2 and 7 days post-injury), intermediate (28 days post-injury), and chronic (3 months post-injury) time-points to investigate whether decreased insulin responsiveness in TBI animals is playing a role in synaptic vulnerability to AD pathology. I was able to detect acute and chronic decreases in insulin responsiveness in isolated hippocampal synaptosomes after TBI. In addition to assessing both $A\beta$ and tau binding on synaptosomes, I performed electrophysiology at the intermediate and chronic time-points to assess the dysfunctional impact of $A\beta$ and tau oligomers as well as the protective effect of insulin. While I found no difference in binding or degree of LTP inhibition by either $A\beta$ or tau oligomers between sham and TBI animals, I did find that

insulin treatment was able to block oligomer-induced LTP inhibition in sham animals but not in TBI animals. Since insulin treatment has been discussed as a therapy for AD, this gives valuable insight into therapeutic implications of treating AD patients based on a patient's history of associated risk factors.

TABLE OF CONTENTS

List of Tables	x
List of Figures	xi
List of Abbreviations	xiii
CHAPTER 1. GENERAL INTRODUCTION	15
Alzheimer’s Disease	15
Overview	15
Pathology	16
Risk Factors	24
Insulin and AD.....	25
Traumatic Brain Injury	28
Overview.....	28
Alzheimer’s disease Consequence.....	30
Insulin and TBI	32
Aim of the Dissertation.....	33
CHAPTER 2. INVESTIGATING SYNAPTIC INSULIN RESISTANCE AFTER FPI	35
Introduction.....	35
Materials and Methods.....	36
Animals.....	36
Parasagittal Fluid-Percussion Injury	37
Craniotomy.	38
Parasagittal Fluid Percussion Injury.	38
Synaptosomal Isolation.....	39
Insulin Responsiveness	39
Insulin Stimulation of synaptosomes.....	40
WES analysis of Insulin Responsiveness.	40
Western Blot Analysis for SOCS3.....	40

Statistical Analysis.....	41
Results.....	41
Development of <i>Ex Vivo</i> Insulin Stimulation Method.....	41
Isolation and confirmation of synaptosomes and IR responsiveness.....	42
Optimization of ex vivo insulin stimulation conditions.....	43
Comparison of ex vivo and in vivo synaptosomal insulin response.....	46
Evaluate Synaptosomal Insulin Responsiveness After TBI	47
Assess Possible Mechanistic Driver of Synaptic Insulin Resistance.....	49
Conclusions.....	51
CHAPTER 3. EVALUATING SYNAPTIC VULNERABILITY TO THE EFFECTS OF Aβ AND TAU AFTER TBI.....	53
Introduction.....	53
Materials and Methods.....	53
Parasagittal Fluid-Percussion Injury	53
Synaptosomal Isolation.....	54
A β -binding.....	54
A β oligomer preparation.....	54
A β oligomer binding challenge.....	54
Tau-binding.....	55
Tau-oligomer preparation.....	55
Ex vivo Tau-oligomer binding.....	55
ELISA Analysis of Tau.....	56
Electrophysiology	56
Insulin's Effect on Properties of Hippocampal Slices	58
Effect on A β binding.....	58
Effect on mitochondria.....	58
Statistical Analysis.....	59
Results.....	59
Quantify Synaptosomal A β Binding After TBI.....	59

Quantify Synaptosomal Tau Binding After TBI.....	62
Electrophysiology Assessment	64
What Could Be Causing the Benefit in LTP By Insulin in the Presence of Oligomers?.....	70
Conclusions.....	73
CHAPTER 4. GENERAL DISCUSSION AND CONCLUDING REMARKS	75
Concluding Remarks.....	80
References.....	82
Vita	92

List of Tables

Table 1.1: Common pathophysiological mechanisms in TBI and AD.	31
---	----

List of Figures

Figure 1.1: Schematic representation of AD progression in relation to symptomatic stage of the disease.	17
Figure 1.2: Coronal section of postmortem human brain.	18
Figure 1.3: Schematic representations of APP and tau processing and aggregation.	20
Figure 1.4: A β and tau oligomers bind to synapses and inhibit LTP.	22
Figure 1.5: AD pathological mechanisms and neuropathology.	24
Figure 1.6: Strength of evidence on risk factors for dementia.	25
Figure 2.1: Schematic of fluid-percussion traumatic brain injury model.	37
Figure 2.2: Synaptosomal characterization and confirmation of insulin stimulation.	43
Figure 2.3: Optimization of ex vivo insulin stimulation method.	45
Figure 2.4: Comparison of in vivo and ex vivo synaptosomal insulin response.	46
Figure 2.5: Insulin responsiveness in ipsilateral hippocampus.	48
Figure 2.6: Insulin responsiveness in contralateral hippocampus.	49
Figure 2.7: SOCS3 expression in the ipsilateral and contralateral hippocampi.	51
Figure 3.1: Amyloid-beta oligomer <i>ex vivo</i> binding curves in the ipsilateral and contralateral hippocampi.	61

Figure 3.2: <i>Ex vivo</i> tau oligomer binding in the ipsilateral and contralateral hippocampi.....	63
Figure 3.3: Electrophysiology experimental design.	64
Figure 3.4: Electrophysiological analysis of A β oligomer-treatment in ipsilateral hippocampus.	66
Figure 3.5: Electrophysiological analysis of tau oligomer-treatment in ipsilateral hippocampus.	67
Figure 3.6: Electrophysiological analysis of A β oligomer-treatment in contralateral hippocampus.	68
Figure 3.7: Electrophysiological analysis of tau oligomer-treatment in contralateral hippocampus.	69
Figure 3.8: Electrophysiological analysis of insulin-treatment alone in ipsilateral and contralateral hippocampi.....	70
Figure 3.9: Insulin's effect on A β binding.....	71
Figure 3.10: Mitochondria analysis after insulin stimulation.	73

List of Abbreviations

A β	Amyloid beta
Ach	Acetylcholine
aCSF	Artificial cerebrospinal fluid
AD	Alzheimer's disease
AICD	Amyloid precursor protein intracellular domain
APOE	Apolipoprotein ϵ
APP	Amyloid precursor protein
BACE-1	Beta-site amyloid precursor protein-cleaving enzyme 1
BBB	Blood brain barrier
BCA	Bicinchoninic acid
CNS	Central nervous system
DPI	Days post-injury
ELISA	Enzyme-linked immunosorbent assay
ENPP	Ecto-nucleotide pyrophosphate phosphodiesterase
fAD	Familial Alzheimer's disease
FDA	Food and Drug Administration
fEPSP	Field excitatory post-synaptic potentials
FPI	Fluid-percussion injury
GWAS	Genome wide association study
HBK	HEPES-buffered Krebs-like buffer
HFS	High frequency stimulation
IGF	Insulin-like growth factor
IP	Intraperitoneal
IR	Insulin receptor
LTP	Long-term potentiation
MAP	Microtubule-associated protein
MAPK	Mitogen-activated protein kinase
MCI	Mild cognitive impairment

mIPSC	miniature inhibitory postsynaptic currents
MPI	Months post-injury
NFTs	Neurofibrillary tangles
NMDAR	N-methyl-D-aspartate receptor
OBTT	Operation brain trauma therapy
PMI	Post-mortem interval
PSD	Post-synaptic density
PS1	Presenilin 1
RCF	Relative centrifugal force
ROS	Reactive oxygen species
sAD	Sporadic Alzheimer's disease
SOCS	Suppressor of cytokine signaling
TBI	Traumatic brain injury
T2DM	Type 2 diabetes mellitus
WT	Wild-type

CHAPTER 1. GENERAL INTRODUCTION

Alzheimer's Disease

OVERVIEW

Alzheimer's disease (AD) is a devastating neurodegenerative disorder that was first reported in 1906 [1,2]. It is the most common form of dementia, affecting over 47 million people worldwide [3,4]. Over 5 million of those affected are Americans which costs the U.S. more than \$200 billion each year [1]. This doesn't even take into account the hours put in by unpaid caregivers. As these numbers are estimated to triple by 2050 [1], this would bankrupt our healthcare system unless we can find a way to combat these growing numbers of AD cases.

Alzheimer's disease can be classified as either familial or sporadic. Familial AD (fAD) is an "early onset" form of AD that represents 2%-5% of all AD cases. This form of AD is driven by genetic mutations in amyloid precursor protein (APP) and presenilin genes (PSEN1 and PSEN2) which effect pathological protein aggregation that drives the disease. Down syndrome patients contain an additional copy of the APP gene due to the trisomy of chromosome 21 and also develop early onset AD [5]. Sporadic AD (sAD) is a "late-onset" form of AD that is more complex and constitutes ~95% of all AD cases. The presence of the APOE4 allele is the major and only undisputed genetic risk factor [6]. However, there are a handful of genes involved in cholesterol metabolism, inflammatory response, and endocytosis where polymorphisms identified by genome wide association study (GWAS) analysis reveals a modest increased effect on AD risk [7].

Since the cause of the majority of AD cases (sAD) is unknown, it has proven very difficult to treat. While there is still no "disease-modifying" cure, current treatments aim at alleviating symptoms which include amnesia, aphasia, agnosia, apathy, language

alterations, loss of spatial orientation, and loss of executive functions [8,9]. There are currently five pharmacological treatments (4 different drugs) that are FDA approved and used in the US which all act on either the cholinergic or glutamatergic circuits affected in AD [1].

Donepezil, rivastigmine, and galantamine are cholinesterase inhibitors whose action is to decrease the extra-synaptic metabolism of acetylcholine (ACh) which therefore allows for an increased amount of time for the neurotransmitter to act on postsynaptic receptors thus increasing neuronal transmission leading to cognitive and behavioral benefits. Memantine acts on the glutamatergic system as an NMDA receptor antagonist by binding the Mg^{2+} binding site which thereby prevents abnormal neurotransmitter glutamatergic signaling. [10]

PATHOLOGY

AD progresses very slowly, and biochemical alterations can accumulate over the course of decades before an affected person begins to show symptoms and memory impairment (Figure 1.1). Pre-symptomatic stages of the disease begin with protein aggregation and synaptic loss while later stages of the disease present with cell death. In the brains of AD patients, neuronal loss is apparent in the cortex and hippocampus, evident by hippocampal shrinkage and ventricle enlargement [11] (Figure 1.2). Protein deposition is found by the presence of extracellular plaques mainly consisting of amyloid beta ($A\beta$) peptide and intracellular inclusions of neurofibrillary tangles (NFT) composed of hyperphosphorylated tau [12].

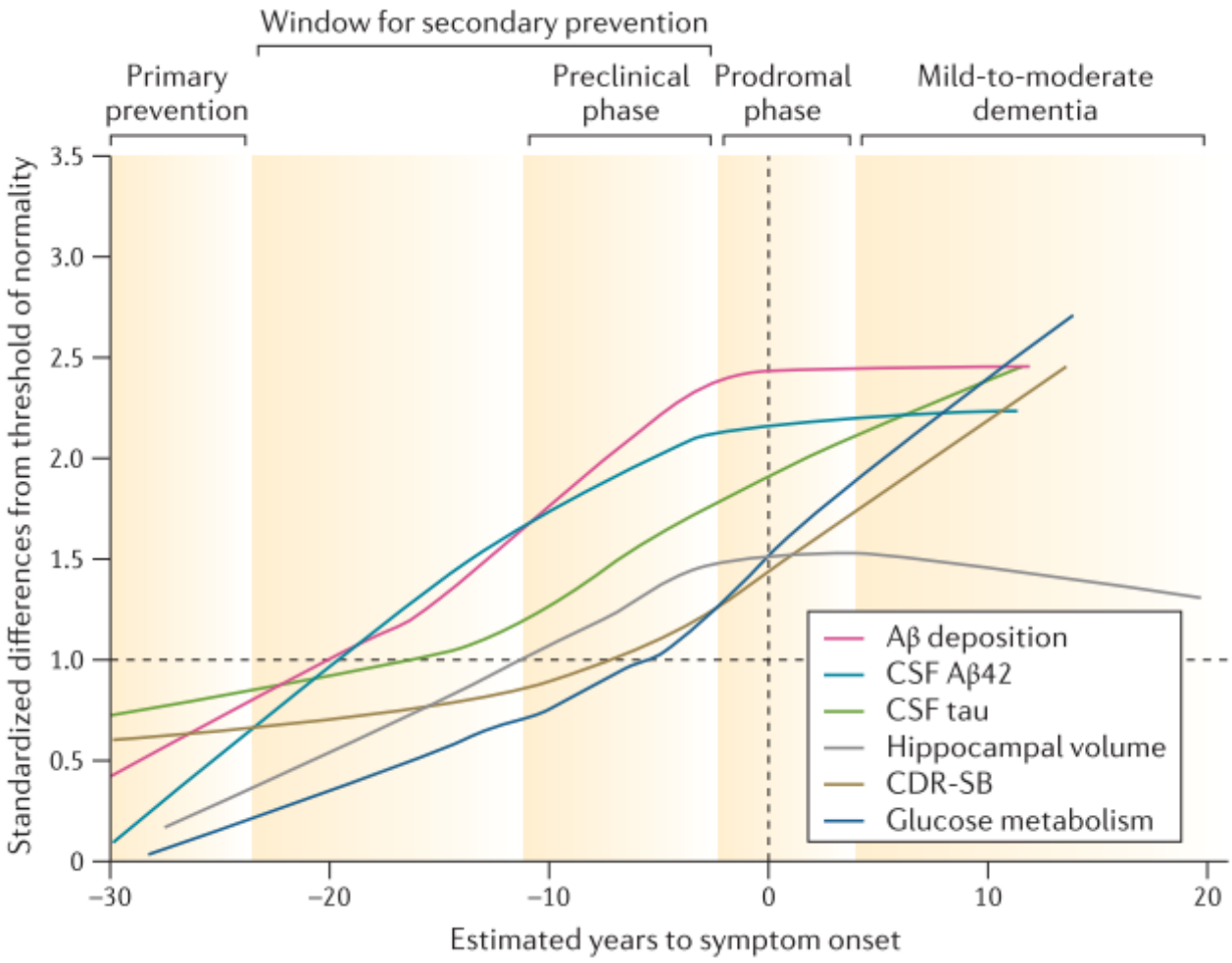


Figure 1.1: Schematic representation of AD progression in relation to symptomatic stage of the disease.

Adapted from Masters et al., 2015 [10].

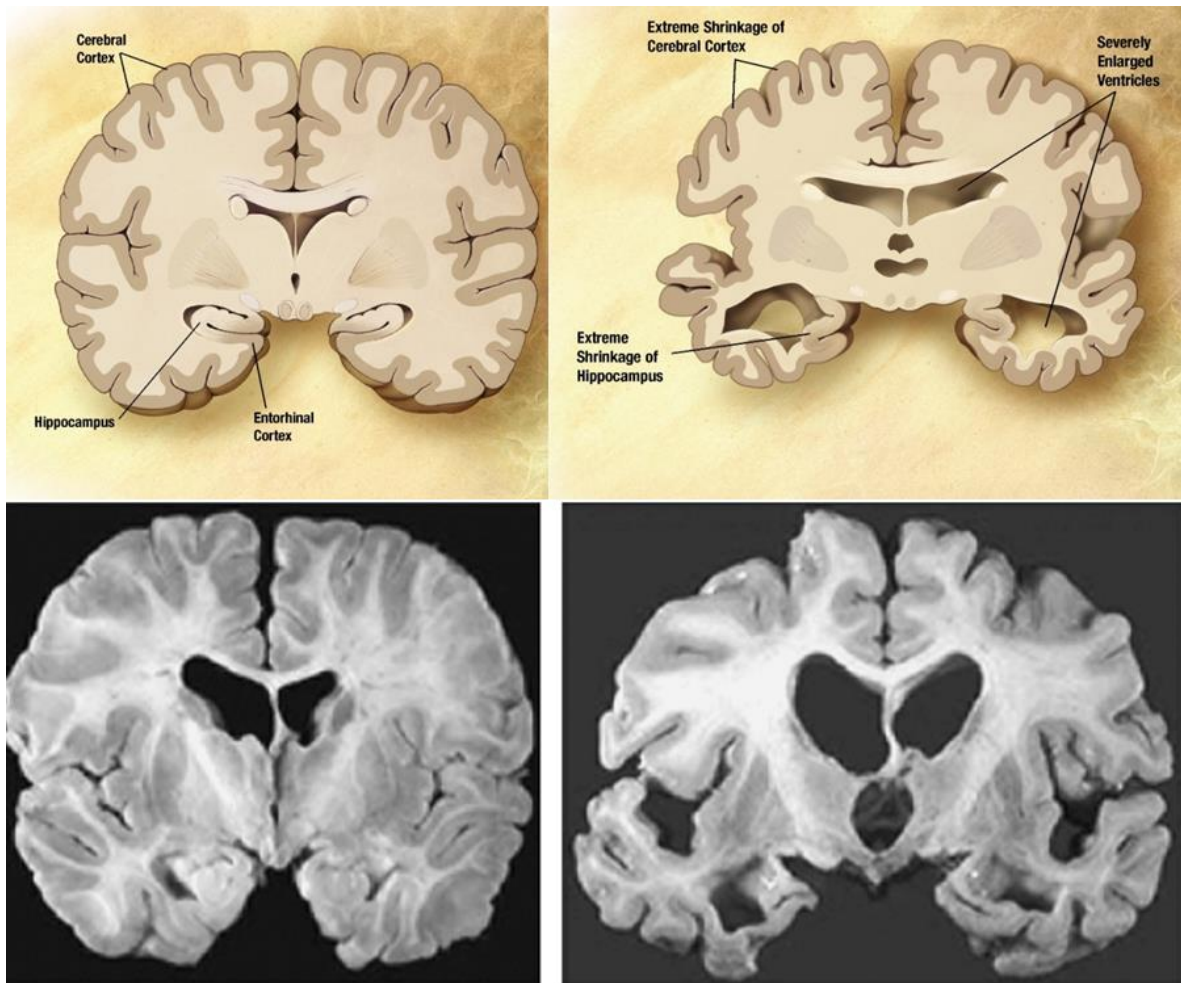


Figure 1.2: Coronal section of postmortem human brain.

Brain slices from an elderly non-demented individual on the left compared with that of a patient with AD on the right, demonstrating hippocampal and cortical shrinkage along with enlarged ventricles in AD. Modified from Figure 1 Yaari et al, 2007 [11].

A β is a cleavage product of APP. APP is a membrane spanning protein that is cleaved by multiple secretases resulting in either a detrimental amyloidogenic or non-toxic, non-amyloidogenic producing pathway depending on the specific secretases involved (Figure 1.3A). For the non-amyloidogenic process, cleavage of APP by α -secretase will produce sAPP α and a remaining c-terminal membrane-bound product (C83) that undergoes further cleavage by γ -secretase to produce p3 and the amyloid intracellular domain (AICD). However, in the amyloidogenic processing pathway, β -secretase beta-site amyloid precursor protein–cleaving enzyme 1 (BACE-1) cleaves rather than α -secretase, resulting in sAPP β and a different C-terminal fragment (C99). C99 is then further processed by γ -secretase cleavage to produce AICD and the potentially toxic A β peptide which is then released into the space outside the neuron and can begin to aggregate [8,13]. The length of the A β peptide can vary from 36-43 amino acids[14]. However, the two primary forms associated with AD are 40 and 42 amino acids in length. A β 42 has a higher propensity for aggregation and is therefore thought to be the more toxic species [8].

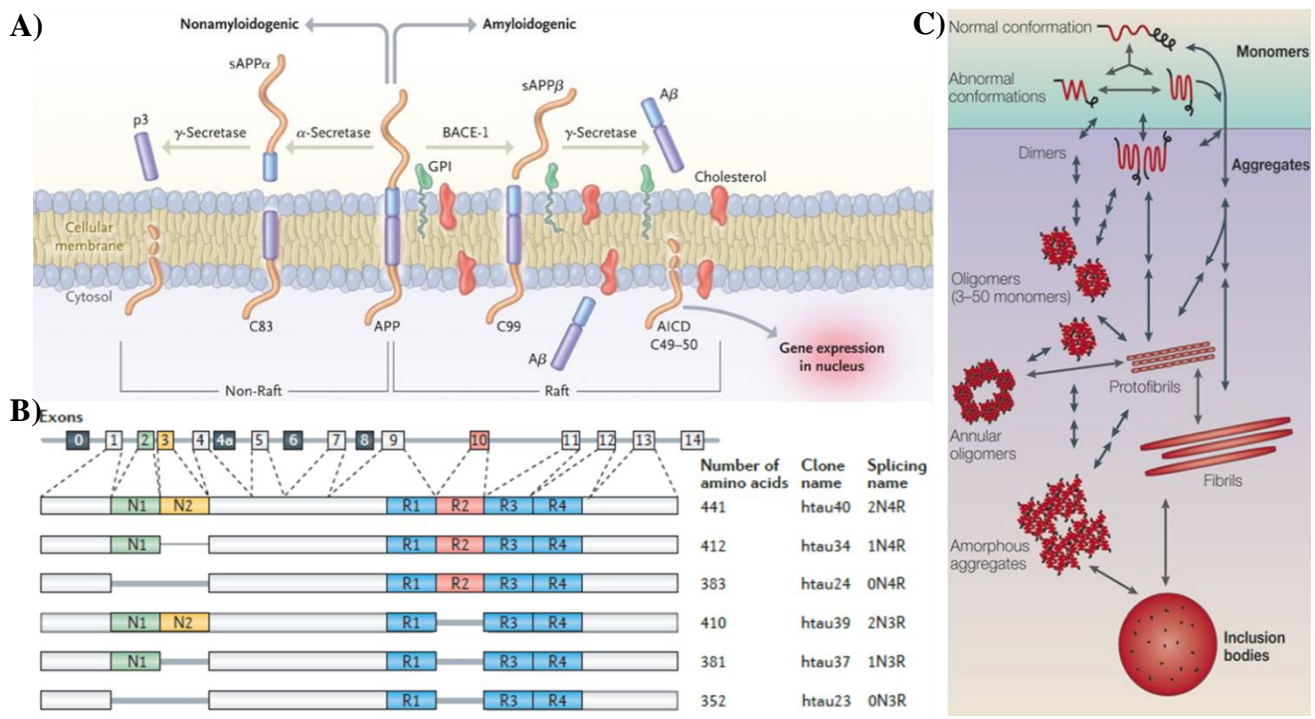


Figure 1.3: Schematic representations of APP and tau processing and aggregation.

A) Processing of amyloid precursor protein (APP) in nonamyloidogenic and amyloidogenic pathways. Adapted from Figure 1 Querfurth et al., 2010[8]. B) The human MAPT gene and the splice isoforms of tau in the human brain. Modified from Figure 1 Wang et al., 2016[15]. C) Aggregation pathways leading to various conformational species including oligomers, annular oligomers, protofibrils, fibrils, and larger aggregates including plaques and tangles. Adapted from Figure 3 Ross et al., 2005[16].

Tau proteins belong to the microtubule-associated proteins (MAP) family and are mainly found in neurons. They are part of the cytoskeletal network and have an important role in microtubule assembly and stabilization. The tau gene contains 16 exons, many of which are constitutively expressed in all of the isoforms. There are 6 isoforms in humans that differ in the addition or the omission of exons 2, 3, and 10 (Figure 1.3B). Exon 2 and 3 are found towards the N-terminus, and, thus, tau isoforms can be designated 0N, 1N, or 2N based on the number of inserts added. Exon 10 is found in the C-terminus of tau and is named 4R for 4 repeats when it is present and 3R designating 3 repeats when exon 10 is absent [15]. The different isoforms vary in localization, efficiency in microtubule assembly, and aggregation potential. The C-terminus of the protein is mainly the site of

phosphorylation and hyperphosphorylation, among other post-translational modifications, which can cause tau to aggregate [17].

Both amyloid beta and tau have been shown to follow similar abnormal aggregation paths (Figure 1.3C) whereby monomers will begin to aggregate together forming soluble oligomers. Oligomers then clump further with either additional monomers or oligomers to grow and become insoluble protofibrils and fibrils [16]. Eventually, other proteins and cellular material are added, and these increasingly insoluble entities combine to become the well-known plaques and hyperphosphorylated tangles that are characteristic of AD [18].

Previously, it was thought that plaques and fibrils might cause all of the damage to neurons that is seen in AD. It has become increasingly evident though that it is the oligomeric aggregates of both A β and tau that contribute to the synaptic dysfunction that precedes the cognitive decline and cell death seen in AD [19,20]. Furthermore, it has been shown that oligomer toxicity is induced by the conformation, regardless of the differing primary structure and sequence of the peptides comprising these oligomers [21,22]. Thus, both A β and tau oligomers have been shown to accumulate at synapses [23] and induce disruptive synaptic alterations (Figure 1.4). A β oligomers can accumulate at the synapse [24], are capable of inducing changes in the composition, shape, and density of the synapse [25,26], can inhibit both early and late phase LTP [27,28], and can disrupt calcium dynamics and calcium-dependent signaling [27,29,30]. Tau also demonstrates these characteristics where it has been seen internalizing into neurons [20] and also inhibiting LTP in its oligomeric aggregation state [19]. It is believed that synaptic dysfunction driven by these oligomers underlies the initiation and progression of AD [31,32].

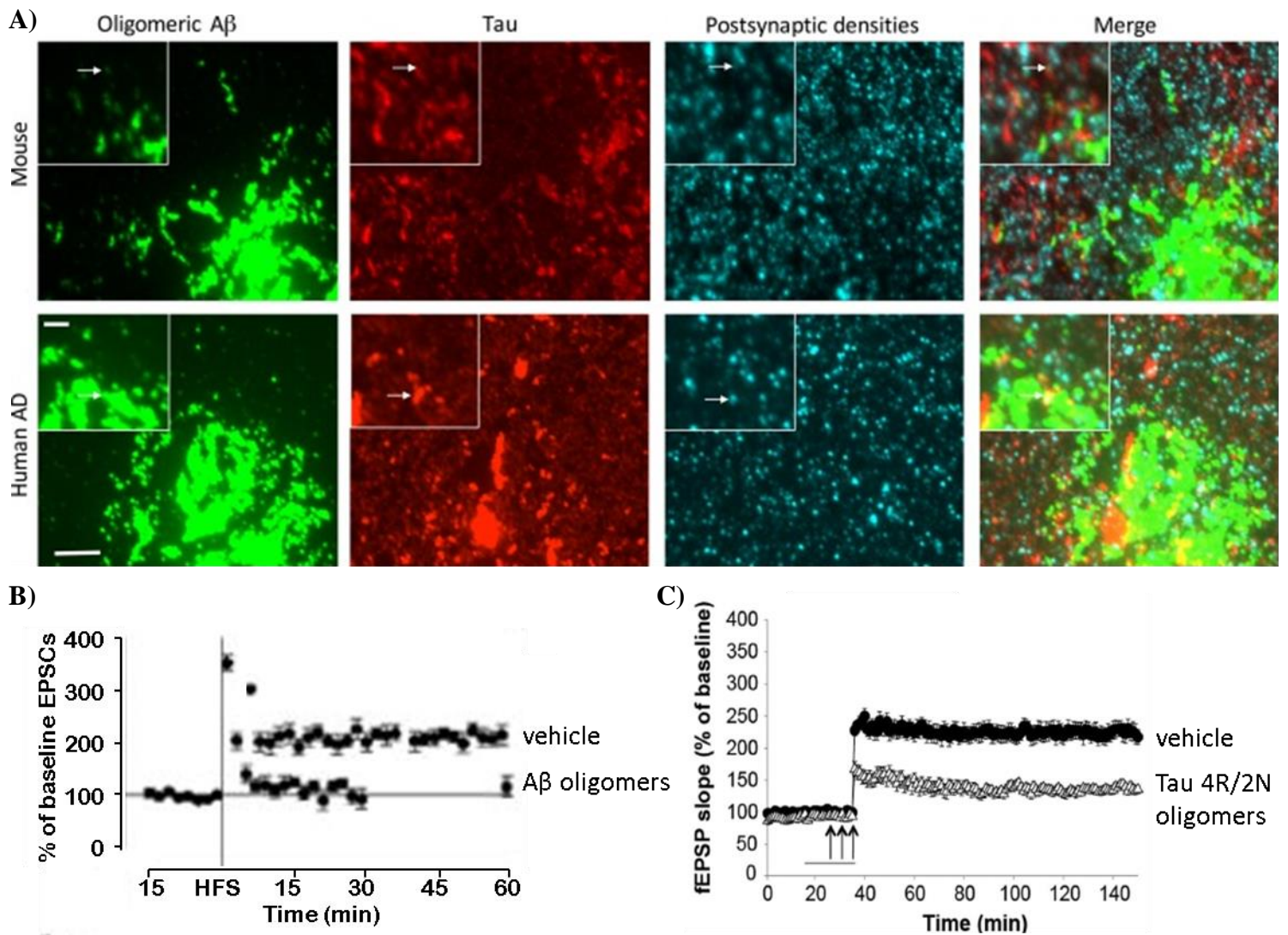


Figure 1.4: A β and tau oligomers bind to synapses and inhibit LTP.

A) Immunofluorescent images demonstrating co-aggregation and localization (arrows) of A β and tau at synapses in an AD mouse model (APP/PS1 mice also expressing human wild-type tau) (top) and human AD brain (bottom) using the array tomography technique. Scale bars represent 5 μ m in large panel and 2 μ m in inset. Adapted from Figure 2 Spiess-Jones et al., 2017 [23]. B) High-frequency synaptic stimulation (HFS)-induced expression of long-term potentiation (LTP) is inhibited in the hippocampus of rat brain slices treated for 1 hr with 0.5 μ M oligomeric A β compared to vehicle. Modified Figure 2 Dineley et al., 2010 [28]. C) HFS-induced expression of LTP is reduced in the hippocampus of mouse brain slices perfused with 2.29 μ g/ml oTau 4R/2N versus 20 minute incubation with vehicle. Adapted from Figure 1 Fa et al., 2016 [19].

In the amyloid hypothesis for AD, it is suggested that there is an accumulation of A β which induces an “A β driven cascade” that triggers the initiation of the disease [3]. A β aggregation drives tau pathology and dysfunction which then leads to neuronal death and memory loss seen in the late stages of AD. These downstream changes eventually become independent of A β pathology [33]. Thus, for this reason, clinical trials investigating therapies using antibodies targeting A β in the late phase of the disease have proven unsuccessful.

Neuropathology of AD is not limited to A β and tau; rather, there are a multitude of additional mechanisms that have been proposed to contribute to AD pathogenesis. Some of these mechanisms that contribute to the complexity of biochemical cascades leading to the induction of AD can be seen in Figure 1.5 and include inflammation, altered autophagy, and vascular dysregulation to name a few [34]. It is evident that AD is complex, and this may contribute to the difficulty and failure in finding a cure for the disease. Therefore, targeting AD associated risk factors can be used as a valid alternative approach to reduce AD incidence.

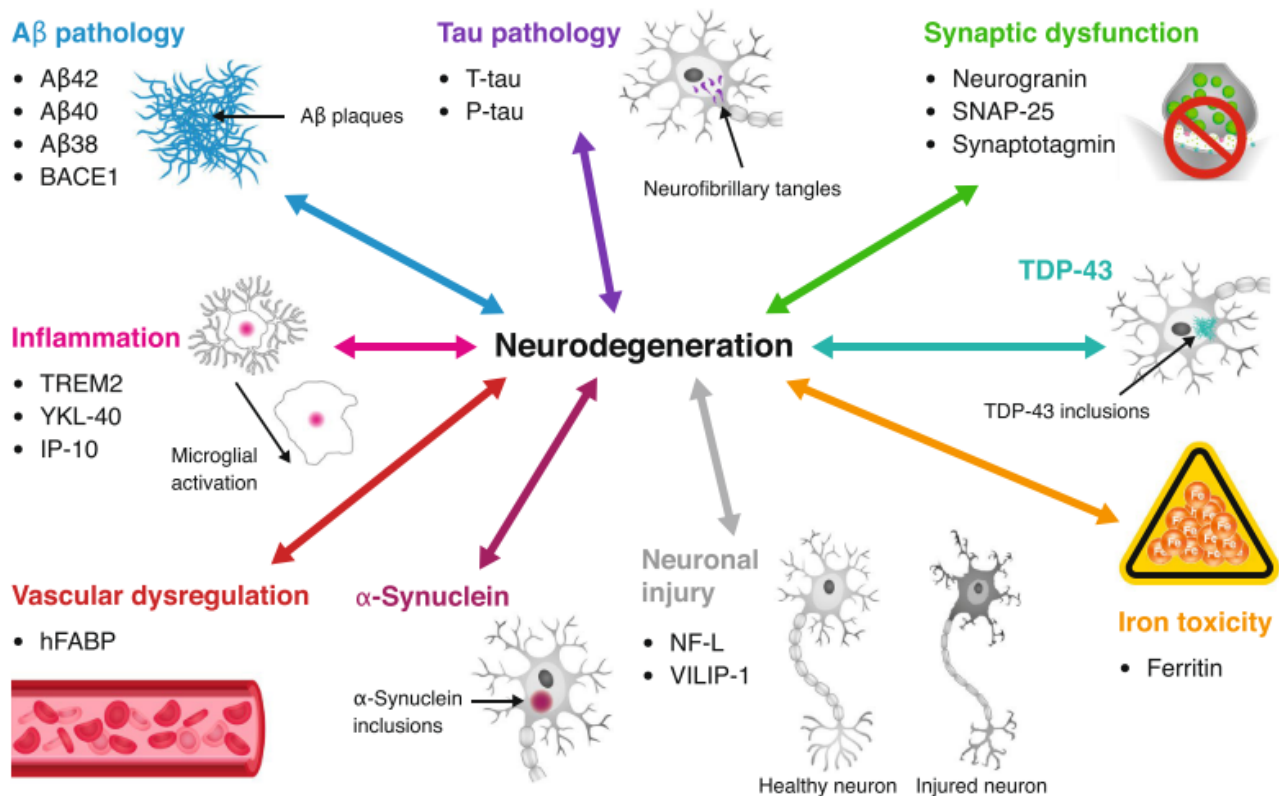


Figure 1.5: AD pathological mechanisms and neuropathology.

Adapted from Figure 1 Molinuevo et al., 2018 [34].

RISK FACTORS

Sporadic AD (sAD) is complex and heterogenous and is responsible for >95% of all AD cases [1,10]. There is a high disease comorbidity with sAD [10], and a large variety of factors increase the risk of developing sAD [4] (Figure 1.6). Some of these risk factors are innate such as old age, family history, and APOE genotype. Other risk factors are due to lifestyle and/or are event-related such as type 2 diabetes mellitus (T2DM) [35–37], central insulin resistance [38], traumatic brain injury (TBI) [39–41], mitochondrial dysfunction [42,43], neuroinflammation [44], obesity [35], smoking, and sleep deprivation. While we cannot control innate factors, event-related risk factors offer an opportunity for us to decrease the growing number of AD patients.

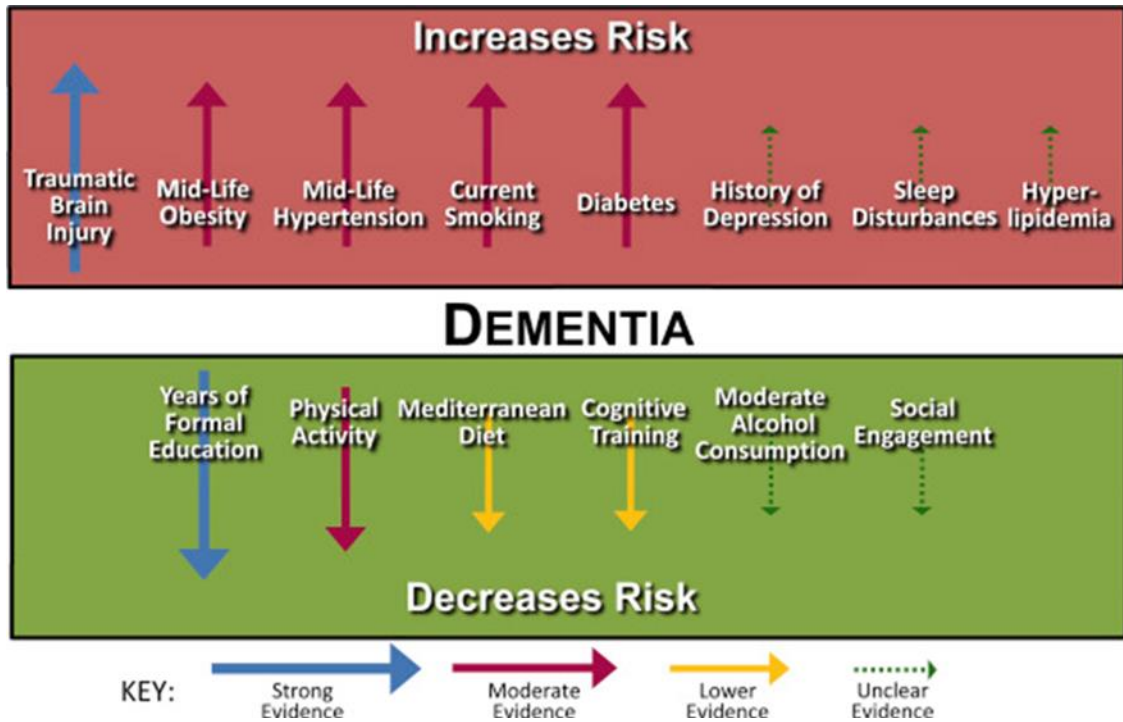


Figure 1.6: Strength of evidence on risk factors for dementia.

Modified from Figure 2 Baumgart et al., 2015 [4].

INSULIN AND AD

The insulin receptor (IR) is a tyrosine kinase receptor that autophosphorylates and can only be phosphorylated in the presence of its substrate, insulin. IRs are located in the periphery as well as the central nervous system. Insulin has been found to be synthesized by neurons in the brain as well as being transported from the periphery via the CSF through receptor-mediated transport [45]. In the CNS, IRs are abundant in the hippocampus and cerebral cortex where they are primarily located at synapses. IRs in the cerebral cortex have a high turnover rate, whereas the hippocampal IRs have a much higher stability [45].

IRs are involved in glucose metabolism in the periphery but have more diverse functions in the brain [45,46]. While the insulin-sensitive glucose transporter GLUT4 can be found in the brain, it is present in a few select nuclei (including the dentate gyrus) and

at a much lower level than the insulin-insensitive glucose transporter isoforms [37]. The most abundant glucose transporter found in neurons is the insulin-insensitive GLUT3 [47]. Therefore, rather than IR primary function being an involvement in glucose uptake in the CNS, the role of insulin signaling in the hippocampus has been implicated in synaptic remodeling, synaptogenesis, and facilitating learning and memory [48].

IRs can affect synaptic activities at both the pre- and post-synapse. Presynaptically, insulin signaling has been found to stimulate membrane phospholipid metabolism in hippocampal slices by enhancing adrenergic activity [45]. Postsynaptically, IR signaling has been shown to enhance NMDA receptor activity in an acute time frame (20 minutes but not after 60 minutes) in hippocampal slices due to tyrosine phosphorylation of NMDA receptor subunits [49]. Additionally, insulin can also act postsynaptically on GABA receptor expression which has been demonstrated to result in increased mIPSCs (miniature inhibitory postsynaptic currents) [50].

Molecular cascades activated by the insulin receptor that underscore long-term memory storage processes through gene expression and protein synthesis involve phosphorylated shc bound to the IR mediating signal transduction through the Grb-2/SOS complex to activate Ras/ mitogen-activated protein kinase (MAPK) cascades. Alternative signaling elements that interact with the insulin receptor to activate pathways involving PI3K, PKC, and AKT/PKB which then are able to interact with the Ras/MEK/MAPK cascades can also modulate memory processes and neuronal survival. [45]

Since insulin signaling is involved in learning and memory processes as well as synaptic health, it's unsurprising that disruptions in this important pathway have been linked to AD. In addition to T2DM being a risk factor for AD[35–37], cerebral glucose metabolism is reported to be decreased in AD[10]. What's more, even in AD patients without diabetes, the hippocampus exhibits insulin resistance shown by decreased insulin signaling and insulin-like growth factor (IGF) signaling response versus cognitively

normal people with doses of 1nM of insulin and IGF-1 that could not be overcome by a 10nM dosage stimulation [51].

Additionally, the protective effects of insulin on A β -oligomer binding and destruction at the synapse has been reported when looking at hippocampal neuronal cultures. In work published by De Felice et al., they showed with immunocytochemistry that A β -oligomers bind to synapses and cause synaptic loss that can be inhibited with the addition of insulin. They went on to show that disruption in the insulin receptor function by pharmacologically inhibiting the tyrosine kinase activity of the receptor abolished the ability of insulin to block A β oligomer binding [52]. This demonstrated that IR function is needed for this protection rather than insulin acting as a competitor on A β binding sites as an explanation for the decreased oligomer binding.

Conversely, they also showed that application and binding of A β oligomers caused a loss of insulin receptor surface expression on dendrites and a loss of autophosphorylation capacity of the receptor [46]. This showed how physiological insulin and pathological A β -oligomers negatively regulate the abundance of each other's binding sites.

In addition to these molecular studies, insulin and insulin-sensitizing therapy has been shown to be effective for cognition and behavior in both mouse models of AD as well as in patients with mild cognitive impairment (MCI) or early AD [52–55].

All of this evidence strongly indicates the existence of an intimate relationship between synaptic insulin responsiveness and neuronal sensitivity to AD neuropathology.

Traumatic Brain Injury

OVERVIEW

Each year, there is an incidence of roughly 2.7 million traumatic brain injuries in the US alone [56,57]. Current treatments for a mild TBI include over-the-counter pain relievers and just focus on treating any resulting symptoms. For those with a severe TBI, the initial treatment focuses on keeping the patient alive as well as preventing any further brain damage through removing blood clots, repairing skull fractures, ensuring adequate oxygen delivery to the brain, assessing blood pressure and intracranial pressure, and monitoring blood flow to the brain as well as brain temperature. For long-term care, these patients are then often transferred to a rehabilitation center where they are cared for by a multidisciplinary team of providers [58,59]. Possible drug interventions for these cases include anti-anxiety medication, anticoagulants, anticonvulsants, antidepressants, muscle relaxants, and stimulants to increase alertness and attention [59].

Molecularly, there are a wide range of effects and complications as a consequence of TBI [60] (Figure 1.7). There is disruption and dysfunction in the vascular system that leads to a variety of problems with the blood brain barrier (BBB), blood flow, and autoregulation. In addition, there are increases of calcium influx resulting in calcium overload. This disrupts mitochondrial function and allows for the generation of reactive oxygen species (ROS). Moreover, there are neuroinflammation consequences that lead to chronic microglia activation which is damaging to the cell. All of these effects are happening concurrently, interacting with and, in some cases, exacerbating each other, leading to a long list of short-term and long-term deficits including the possibility of AD. Even though these disruptions and consequences are known to occur, the exact mechanisms contributing to the increased risk of AD after TBI are unknown. Furthermore, despite this progress in understanding these molecular changes that occur, this has not led to a translational therapeutic benefit since over 30 clinical trials have

failed to find a drug intervention that can lead to measurable benefit in TBI patients [58].

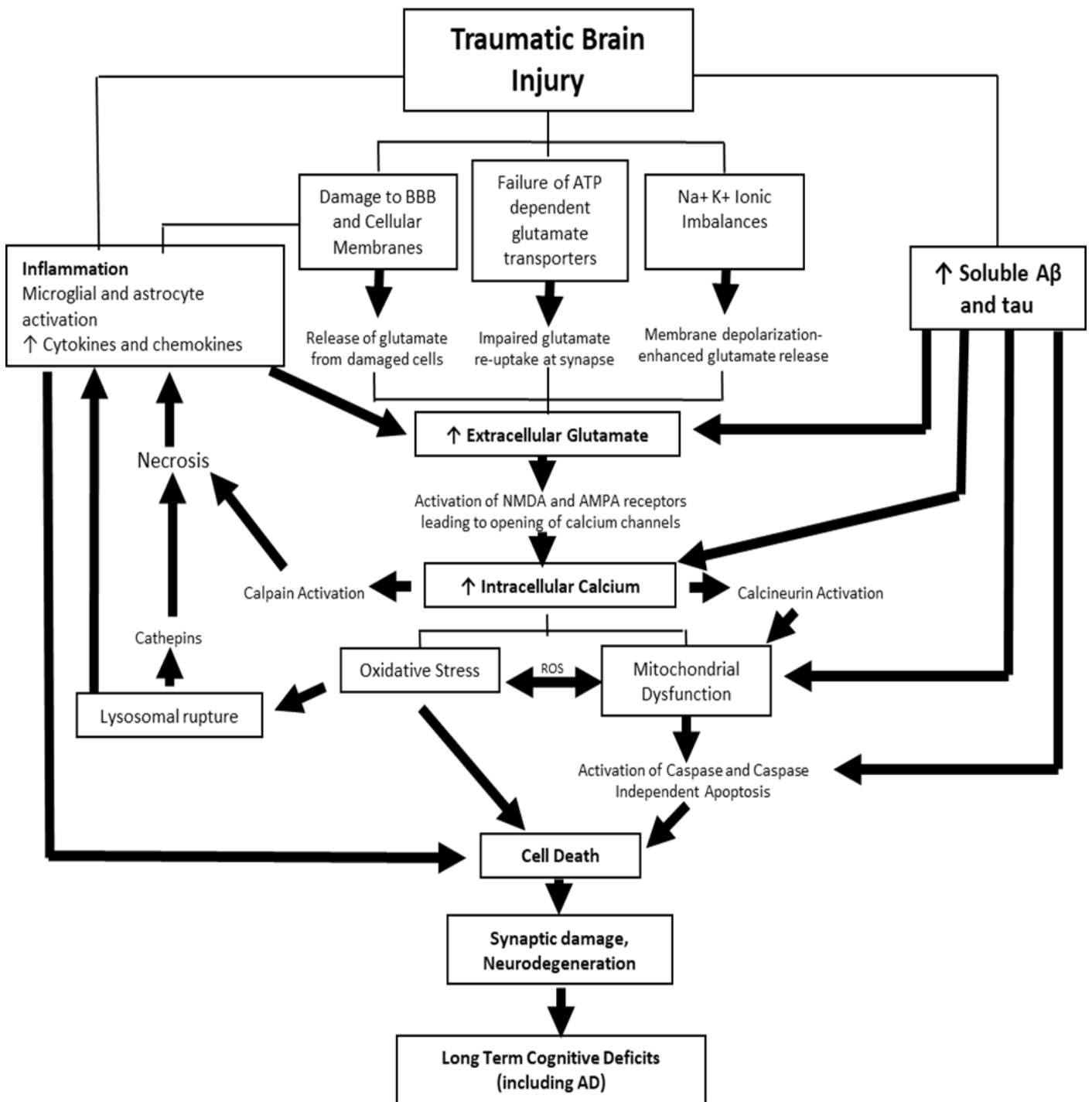


Figure 1.7: Consequences of traumatic brain injury. Molecular alterations after TBI leading to various acute and chronic diseases and consequences.

ALZHEIMER'S DISEASE CONSEQUENCE

TBI-induced dementia, in particular, is becoming a more central concern as the cost and incidence of AD continue to rise without any effective treatments. There is a dose-response relationship whereby the risk for dementia increases with the severity and number of injuries, but a single moderate or severe injury can still increase the risk of developing dementia diseases.

There are several things that have been postulated and investigated to contribute to the increased susceptibility to AD after TBI. Among these are the presence of the APOE 4 allele (which can increase your chance of generating AD after TBI by 10-fold), phosphorylated tau, and accumulating A β after TBI [44,61]. The accumulation of A β plaques that has been seen in about 30% of TBI cases in humans [62–64] has been thought to possibly correlate with many things, including elevated levels of soluble A β after TBI [41], increased A β 42:40 ratio [63,65], increase in APP processing since both APP [66] and β -secretase concentration have been shown to increase after TBI [64,67–69], and/or decreased A β clearance from the brain. However, the increase in soluble A β oligomers, APP, and β -secretase seen after TBI is transient whereby there is an increase followed by a decrease to normal levels within just a few days [65]. This acute accumulation therefore could not account for the susceptibility to AD since the patients do not generate dementia within a short time span. Rather, there is a long-term susceptibility causing the patient to be more likely to develop Alzheimer's decades down the road. Ergo, the systemic alteration linking the two diseases must be one that is chronic.

Molecular dysfunction	TBI (clinical and experimental)	AD (human brain and transgenic mouse model)
Impaired synaptic plasticity ↓LTP ↑LTD	Albensi et al., 2000; Scheff et al., 2005	Oddo et al., 2003; Trinchese et al., 2004
Impaired glutamate transport ↓GLAST/EAAT1 ↓GLT-1/EAAT2	Rao et al., 1998; van Landeghem et al., 2006; Yi and Hazell, 2006	Masliah et al., 1996; Li et al., 1997; Scott et al., 2011
↑NMDA receptor activation	Palmer et al., 1993	Revett et al., 2013
Intracellular calcium dysregulation	Sun et al., 2008; Saatman et al., 2010	See review Supnet and Bezprozvanny, 2010
Mitochondrial dysfunction	Xiong et al., 1997; Gilmer et al., 2009	Dragicevic et al., 2010; Reddy et al., 2010
Oxidative stress	Ansari et al., 2008; Cheng et al., 2012	Ansari and Scheff, 2010
Calcineurin activation	Kurz et al., 2005a,b	Liu et al., 2005; Wu et al., 2010
Calpain activation	Vosler et al., 2008; Saatman et al., 2010	Trinchese et al., 2008; Ferreira, 2012
Apoptosis	Minambres et al., 2008; Stoica and Faden, 2010	Castro et al., 2010; Rohn, 2010
Caspase-3 activation	Clark et al., 2000; Stone et al., 2002; Abrahamson et al., 2006; Walker et al., 2012	Tesco et al., 2007; see review Castro et al., 2010; Rohn, 2010
↑BACE1 level and activity	Blasko et al., 2004; Loane et al., 2009; Walker et al., 2012	Fukumoto et al., 2002; Holsinger et al., 2002; Sun et al., 2002; Tyler et al., 2002; Tesco et al., 2007; Cole and Vassar, 2008
↓GGA3 and GGA1 adaptor proteins	Walker et al., 2012	Tesco et al., 2007; Walker et al., 2012
Inflammation and chronic microglial activation	Ramlackhansingh et al., 2011; Acosta et al., 2013	Cagnin et al., 2001; Heneka et al., 2005; Schindowski et al., 2006; Parachikova et al., 2007; Garwood et al., 2010; Ferretti et al., 2012

Table 1.1: Common pathophysiological mechanisms in TBI and AD.

Adapted from Table 2 Walker et al., 2013 [61].

In addition to the A β and tau-related changes, there are also several pathophysiological mechanisms that are shared between the two diseases that have been described and investigated including problems with synaptic plasticity, calcium

dysregulation, oxidative stress, etc [61] (Table 1.1). However, all of these have fallen short in finding effective therapies that help alleviate this TBI/AD risk factor connection.

According to the NIH database clinicaltrials.gov, current ongoing drug interventional clinical trials on TBI include near infrared light therapy, intracranial administration of SB623 modified stem cells (phase 2), huperzine A in patients who have sustained a moderate to severe TBI and looking at memory function (phase 2), melatonin treatment in children after mild TBI (phase 2), citicholine/amantadine and its combinations on neuro-recovery in the early phase of moderate TBI (phase 4).

Due to the lack of success in clinical translation of TBI therapies, a group of researchers have collaborated in an attempt to streamline and standardize TBI research efforts with animal studies. To more adequately find the best drug candidates that hold the most potential in translating to a therapy in humans, they formed a preclinical consortium known as Operation Brain Trauma Therapy (OBTT) to test drug interventions using multiple TBI animal models. Four (nicotinamide, erythropoietin, cyclosporine A, and simvastatin) of the five drugs that have been tested so far by this consortium have shown sub-par performances compared to expectations based on the published literature. The only therapy that was found to have promising results in behavioral outcomes in more than one model of TBI was an early post-TBI administration of levetiracetam, which they have since advanced to the next phase of testing via a model of TBI using large animals (micropigs). [70]

INSULIN AND TBI

There are a multitude of consequences after TBI that suggest that normal insulin functioning can affect TBI recovery and that disruptions may be playing a role in the consequences. Several groups have reported hyperglycemia after TBI and found that uncontrolled blood glucose levels lead to a poorer outcome and recovery [71,72].

Moreover, previous reports have also found an increased mortality after head injury in people with T2DM [73]. One previous report found acute decreased insulin signaling in homogenate from the frontal cortex after a controlled cortical impact (CCI)-induced mild TBI [74]. They found decreased phosphorylation of the downstream insulin signaling element AKT in response to a 10nM insulin stimulation at 2DPI that recovered by 7DPI. In this same study, they also found that a repeated mild injury resulted in this decreased insulin signaling at 2 DPI, 7 DPI, and 14 DPI and recovered by 28 DPI.

While this previous finding of acute insulin resistance after a mild TBI is a promising start, no studies have investigated TBI-driven insulin resistance at the synapses. My research further attempts to evaluate synaptic insulin response specifically in the hippocampus to provide valuable insight into whether any changes in this synaptic health mechanism contributes to a vulnerable window to AD pathology since insulin resistance found here could leave synapses in a weakened state and more susceptible to the toxicity exerted by A β and tau oligomers.

Aim of the Dissertation

Traumatic brain injury (TBI) increases the risk of developing Alzheimer's disease (AD) later in life through unknown mechanisms [39–41,61]. Synaptic dysfunction stemming from the interaction and binding of toxic amyloid beta (A β) and tau oligomeric species to the pre- and post-synapse is an early event in AD that leads to the cognitive decline that characterizes this disease [20]. Since insulin signaling plays a role in synaptic health and function, disruption of this pathway due to insulin resistance has been implicated in the susceptibility of the synapse to AD pathology [46,52].

The aim of this dissertation was to investigate an altered susceptibility of the synapses to AD pathology in relation to TBI-induced changes in signaling and support systems to give novel insights into the link between the two conditions. My central hypothesis is that TBI promotes insulin resistance at the synapse resulting in increased synaptic sensitivity to the dysfunctional effects of A β and tau oligomers. I addressed my central hypothesis with two specific aims. In my first aim, I confirmed that TBI alters insulin responsiveness at the synapse by characterizing hippocampal synaptic insulin responsiveness using an *ex vivo* stimulation method. In my second aim, I tested the hypothesis that synaptic vulnerability to the effects of A β and tau is increased after TBI. I addressed this aim by utilizing *ex vivo* binding methods with flow cytometry and ELISA analysis to specifically determine any binding alterations. I additionally performed electrophysiology to investigate changes in functional susceptibility to the oligomers.

This research will contribute to understanding mechanism(s) underscoring the increased risk linking the two diseases, which is critical to develop effective interventions to reduce the incidence of AD in TBI subjects. Additionally, this work further illustrates the importance of considering a prior history of associated risk factors and how these may impact the efficacy of particular treatments that are being investigated for AD in the general population.

CHAPTER 2. INVESTIGATING SYNAPTIC INSULIN RESISTANCE AFTER FPI

Modified in part from:

Franklin W, Taglialatela G (2016) A method to determine insulin responsiveness in synaptosomes isolated from frozen brain tissue. *J. Neurosci. Methods* **261**, 128–134.

And

Franklin W, Krishnan B, Taglialatela G. Chronic synaptic insulin resistance after traumatic brain injury abolishes insulin protection from amyloid beta and tau oligomer-induced synaptic dysfunction. Submitted to *Scientific Reports*. 26 Feb, 2019.

Introduction

Alterations of insulin signaling in neurons have been linked to many different disorders including Type 2 diabetes, inflammation, and Alzheimer's disease (AD) [75]. Synapses are rich with insulin receptors, and insulin has been shown to be an important component for maintaining synaptic health/integrity [46,52]. Notably, disruption of this pathway due to insulin resistance has been implicated in the susceptibility of the synapse to AD pathology [46,52]. Since the risk of developing AD increases after a traumatic brain injury, in this chapter, I decided to first investigate if there are changes in synaptic insulin responsiveness after TBI by using rats that underwent a lateral fluid percussion injury at acute and chronic time points.

Materials and Methods

ANIMALS

Male Sprague-Dawley rats were utilized for the traumatic brain injuries and subsequent experiments in this study. All rats were 2-4 months old (300-450 grams) at the time of surgery/injury. All experimental protocols involving animals in this study were approved by Institutional Animal Care and Use Committee of the University of Texas Medical Branch. Animals were housed under USDA standards (12:12 hour light dark cycle, food and water ad libitum) at the UTMB vivarium. After the designated amount of time after surgery/injury, the rats were sacrificed by isoflurane overdose and decapitated. The brains were quickly removed, dissected into major regions (frontal cortex, parieto-occipital cortex, hippocampus, midbrain, and cerebellum) and opposing hemispheres (“ipsilateral” referring to the brain hemisphere that underwent the craniotomy in the lateral FPI procedure and “contralateral” for the opposite hemisphere), snap frozen, and stored at -80°C until ready for further analysis.

An adipocyte-specific ecto-nucleotide pyrophosphate phosphodiesterase (ENPP) over-expressing transgenic mouse model of metabolic syndrome and systemic insulin resistance, AtENPP1-Tg, was used to confirm the validity of the *ex vivo* insulin responsiveness assay. This mouse model has previously been shown to present with marked synaptic insulin resistance [76]. Samples from an adult male AtENPP1-Tg mouse that had been fed with high-fat chow (60% calories from fat – 37.1% saturated) for 12 weeks and a C57Bl/6J (wild-type) mouse that had been fed a regular chow diet (4% calories from fat) as previously described in Sallam et al., 2015 were graciously donated by Dr. Nicola Abate.

PARASAGITTAL FLUID-PERCUSSION INJURY

For laboratory models used to induce TBI, there are those that induce either static or dynamic trauma. Dynamic models can induce impact injury through penetration, closed head injuries, acceleration, and direct brain deformation [77]. The TBI model that was used for these experiments is a dynamic model of direct brain deformation impact injury called fluid percussion injury (FPI).

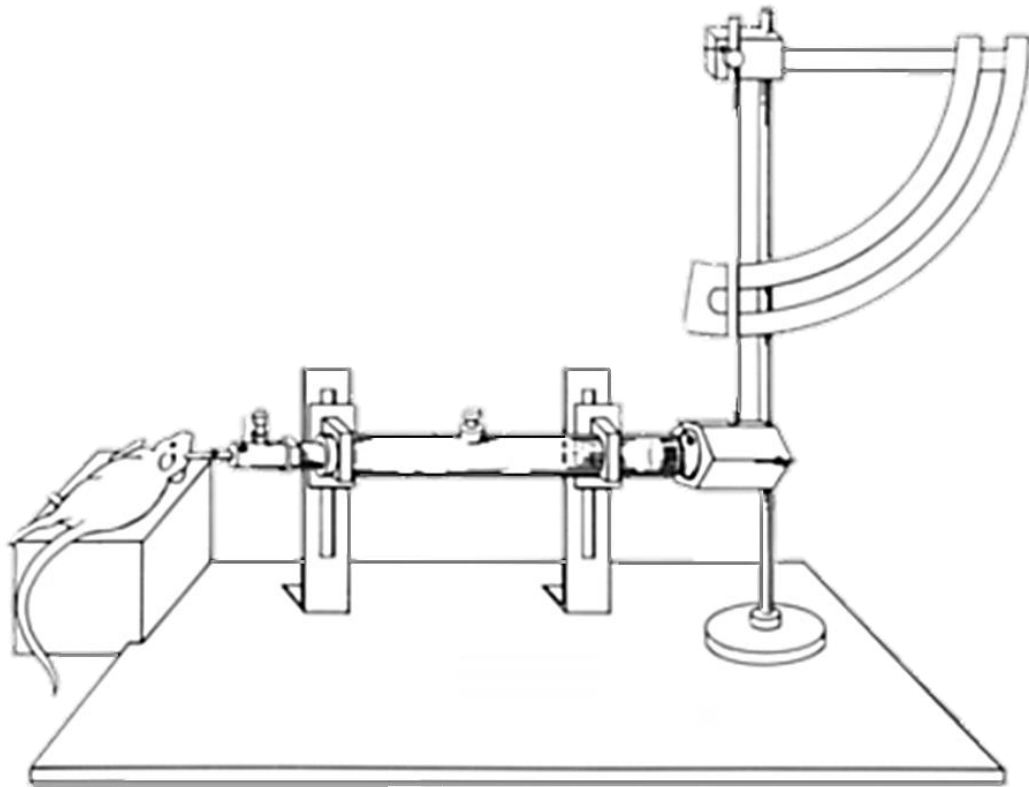


Figure 2.1: Schematic of fluid-percussion traumatic brain injury model.

This model of TBI is one of the most widely used and established models. First, a craniotomy is performed to expose part of the brain where fluid pressure will later be applied. The position, lateral or midline, of the craniotomy can be altered to fit the type of brain injury classification desired: focal versus diffuse.

The animal's craniotomy site is then connected to the transducer end of the injury device. The pendulum of this device is lifted to a specified height that corresponds to the intensity of injury desired. The higher the pendulum, the more severe the injury. Once the pendulum is released, it strikes the back of a saline-filled cylinder that acts as a piston by then pushing saline through the craniotomy site causing a direct brain deformation injury. The pressure with which the fluid is injected causes the injury. The righting reflex time is used as an indication of injury severity.

The controls used in these experiments are sham injured animals who have undergone the craniotomy and the same procedures as the injured animals with the exception of the fluid percussion injury itself. The term "ipsilateral" will be used when referring to the brain hemisphere that underwent the craniotomy in the lateral FPI procedure while "contralateral" refers to the opposite brain hemisphere.

Craniotomy. Male Sprague-Dawley rats (300–450 grams) were anesthetized (4% isoflurane) and prepared for moderate or sham parasagittal FPI. Rectal temperatures were monitored using telethermometers (Yellow Spring Instrument Co., Yellow Springs, OH), and temperatures were maintained within a range of 37.5 ± 0.5 °C using an overhead lamp and a thermostatically controlled water blanket (Gaymar, Orchard Park, NY). Rats were placed in a stereotaxic apparatus, a midline incision of the skin was performed, and the skull was exposed. A craniotomy was performed using a 5mm diameter Michele trephine at 1 mm lateral (right) to the sagittal suture, midway between the lambda and bregma. The bone chip was removed, leaving the dura intact. A modified 20-gauge needle hub was secured in place over the exposed dura with superglue and cemented into place with hygienic dental acrylic.

Parasagittal Fluid Percussion Injury. TBI was administered by means of a FPI device (AmScien Instruments, Richmond, VA) consisting of a fluid-filled Plexiglass cylinder 25-inches-long and 2.5 inches in outside diameter, with one end connected to a pressure transducer and the other end closed by a Plexiglass piston mounted on O rings.

The animal's craniotomy hub site was directly connected to the transducer end of the injury device. The 3.6-kg pendulum of the device was lifted to a specified height to correspond to the intensity of injury desired, moderate injury level for these studies. The pendulum was released and struck the back of the sterile saline-filled cylinder causing a direct brain deformation injury. The fluid pressure pulse is triggered photoelectrically by the strike of the pendulum and was recorded using a FP-302 signal conditioner connected to a Windows 8 operating computer. The righting reflex time was recorded and further used as an indication of injury severity. At 2 days, 7 days, 1 month, or 3 months after TBI or sham injury, the rats were euthanized and brain tissue collected as described above.

SYNAPTOSOMAL ISOLATION

Synaptosomes containing both pre- and post-synaptic components were isolated from frozen tissue that had been snap frozen on dry ice and transferred to -80°C . Left and right hippocampi were homogenized separately in SynPER (Thermo Scientific, Waltham, MA) with 1% protease (Sigma, St. Louis, MO) and phosphatase cocktail inhibitors (Thermo Scientific, Waltham, MA) on ice. Homogenate was centrifuged (Eppendorf, Mississauga, Canada) at $1,200 \times g$ RCF for 10 minutes at 4°C . Supernatant was collected and centrifuged (Eppendorf, Mississauga, Canada) at $15,000 \times g$ RCF for 20 minutes at 4°C . The supernatant was removed, and the pellet was resuspended in $48\mu\text{L}$ HEPES-buffered Krebs-like (HBK) buffer (143-mM NaCl, 4.7-mM KCl, 1.3-mM MgSO_4 , 1.2-mM CaCl_2 , 20-mM HEPES, 0.1-mM NaH_2PO_4 , and 10-mM D-glucose, pH 7.4). The quality of the synaptosomes are routinely verified by Western blot and electron microscopy as previously reported [78].

Michael Woodson from the UTMB electron microscopy core used frozen, isolated synaptosomes to generate the electron microscopy images shown in Figure 2.2D.

INSULIN RESPONSIVENESS

Insulin Stimulation of synaptosomes. After isolation of synaptosomes, insulin stimulations were performed as previously described [78–80]. In short, 100mM ATP stock was added for final concentration of 8mM to synaptosomes in HBK for both unstimulated and stimulated samples, and U-100 insulin was added for 200nM final insulin concentration to insulin-stimulated samples. Samples were vortexed and incubated for 15 minutes at 37°C. Synaptosomes were pelleted by centrifugation at 10,000 x g RCF for 10 minutes at 4°C. Pellets were resuspended in 1X RIPA (75-mM NaCl, 25- mM Na₂PO₄, 1-mM EDTA, 0.5% NP-40, and 0.5% TritonX-100) plus 1% protease (Sigma, St. Louis, MO) and phosphatase cocktail inhibitors (Thermo Scientific, Waltham, MA) to solubilize the proteins for Western blot and WES detection. Samples were then stored at -80°C.

WES analysis of Insulin Responsiveness. IR phosphorylation extent was analyzed using WES (Protein Simple, San Jose, CA) with specific antibodies against the phosphorylated form of the 1150/1151 tyrosine residue of the insulin receptor (Cell Signaling Cat. #3024L). The phosphorylated form was normalized against β -tubulin (Cell Signaling Cat. #2146S). Another WES was run for the total amount of IR (Cell Signaling Cat. #3025S) which was normalized to β -tubulin as well. The ratio of normalized phosphorylated-IR over normalized total IR was used to assess the extent of insulin responsiveness.

WESTERN BLOT ANALYSIS FOR SOCS3

The bicinchoninic acid (BCA) assay method was used for protein estimation to prepare samples of equal protein concentration. Samples were prepared in 2-mercaptoethanol (2-ME) and boiled prior to loading. Thirty micrograms of protein were loaded with appropriate marker on 10% sodium dodecyl sulfate polyacrylamide gel electrophoresis (SDS-PAGE) gels followed by transfer to Amersham Protran nitrocellulose transfer membrane (GE Healthcare-Life Sciences) for 1 hour at 100V. The

membrane was blocked using Odyssey blocking buffer (LI-COR, Lincoln, Nebraska) for 1 hour at room temperature. Primary antibodies were diluted 1:1000 in 1X TBST and incubated with the membrane at 4°C overnight for SOCS3 (Cell Signaling Cat. #2923S) and 1 hour at room temperature for β -tubulin (Cell Signaling Cat. #2146S). The membrane was washed twice with 1X TBST for 15 minutes each and incubated with LI-COR secondary antibodies diluted at 1:10,000 in 1X TBST with 3% non-fat dry milk for 1 hour at room temperature. The membrane was again washed twice with 1X TBST for 15 minutes each.

Western blots were imaged using LI-COR Odyssey infrared imaging system (LI-COR, Lincoln, Nebraska), application software version 3.0.30. The density of each immunoreactive band was measured using Image J software.

STATISTICAL ANALYSIS

Data is represented as mean \pm SEM. All data were statistically analyzed using Graphpad Prism6. Unpaired t-tests were used to determine statistical significance between sham and TBI animals for each time point individually for the insulin stimulations.

Results

DEVELOPMENT OF *EX VIVO* INSULIN STIMULATION METHOD

In order to investigate and assess insulin responsiveness, I had to develop a method whereby I would be able to detect phosphorylation of the insulin receptor directly, rather than probing for downstream elements. Additionally, I wanted to isolate responses of neurons at the synapse to avoid picking up IR activation at the cell body or

in other cell types such as glia. Therefore, I developed an *ex vivo* insulin stimulation method on isolated synaptosomes, details of which can be found in my published method paper in Journal of Neuroscience Methods [78].

To accomplish this detection method, I isolate functional synaptosomes containing both pre- and post-synaptic elements (Figure 2.2A) from fresh or frozen tissue by fractionation (either using a Percoll sucrose gradient or using synPER reagent (Thermo Scientific)) and expose them to insulin in the presence of ATP to detect insulin receptor phosphorylation using either Western blot or WES analysis.

Isolation and confirmation of synaptosomes and IR responsiveness. Upon initially developing the method, I used electron microscopy to visually confirm synaptosomal isolation (Figure 2.2D). I additionally confirmed the isolation of the synaptosomes by checking for enrichment of post-synaptic density marker PSD-95 in the synaptosomal fraction versus total homogenate using Western blot analysis (Figure 2.2B). I saw an enrichment of this marker in the synaptosomal protein fraction indicating that the fractionation procedure was successful. Moreover, I demonstrated a reliable phosphorylation of the insulin receptor via Western blot analysis using this method (Figure 2.2C).

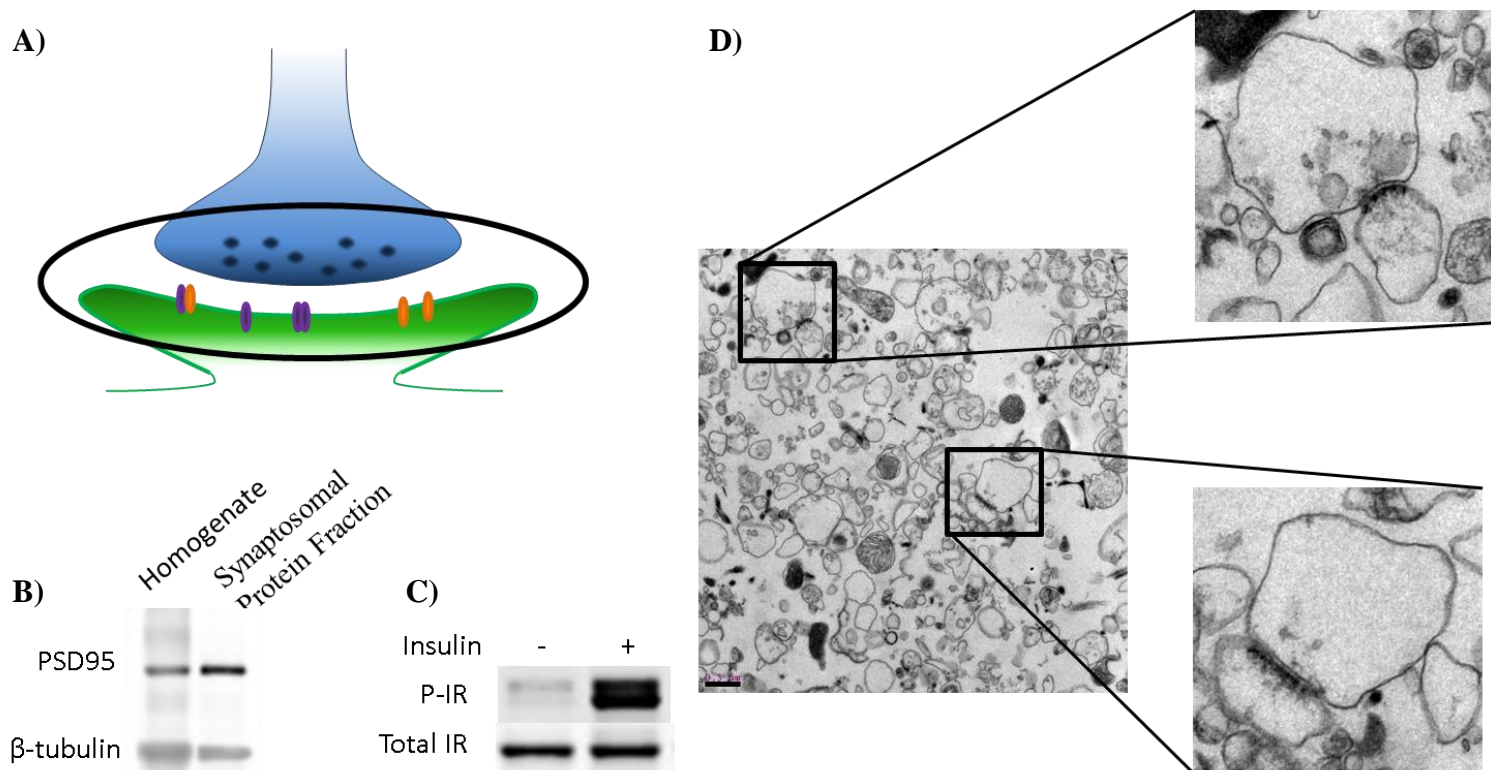


Figure 2.2: Synaptosomal characterization and confirmation of insulin stimulation.

A) A schematic showing the pre- and post-synaptic areas retained in the synaptosomal isolation. B) Representative Western blot detecting enrichment of the post-synaptic marker PSD95 in synaptosomal fraction versus total homogenate, indicating successful synaptosomal isolation. C) Representative Western blot detecting insulin-stimulated IR phosphorylation in synaptosomes isolated from frozen rat brain and stimulated with 0.333 units/mL of insulin for 15 min at 37°C with 8mM ATP. D) Representative transmission electron microscopy image (3,000 x) of synaptosomal protein fraction. Scale bar represents 0.5 μ m. Blow-out insert images illustrate examples of synaptosomes characterized by the presence of the post-synaptic density area (arrows). Modified from Figure 1 and Supplemental Figure 2 from Franklin et al., 2016 [78].

Optimization of ex vivo insulin stimulation conditions. After confirming synaptosomal isolation as well as confirmation that this ex vivo insulin stimulation allows for detection of the insulin receptor directly, I optimized this technique with ATP dosage curves, insulin dosage curves, and insulin time course responses. From the data investigating insulin-stimulated IR phosphorylation of synaptosomes isolated from frozen rat brain tissue that were stimulated with 1.67 units/mL of insulin for 15 min at 37 °C in the presence of increasing concentrations of ATP (0–6 mM) in the incubation buffer, I

saw no plateau in insulin receptor activity in this concentration range as determined by Western blot (Figure 2.3A). Since the ATP concentration inside the cell is between 0 and 10 mM, I decided to use an ATP concentration of 8mM for all future experiments. Using synaptosomes from frozen mouse brain and stimulating with increasing concentrations of insulin for 15 min at 37 °C in the presence of 8 mM ATP, I saw a plateaued response beginning at 0.154units/mL of insulin (Figure 2.3B). An insulin-receptor activation curve of synaptosomes exposed to 0.333 units/mL of insulin for varying amounts of time from 0 to 1 h at 37°C with 8 mM ATP was performed and analyzed by Western blot. I found maximal IR phosphorylation 10 to 15 minutes after addition of insulin (Figure 2.3C) and thus used 15-minute incubations for the remaining experiments.

Furthermore, I looked at other factors that may influence the ability of the IR to activate including post-mortem intervals (PMI) (Figure 2.3D). I looked at PMIs that modeled the conditions that would normally occur for collection of autopsy brain human specimens (PMI of 8 hours, 12 hours, and 21 hours). To accomplish this, I assessed insulin-stimulated phosphorylation of the IR in synaptosomes isolated from brain tissue collected from mice at varying times after sacrifice. Mice were sacrificed by CO₂ asphyxiation followed by cervical dislocation and left at room temperature for 1 hour prior to being placed at 4°C for the remainder of the specified PMI times. Afterwards, brains were collected, snap frozen, and stored at -80°C. Synaptosomes were isolated from the frozen mouse brains and stimulated with 0.333 units/mL of insulin for 15 min at 37°C with 8mM ATP. I found no significant differences in the ratio of P- IR/IR in the various PMI samples versus control where the brain was immediately collected and placed at -80°C upon sacrifice.

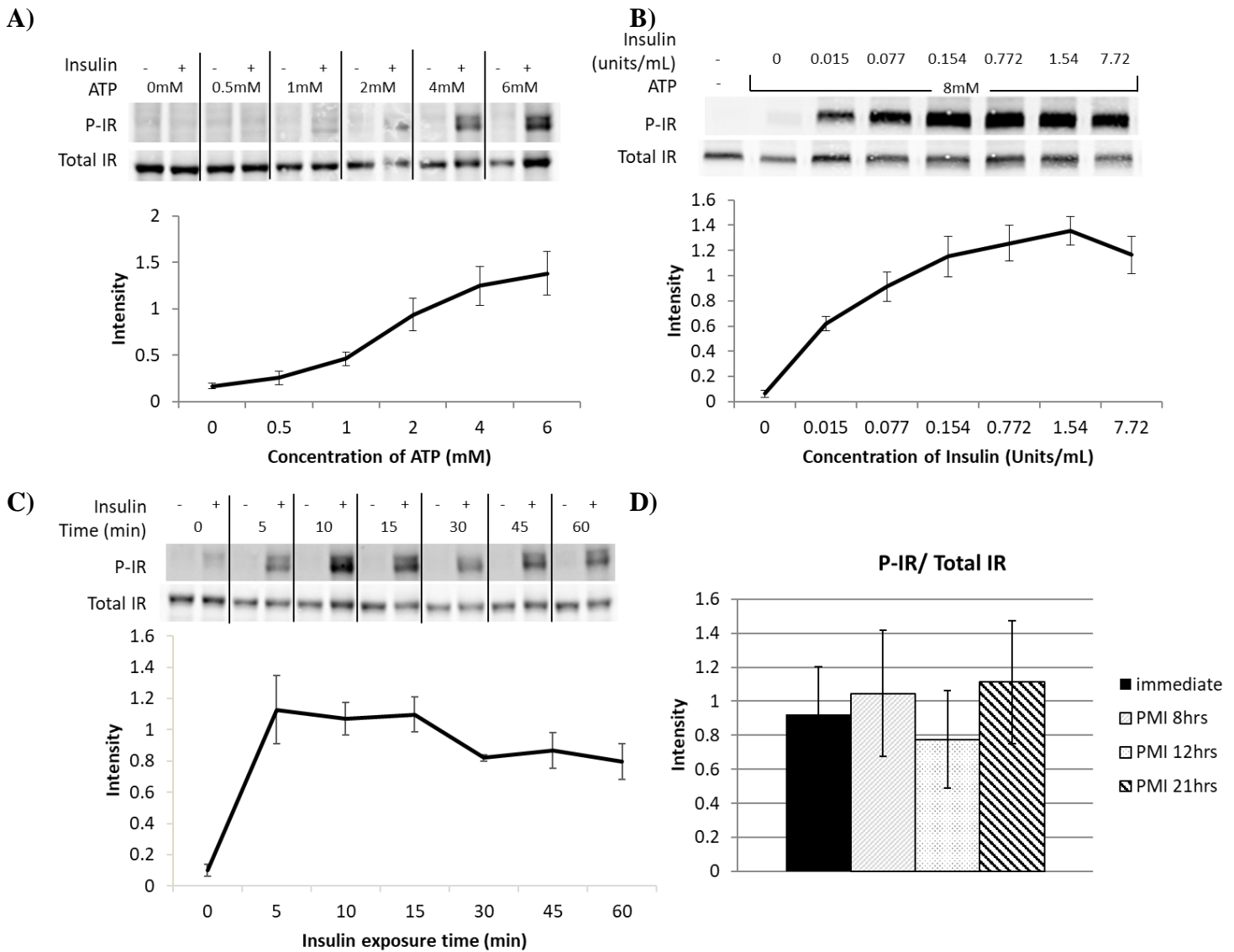


Figure 2.3: Optimization of ex vivo insulin stimulation method

A) Representative Western blot of insulin-stimulated IR phosphorylation in the presence of increasing concentrations of ATP in the incubation buffer and quantification of the ratio p-IR/Total IR expressed as average \pm SEM from 3 independent experiments. B) Representative Western blot showing IR phosphorylation in response to increasing concentrations of insulin and quantification of the ratio p-IR/Total IR expressed as average \pm SEM from 3 independent experiments. C) Representative Western blot showing IR phosphorylation at different time points after insulin addition and quantification of the ratio p-IR/Total IR expressed as average \pm SEM from 3 independent experiments. D) Quantification of Western blot's immunoreactivity from insulin-stimulated phosphorylation of the IR in synaptosomes isolated from brain tissue collected from mice at varying post-mortem intervals. Modified from Figure 2 and Figure 4 from Franklin et al., 2016 [78].

Comparison of *ex vivo* and *in vivo* synaptosomal insulin response. After optimization of the method, I wanted to verify that the *ex vivo* insulin stimulation protocol yields results consistent with *in vivo* physiology by using a transgenic mouse model of metabolic syndrome and systemic insulin resistance, AtENPP1-Tg. This mouse model has previously been shown to present with marked synaptic insulin resistance when assessing downstream insulin signaling elements (AKT and GSK3 β) after an intraperitoneal (IP) insulin injection (*in vivo* insulin stimulation), contrary to the response seen in wild-type (WT) mice [76] (Figure 2.4A).

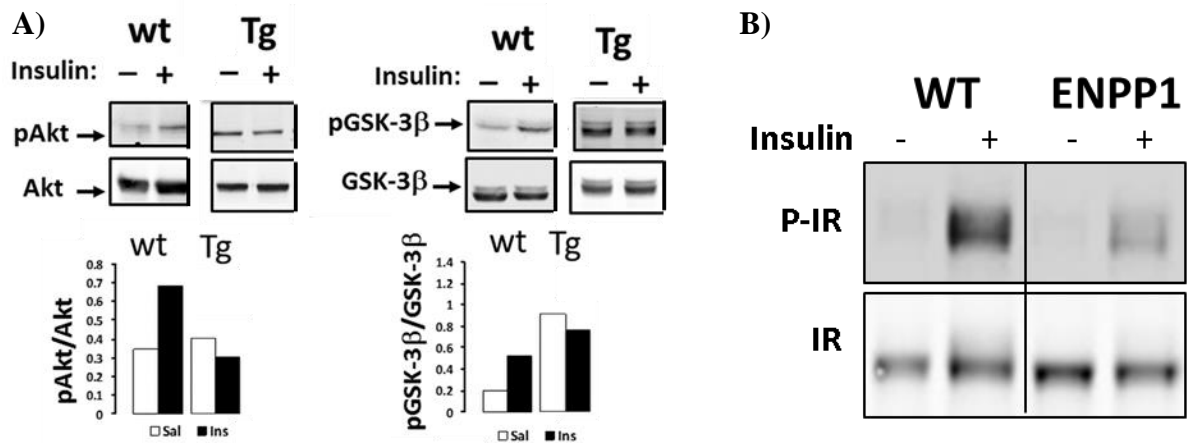


Figure 2.4: Comparison of *in vivo* and *ex vivo* synaptosomal insulin response.

A) *In vivo* insulin response in the hippocampus of AtENPP1-Tg mice showing blunted post-receptor response to systemic insulin elevation (IP insulin injection) compared to their WT littermates. Modified from Figure 1S Sallam et al., 2015 [76]. B) Representative Western blot detecting insulin-driven phosphorylated IR in isolated hippocampal synaptosomes from AtENPP1-Tg and WT mice using the *ex vivo* insulin stimulation technique. Adapted from Figure 5 Franklin et al., 2016 [78].

Thus, to confirm that the *ex vivo* results were consistent with the *in vivo* situation, I isolated synaptosomes from both the WT and AtENPP1-Tg mice, performed this *ex vivo* insulin stimulation protocol, and observed IR phosphorylation/activation to a lesser extent in the transgenic animals compared to controls (Figure 2.4B). This data clearly

shows that this *ex vivo* stimulation correlates and represents the physiology *in vivo* due to detection of a decreased response of the insulin receptor in an animal model of known insulin resistance.

EVALUATE SYNAPTOSOMAL INSULIN RESPONSIVENESS AFTER TBI

Now with an established technique in place to evaluate synaptic insulin receptor responsiveness, I tested the hypothesis that TBI alters insulin responsiveness at the synapse after FPI in rats. I performed lateral FPI to induce TBI, collected and dissected the brain, and performed *ex vivo* insulin stimulations and WES analyses on isolated synaptosomes of frozen brain tissue prepared from the hippocampi of both the ipsilateral-hemisphere (side of injury) and contralateral-hemisphere (opposite to the lateral injury). I evaluated multiple time-points after injury (2 days post injury (DPI), 7 DPI, 1-month post injury (MPI), and 3 MPI).

In the ipsilateral hippocampus, I found a significant decrease in synaptic insulin responsiveness by 7 DPI (Figure 2.5B) that was further decreased by 3 MPI. Moreover, I observed a significantly decreased level of IR at the synapse at 7DPI, as compared to sham-injured animals (Figure 2.5C). However, this decrease in IR level cannot account for the decreased insulin response at this time-point after injury. At 1 MPI, the synaptic IR level was normalized back to the level of sham-injured animals, and there was a further significant increase in IR level at the synapse at 3 MPI which could be indicative of an attempted compensatory mechanism. I also found a significant increase in basal (unstimulated) level of IR phosphorylation at 2 DPI (data not shown). Whereas at both 7 DPI and 3 MPI, the basal level of IR phosphorylation was significantly decreased (data not shown).

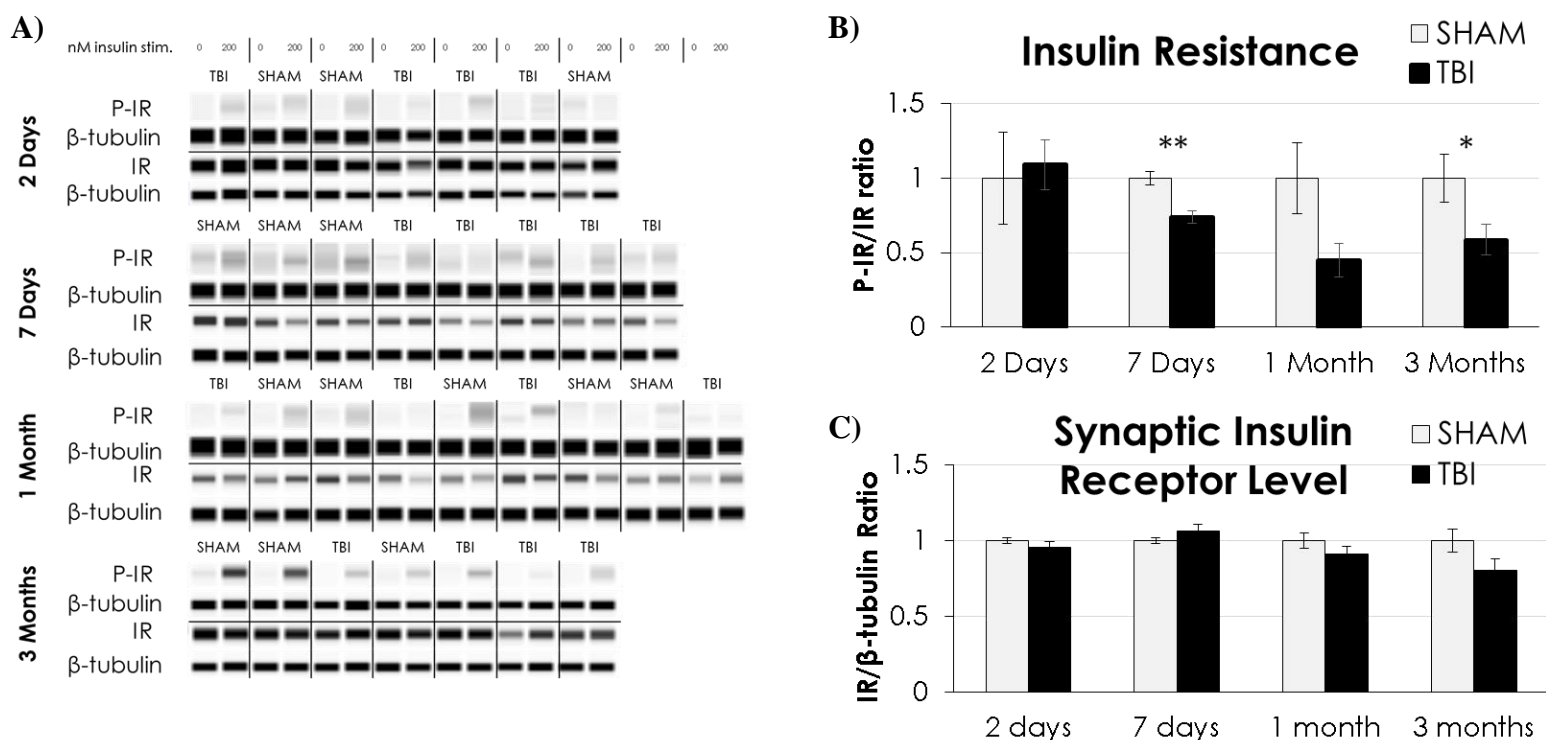


Figure 2.6: Insulin responsiveness in contralateral hippocampus.

A) Representative WES analysis of insulin stimulated and unstimulated isolated synaptosomes from 2 DPI (n=3 sham, n=4 TBI), 7 DPI (n= 3 sham, n=5 TBI), 1 MPI (n= 5 sham, n=4 TBI), and 3 MPI (n= 3 sham, n= 4 TBI) animals. Quantitative graph of WES analysis showing B) the ratio of P-IR/ β -tubulin to IR/ β -tubulin demonstrating that synaptosomal insulin responsiveness is chronically decreased after TBI and C) IR/ β -tubulin showing that the insulin receptor level at the synapse is unchanged. Statistical significance was determined by unpaired t-test analysis. Error bars represent standard error. * $p < 0.05$; ** $p < 0.01$.

In summary, I found a significant decrease in the synaptic insulin receptor's response to insulin at 7 DPI, 1 MPI, and 3 MPI but not at 2 DPI. These data indicate that there are chronic deficits in synaptic insulin responsiveness in both the ipsilateral and contralateral hippocampi after lateral FPI.

ASSESS POSSIBLE MECHANISTIC DRIVER OF SYNAPTIC INSULIN RESISTANCE

I then decided to turn my attention to a possible mechanistic driver of this chronic synaptic insulin resistance that I found. Thus, I thought to look for an increased protein

level of an insulin receptor inhibitor that could directly bind to the insulin receptor. I first decided to try and look at ENPP1, a pyrophosphatase that not only degrades ATP but can directly bind to the insulin receptor to remove and prevent phosphorylation. After multiple attempts in a variety of samples, I determined that I could not see a sufficient amount of ENPP1 in any hippocampal rodent brain samples (homogenate, cytosol, synaptosomes \pm insulin) (data not shown) which suggests that either ENPP1 is not at a detectable protein level in the brain or that the antibody for this protein is not specific enough to prove to be a viable method of detection and analysis.

I then performed a more in-depth literature search for inhibitor candidates, and, with the help of employing the brain atlas protein database, I determined an alternative protein to investigate as the insulin receptor inhibitor. I decided to look for an upregulation of SOCS3. SOCS3 is a protein of the suppressor of cytokine signaling (SOCS) family that acts as negative regulators of cytokine and growth factor signaling. SOCS3 expression can be induced by IL6 as well as IL10 and has previously been shown to negatively regulate insulin signaling [81]. I analyzed the level of this protein in synaptic fractions from hippocampi of both brain hemispheres in sham and TBI animals at all of my time points (2 DPI, 7 DPI, 1 MPI, and 3 MPI) using Western blot analysis (Figure 2.7).

In the ipsilateral hippocampus, I found a significantly increased level of SOCS3 at the synapse in TBI animals versus sham animals at 2 DPI, 7 DPI, and 1 MPI as well as a trend of a remaining but not significant increase at 3 MPI (Figure 2.7A/C). Since this occurs prior to insulin resistance being found at the synapse at 7 DPI, this could be a driving factor in initiating the dysregulation and insulin resistance. In the contralateral hemisphere, however, I did not find altered levels of SOCS3 at the synapse at any of the time points (Figure 2.7B/D). While I still found synaptic insulin resistance beginning at 7 DPI in this hemisphere too, it is possible that the two hemispheres have resulting insulin resistance from different mechanisms.

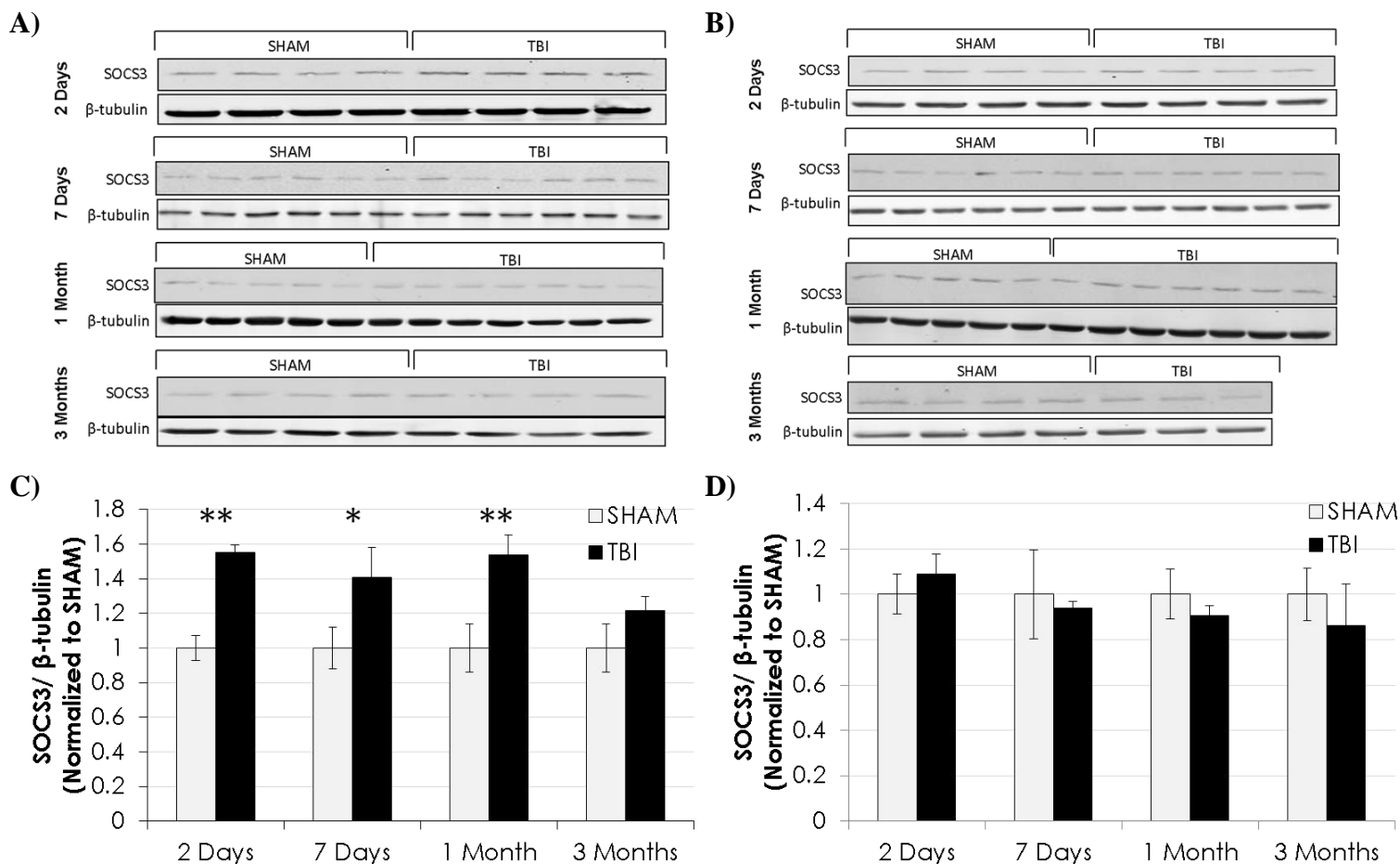


Figure 2.7: SOCS3 expression in the ipsilateral and contralateral hippocampi.

Western blots of isolated synaptosomes from 2 DPI (n = 4 for both sham and TBI), 7 DPI (n= 6 for both sham and TBI), 1 MPI (n= 5 sham, n=7 TBI), and 3 MPI (n= 4 sham, n= 4 TBI ipsi and n=3 TBI contra) animals isolated from the A) ipsilateral hippocampus and B) contralateral hippocampus. Quantitative graphs of the Western blot analysis showing SOCS3 normalized to β -tubulin for the C) ipsilateral hippocampus and D) contralateral hippocampus. Statistical significance was determined by unpaired t-test analysis. *p < 0.05; **p < 0.01.

Conclusions

I first developed and optimized a consistent, efficient method to measure insulin-driven *ex vivo* phosphorylation of the synaptosomal insulin receptor that can reliably

reflect the pre-existing insulin responsiveness status in the CNS of the animal. This method is advantageous over other methods detecting IR in total brain homogenates due to the ability to detect IR response without confounding contributions from other cell areas (e.g. cell soma) and cell types (glia) also expressing substantial levels of IR. This unique characteristic makes this new method particularly useful in situations when insulin responsiveness at the synapses must be differentiated from other subcellular compartments as it has been found that A β -oligomers induced an IR redistribution from the dendrites to the cell body in a hippocampal neuronal culture [52].

After the *ex vivo* synaptic insulin response assay was developed, I longitudinally characterized synaptic insulin responsiveness in the hippocampus of rats at different time points after FPI. I found a significant decrease in the synaptic insulin receptor's response to insulin at 7 DPI, 1 MPI, and 3 MPI but not at 2 DPI. These data indicate that there are chronic deficits in synaptic insulin responsiveness in both the ipsilateral and contralateral hippocampi after lateral FPI.

Moreover, I found a significantly increased level of an insulin receptor signaling inhibitor, SOCS3, in synaptosomes at 2DPI, 7 DPI, and 1 MPI in the ipsilateral hippocampus which precedes the decreased insulin responsiveness. However, I did not find any changes in SOCS3 expression in the contralateral hippocampus.

CHAPTER 3. EVALUATING SYNAPTIC VULNERABILITY TO THE EFFECTS OF AB AND TAU AFTER TBI

Modified from:

Franklin W, Krishnan B, Taglialatela G. Chronic synaptic insulin resistance after traumatic brain injury abolishes insulin protection from amyloid beta and tau oligomer-induced synaptic dysfunction. Submitted to *Scientific Reports*. 26 Feb, 2019.

Introduction

In the previous chapter, I demonstrated that there is chronic synaptic insulin resistance after TBI. In the current chapter, I wanted to investigate whether this decreased insulin responsiveness may lead to increased synaptic sensitivity to AD pathology. I decided to evaluate synaptic vulnerability to these proteinaceous species in two ways; 1) binding susceptibility using flow cytometry for A β oligomers and ELISA analysis for tau oligomers and 2) functional vulnerability using electrophysiology to assess oligomer-induced LTP inhibition as well as any afforded protection by insulin against this impairment.

Materials and Methods

PARASAGITTAL FLUID-PERCUSSION INJURY

Craniotomy and fluid-percussion injury were induced using male Sprague-Dawley rats as previously described in chapter 2. At 1 month or 3 months after TBI or sham injury, the rats were euthanized and brain tissue collected for synaptosomal isolation as previously described for binding experiments. For electrophysiology

experiments, animals were euthanized with an overdose of isoflurane and decapitated with a guillotine, and immediately brain tissue was sliced and treated as described below.

SYNAPTOSOMAL ISOLATION

Synaptosomes were isolated from frozen tissue using SynPER (Thermo Scientific, Waltham, MA) and resuspended in HBK buffer as described in chapter 2.

AB-BINDING

A β oligomer preparation. Human A β 1–42 peptide was purchased from Department of Biophysics and Biochemistry, Harvard University, MA. Human A β oligomers are routinely prepared in our lab [82] from lyophilized synthetic A β aliquots of 0.3mg. 200 μ L of 1,1,1,3,3,3- Hexafluoro-2-propanol (HFP) was used to dissolve the lyophilized aliquots. 700 μ L of DDI water was then added, and a cap with four holes was placed on the tube. The sample was magnetically stirred under a fume hood for 48 hours. The A β oligomers were aliquoted, frozen at -80°C, and used within 3 months. For the flow cytometry analysis of A β oligomer-binding to synaptosomes, A β oligomers spiked with Flour 647 tagged A β (AnaSpec Inc., Fremont, CA) were utilized. These A β oligomers were prepared by adding 7 μ L of the tagged A β to the HFP-A β mixture described above, prior to the addition of water. The quality of the oligomeric preparations was routinely checked by Western blot and dot blot analysis using 6E10 and A-11 antibodies (A β oligomer specific).

A β oligomer binding challenge. Oligomeric A β to be employed in the same experiment was always used from aliquots of the same batch of A β . Hippocampal synaptosomes were treated with A β oligomers for an *ex vivo* binding challenge and evaluated using flow cytometry as previously performed in our lab [83]. An equal number of isolated synaptosomes per animal determined by flow cytometry were pooled for each experimental group. For each group, the pooled samples were then aliquoted into

10 separate tubes containing 10 million synaptosomes each. This was repeated 3 times for 3 separate curves. Each sample was incubated with A β oligomers tagged with HyLite Fluor 647 for the desired μ M concentration, ranging from 0 μ M to 20 μ M, for 1 hour at room temp. Synaptosomes were then centrifuged at 15,000 x g RCF for 10 minutes at 4°C, washed 3 times with HBK buffer, and resuspended in PBS. Data was acquired by a Guava EasyCyte flow cytometer (EMD Millipore, Burlington, MA) and analyzed using Incyte software (EMD Millipore).

TAU-BINDING

Tau-oligomer preparation. Prepared recombinant tau oligomers were graciously given to us by Dr. Rakez Kayed's laboratory. The tau oligomers were produced as previously described [84]. Briefly, full-length human recombinant tau was expressed, purified, and aliquoted into a monomeric tau stock solution of 1mg/mL in 1XPBS buffer at pH 7.4. A β 42 oligomers seeds were added to a 0.3 mg/ml tau solution in 1XPBS and incubated on an orbital shaker for 1 hour at room temperature. The tau oligomers produced were purified by FPLC and used as seeds in a fresh batch of tau monomers. After three rounds of seeding with purified tau oligomers, detection of the original A β seeds was eliminated due to sufficient dilution. Each batch of oligomers is tested using dot blot with T22 (a tau oligomer-specific antibody), Western blot analysis, and atomic force microscopy (AFM) to verify the quality of the tau oligomer preparation.

Ex vivo Tau-oligomer binding. Synaptosomes were treated with tau oligomers for an *ex vivo* binding challenge and evaluated using ELISA as previously performed in our lab [85]. Hippocampal synaptosomes from each animal were challenged and evaluated independently. Using flow cytometry, 10 million synaptosomes from each animal were aliquoted and challenged with 2 μ M of tau oligomers for 1 hour at room temperature. The samples were then centrifuged and washed with HBK buffer 3 times to thoroughly remove any unbound tau oligomers. Synapse number was acquired using flow

cytometry once again, and an equal amount of synaptosomes per sample were analyzed by tau5 (total tau) ELISA.

ELISA Analysis of Tau. Total tau levels were measured by ELISA analysis using the total tau antibody tau5 (Biolegend Cat. # 806401). Samples were incubated on the ELISA plate at 4 °C overnight with the coating buffer 0.1 M sodium bicarbonate (pH 9.6). Samples were discarded and each well was washed with Tris-buffered saline with low Tween 20 (0.01%) (TBS-low T) followed by blocking with 10% nonfat milk for 2 hours. After a second wash, the primary tau5 antibody (1:1000 in 5% nonfat milk in TBS-low T; Thermo Scientific) was incubated in each well for 1 hour at room temperature. After a third wash, the plates were incubated for 1 hour at room temperature with horseradish peroxidase-conjugated anti-rabbit IgG secondary antibody (1:10,000 in 5% nonfat milk in TBS-low T; Promega). Following the fourth wash, 3,3',5,5'-tetramethylbenzidine (TMB-1 component substrate; Sigma-Aldrich) was added to each well. After 30 min of incubation in the dark, 1 M HCl was added to stop the reaction, and the plate was read at 450 nm for tau detection and quantification.

ELECTROPHYSIOLOGY

Animals were euthanized with deep isoflurane anesthesia, decapitated by guillotine, and brains were harvested and sliced using Compressstome VF-300 (Precisionary Instruments, Greenville, NC) in NMDG-aCSF (93 mM NMDG, 2.5 mM KCl, 1.2 mM NaH₂PO₄, 30 mM NaHCO₃, 20 mM HEPES, 25 mM glucose, 5 M sodium ascorbate, 2 mM thiourea, 3 mM sodium pyruvate, 10 mM MagSO₄ ·7H₂O, 0.5 mM CaCl₂ ·2H₂O, and 12 mM N-acetyl L-Cysteine) to obtain 450 μm transverse brain sections. Slices were allowed to recover for 10 minutes in NMDG-aCSF at 35°C. Slices were then maintained at room temperature in a modified HEPES holding aCSF solution (92 mM NaCl, 2.5 mM KCl, 1.2 NaH₂PO₄, 30 mM NaHCO₃, 20 mM HEPES, 25 mM Glucose, 5 mM sodium ascorbate, 2 mM thiourea, 3 mM sodium pyruvate, 2 mM

MgSO₄·7H₂O, 2 CaCl₂·2H₂O, 12 N-Acetyl L-Cysteine). Slices were recorded in standard recording aCSF (124 mM NaCl, 2.5 mM KCl, 1.2 mM NaH₂PO₄, 24 mM NaHCO₃, 5 mM HEPES, 12.5 mM glucose, 2 mM MgSO₄·7H₂O and 2 mM CaCl₂·2H₂O). All solutions were aerated using 95% O₂ with 5% CO₂.

For oligomer challenges, the slices were incubated for 1 hour at room temperature prior to recording with 200nM A β oligomers, 50nM tau oligomers, and/or 200nM insulin. For slices treated with insulin, 200nM insulin was also present in the aCSF recording solution.

Using a horizontal P-97 Flaming/Brown micropipette puller (Sutter Instruments, Novato, CA), borosilicate glass capillaries were used to pull electrodes and filled with nACSF to get a resistance of 1–2 M Ω . Evoked field excitatory post-synaptic potentials (fEPSPs) recordings were performed by stimulating the Schaffer collateral pathway using a stimulating electrode of 22 k Ω resistance placed in the CA3 region and recording in the CA1 region. LTP was induced using an HFS protocol (3 x 100 Hz, 20 seconds) as previously described [86]. Recordings were digitized with Digidata 1550B (Molecular Devices, Sunnyvale, CA), collected using an Axon MultiClamp 700B differential amplifier (Molecular Devices), and analyzed using Clampex 10.6 software (Molecular Devices). Current stimulation was delivered through a digital stimulus isolation amplifier (A.M.P.I, ISRAEL) and set to elicit an fEPSP approximately 30% of maximum for synaptic potentiation experiments using platinum-iridium tipped concentric bipolar electrodes (FHC Inc., Bowdoin, ME). Baseline recordings were obtained by delivering single pulse stimulations at 20 second intervals. All data are represented as a percentage change from the initial average baseline fEPSP slope obtained for the 10 minutes prior to HFS.

INSULIN'S EFFECT ON PROPERTIES OF HIPPOCAMPAL SLICES

Naïve, male Sprague-Dawley rats were euthanized with deep isoflurane anesthesia, decapitated by guillotine, and brains were harvested and sliced as performed for the electrophysiology experiments. Slices were then maintained at room temperature in a modified HEPES holding aCSF solution and aerated using 95% O₂ with 5% CO₂.

Effect on A β binding. Hippocampal brain slices were treated with A β oligomers \pm insulin, synaptosomes isolated, and binding evaluated using flow cytometry. Slices were challenged with 2.5 μ M A β -oligomers tagged with HyLite Fluor 647 diluted in HEPES holding aCSF solution with or without 200nM insulin to mimic the insulin stimulation used for the electrophysiology paradigm. A higher concentration of A β -oligomers was used for these experiments than for the electrophysiology (2.5 μ M rather than 200nM) because the flow cytometry detection method used here cannot detect 200nM A β binding parameters. Each slice was incubated in 0.5mL total solution in a 48 well cell/tissue culture plate (Costar, Corning, NY) for 1 hour in the dark in a 37°C tissue incubator maintained with 95% O₂ with 5% CO₂. Slices were transferred to 1.5mL tubes and washed with HEPES-aCSF to remove any unbound oligomers. Synaptosomes were isolated using SynPER as described above and resuspended in PBS. Data was acquired by a Guava EasyCyte flow cytometer (EMD Millipore, Burlington, MA) and analyzed using Incyte software (EMD Millipore).

Effect on mitochondria. Hippocampal brain slices were treated with insulin, synaptosomes isolated, mitochondria labeled, and flow cytometry used to evaluate mitochondria. Slices were treated with either 200nM or 2.5 μ M of insulin diluted in HEPES holding aCSF solution for 1 hour in a 37°C tissue incubator maintained with 95% O₂ with 5% CO₂. Slices were transferred to 1.5mL tubes and washed with HEPES-aCSF, and synaptosomes were isolated using SynPER as described above. Synaptosomes were then treated with Mitotracker green FM (Invitrogen, Carlsbad, CA) and MitoSense Red

(1,1',3,3',3',3'- Hexamethylindodicarbocyanine iodide) (EMD Millipore, Burlington, MA) for 15 minutes at 37 °C. MitoTracker is a fluorescent dye that diffuses across the mitochondrial membrane and reacts with thiol groups of specific mitochondrial proteins[87]. The fluorescent dye MitoSense correlates with mitochondria membrane potential[88]. The synaptosomes were washed twice with HBK buffer and then resuspended in PBS. Fluorescent emittance was acquired by a Guava EasyCyte flow cytometer (EMD Millipore, Burlington, MA) and analyzed using Incyte software (EMD Millipore).

STATISTICAL ANALYSIS

Data is represented as mean \pm SEM except for electrophysiology data represented as mean \pm SD. All data were statistically analyzed using Graphpad Prism6. Unpaired t-tests were used to determine statistical significance between sham and TBI animals for each time point individually for the oligomer binding experiments. For the electrophysiology experiments, a one-way ANOVA with Bonferroni's post hoc test was used to determine statistical significance between the LTP of each condition.

Results

QUANTIFY SYNAPTOSOMAL A β BINDING AFTER TBI

I tested the hypothesis that synaptic vulnerability to A β binding is increased after TBI by utilizing an *ex vivo* A β binding protocol with flow cytometry analysis to generate a binding concentration curve for A β . After learning flow cytometry and optimizing this experiment, I used isolated synaptosomes and performed an A β binding curve using 10 different concentrations of A β oligomers labeled with Flour 647 (from 0 μ M to 20 μ M)

with 3 replicates of pooled samples of 1 and 3 MPI animals from the ipsilateral (Figure 3.1B/C) and contralateral hippocampi (Figure 3.1D/E). To exclude non-synaptosomal particles in my analysis and eliminate any nonspecific A β oligomer-binding, I used size particle standards to size-gate for synaptosomes with parameters set to include particle sizes from 1–5 μ m. Data were transformed for Scatchard plot analysis to estimate the maximum binding capacity (B_{\max}) and affinity (K_d) of A β binding. I did not find increases in A β binding (neither in B_{\max} nor in K_d) in hippocampal synaptosomes from TBI versus sham animals at either the 1 month or 3 months post-injury time points. These results suggest that despite onset of insulin resistance, synapses are not more susceptible to A β oligomer binding at these intermediate and chronic time points.

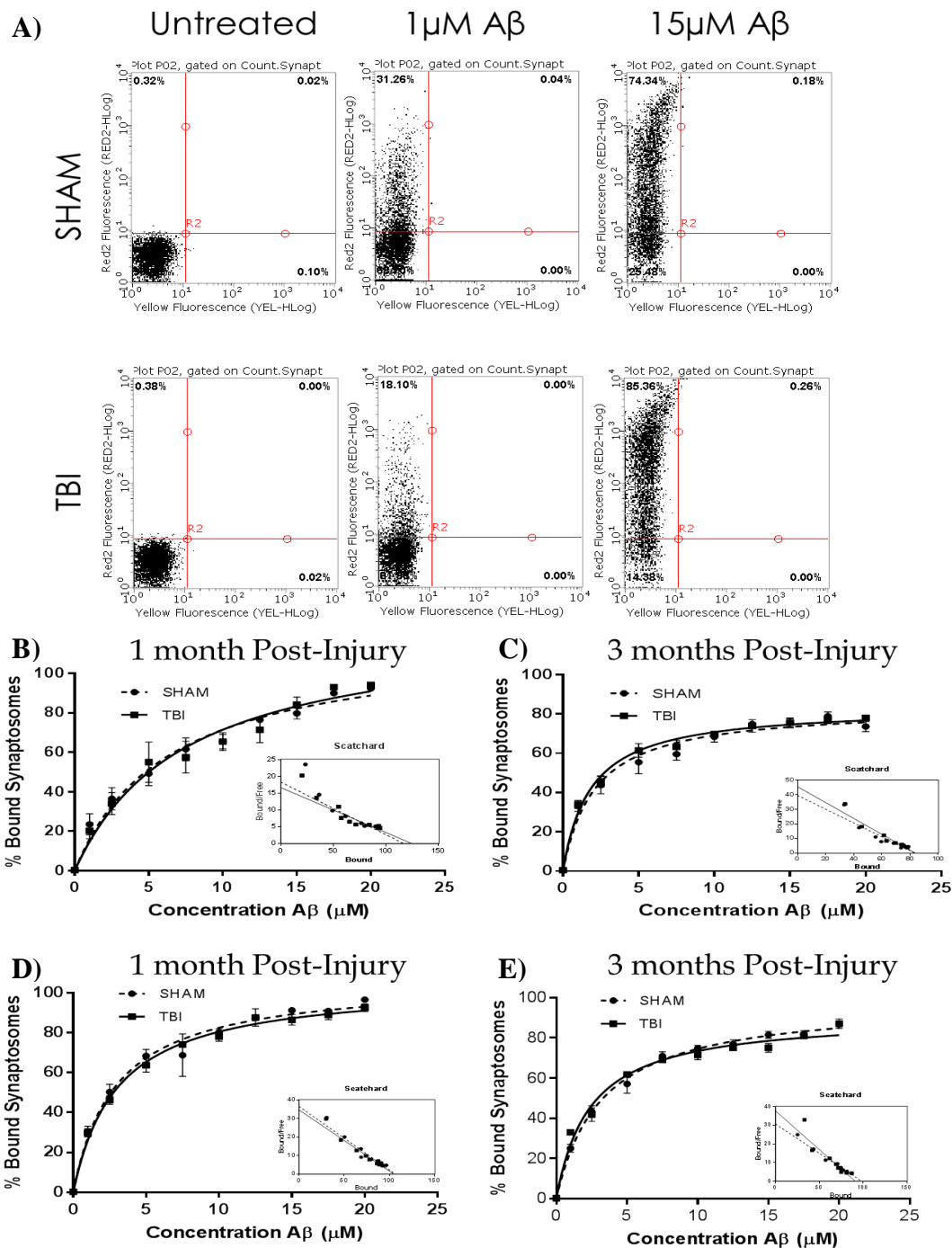


Figure 3.1: Amyloid-beta oligomer *ex vivo* binding curves in the ipsilateral and contralateral hippocampi.

A) Representative flow cytometry analysis of pooled synaptosomes isolated from 1 MPI sham and TBI animals challenged with increasing concentrations of A β oligomers tagged with HyLite Fluor 647. Michaelis-Menton graphs with Scatchard plot transformation from three separate binding curve analysis showing the percent of synaptosomes with bound A β oligomers determined by flow cytometry analysis in the ipsilateral hippocampus at B) 1 month post-injury (n= 5 sham, n= 7 TBI) and C) 3 months post-injury (n= 4 for both sham and TBI) and in the contralateral hippocampus at D) 1 month post-injury (n= 5 sham, n= 7 TBI) and E) 3 months post-injury (n= 4 sham, n=3 TBI).

QUANTIFY SYNAPTOSOMAL TAU BINDING AFTER TBI

To complement the A β oligomer binding data at the intermediate and chronic time-points after TBI, my next goal was to determine tau oligomer binding in isolated hippocampal synaptosomes at these same time-points.

Therefore, to assess tau oligomer binding at the synapse, I performed an *ex vivo* binding experiment using a single concentration of tau oligomer on isolated hippocampal synapses and quantified the binding with an ELISA. I first optimized conditions for both the tau oligomer challenge as well as for the tau-5 ELISA on isolated rat synaptosomes. Tau-5 antibody showed high background from endogenous rat tau and thus took several experiments to optimize concentration/ incubation time of tau as well as sample concentration to load for the ELISA.

After optimization, to determine whether the chronically decreased synaptic insulin responsiveness would affect synaptic vulnerability to tau oligomers, I performed an *ex vivo* tau binding on hippocampal synaptosomes isolated from both sham and TBI animals at 1 month and 3 months post-injury using ten million synaptosomes from each animal and exposing them to 2 μ M of tau oligomers for 1 hour, as described in the Materials and Methods section. After washing synaptosomes to remove unbound oligomers, flow cytometry was used to ensure an equal number of synaptosomes were loaded per well for ELISA analysis. Tau-5 antibody was used to quantify the amount of tau bound to synaptosomes. I found that both ipsilateral (Figure 3.2A/B) and contralateral (Figure 3.2C/D) hippocampal synaptosomes from TBI animals at both time points bound similar levels of exogenously added tau oligomers as compared to sham animals. These data suggest that, similar to what I found for A β -oligomer binding, synapses are not more susceptible to tau oligomer binding at the late time points of 1 month or 3 months after TBI.

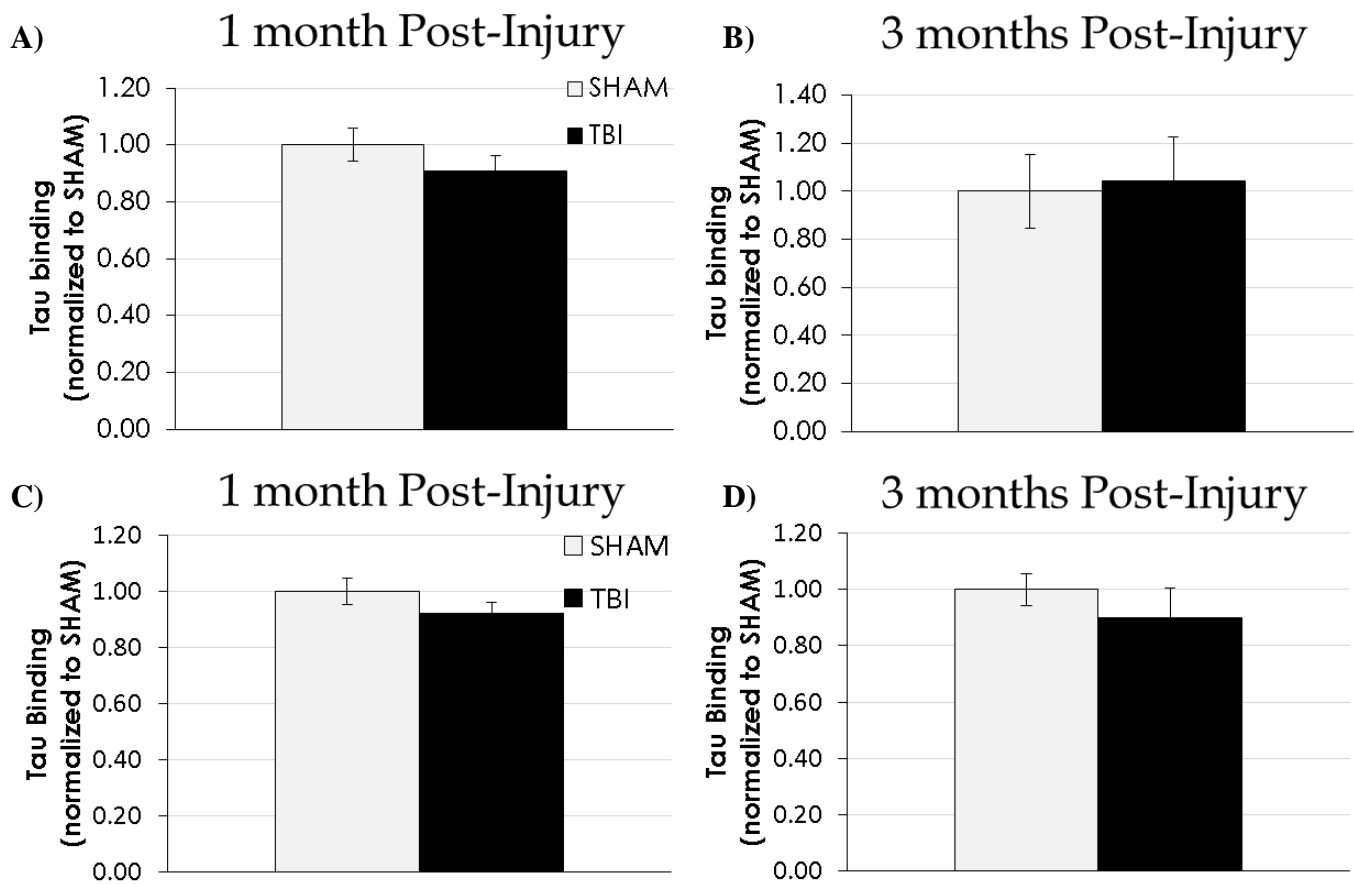


Figure 3.2: *Ex vivo* tau oligomer binding in the ipsilateral and contralateral hippocampi.

Quantification of $2\mu\text{M}$ tau-oligomer *ex vivo* binding on isolated synaptosomes determined by tau-5 ELISA analysis in the ipsilateral hippocampus at A) 1 MPI (n= 5 sham, n= 7 TBI) and B) 3 MPI (n= 4 for both sham and TBI) and in the contralateral hippocampus at C) 1 MPI (n= 5 sham, n= 7 TBI) and D) 3 MPI (n= 4 sham, n= 3 TBI). Error bars represent standard error.

ELECTROPHYSIOLOGY ASSESSMENT

While I did not observe any increases in hippocampal synaptic vulnerability to the binding of A β or tau oligomers in TBI animals, I wanted to test the hypothesis that there is an increase in functional vulnerability of synapses to AD pathology after TBI. Therefore, I decided to use electrophysiology to determine if there are functional disturbances that are commonly observed in both A β and tau oligomer-bound synapses, i.e. LTP inhibition. I sought to additionally evaluate whether an application of insulin in coordination with the presence of the oligomers can block the oligomer-induced LTP suppression.

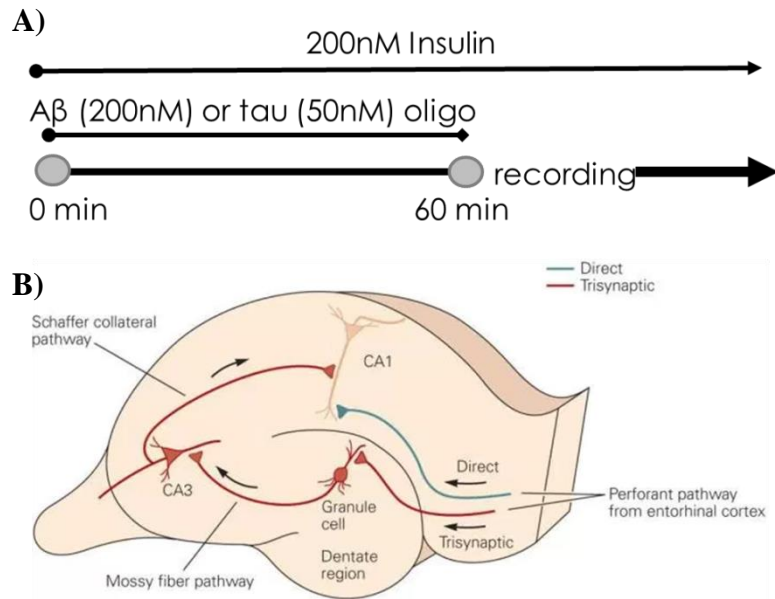


Figure 3.3: Electrophysiology experimental design.

A) Oligomer challenge paradigm for electrophysiological assessment of LTP suppression. B) Hippocampal slice schematic of various neural pathways. Electrophysiological recording of the Schaffer collateral pathway was performed by stimulating at the CA3 and recording from the CA1 region.

Hippocampal slices of the ipsilateral and contralateral hemispheres prepared from sham and TBI animals at both the 1 MPI and 3 MPI time points were evaluated for LTP impairment after a treatment challenge with 200nM of A β oligomers (Figure 3.4 and Figure 3.6), 50nM of tau oligomers (Figure 3.5 and Figure 3.7), and/or 200nM insulin for

1 hour prior to recording. The electrophysiological assessment recorded from the Schaffer collateral pathway in untreated and oligomer-treated slices was performed using standard recording aCSF. When insulin treatment was used, slices were recorded using standard recording aCSF containing 200nM insulin.

I saw a reduction in the magnitude of LTP from untreated brain slices in both the ipsilateral and contralateral hippocampi from the injured animals' vs sham animals at 1 MPI. At 3 MPI, I found this same significant reduction in the magnitude of LTP from untreated brain slices from the injured animals' vs sham animals in the ipsilateral hippocampus only.

In slices treated with A β oligomers for 1 hour prior to recording, the magnitude of LTP was significantly lower in the TBI versus sham group in the ipsilateral hippocampus at 1 MPI (Figure 3.4B). However, in the contralateral hippocampus, I saw the opposite effect where the magnitude of LTP, while only modestly higher, was significantly increased compared to slices from sham animals when treated with A β (Figure 3.6B). For tau oligomer-treated slices at 1 MPI, the magnitude of LTP was significantly decreased in slices taken from TBI versus sham animals in the contralateral hippocampus only (Figure 3.7B). However, for 3 MPI, in both hemispheres' hippocampi, I found no significant differences in LTP suppression due to either the A β (Figure 3.4D and Figure 3.6D) or tau oligomer (Figure 3.5D and Figure 3.7D) treatments for the TBI versus sham group.

The 200nM insulin treatment during both the A β and tau oligomer-challenge was able to block LTP suppression in sham hippocampal slices at both time points in the ipsilateral (Figure 3.4B/D and Figure 3.5B/D) and contralateral hemispheres (Figure 3.6B/D and Figure 3.7B/D). Notably, however, the insulin treatment did not block the A β -induced LTP inhibition in slices from TBI animals in any of these groups (Figure 3.4B/D and Figure 3.6B/D). While the insulin provided no protection against the tau-induced LTP reduction in slices from TBI animals in the ipsilateral hemisphere (Figure 3.5B/D), I did find that insulin provided a partial protection against tau in the

contralateral hemisphere at both time points (Figure 3.7B/D). Importantly, in slices treated with insulin alone (Figure 3.8), insulin did not enhance LTP expression in sham nor in TBI animals in either hemisphere.

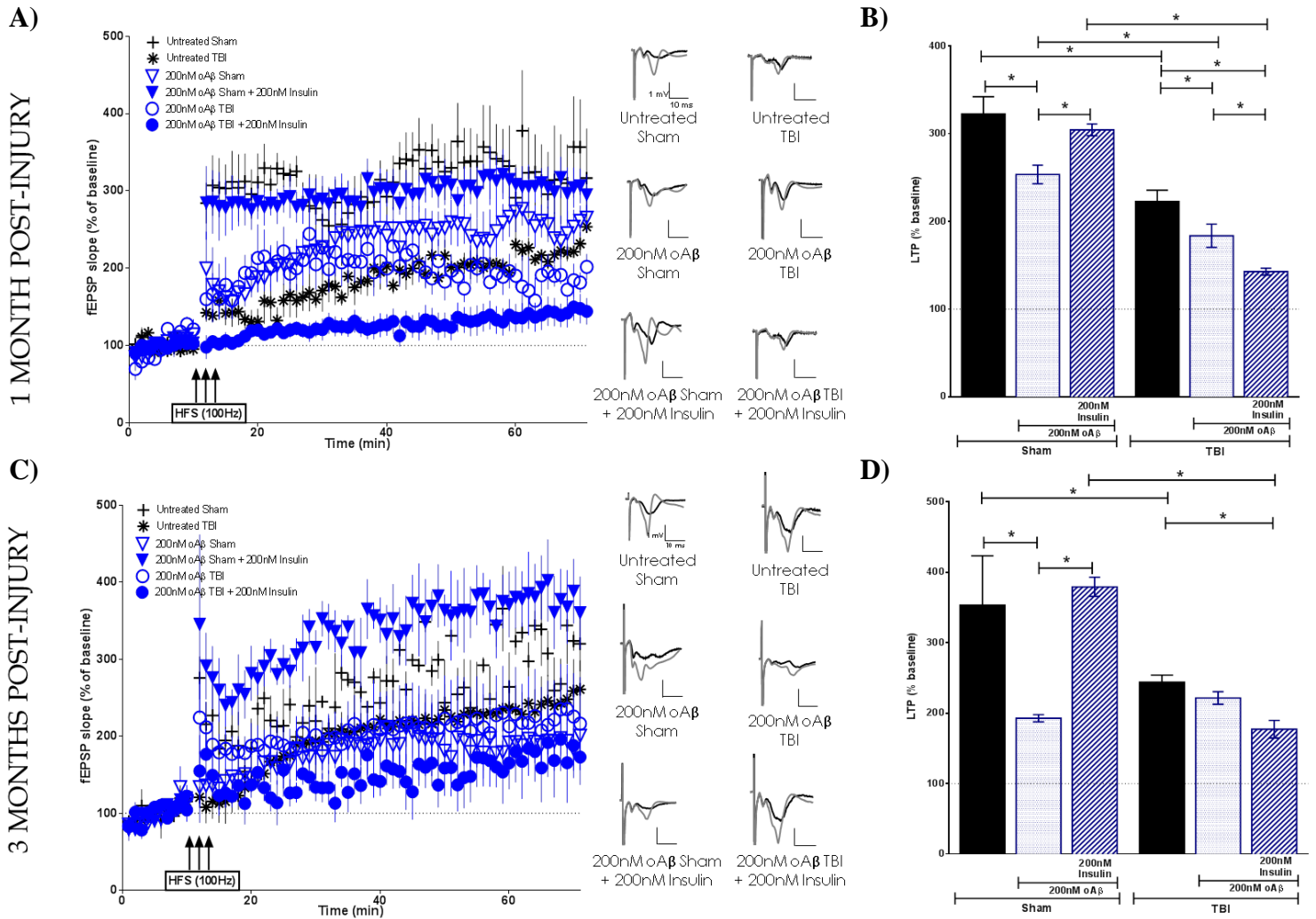


Figure 3.4: Electrophysiological analysis of A β oligomer-treatment in ipsilateral hippocampus.

Schaffer collateral field recordings were performed to determine oligomer-induced LTP impairment in slices from sham and TBI animals. Graphs of fEPSP's slopes as a percentage of the baseline with representative traces for each condition at A) 1 month post-injury and C) 3 months post-injury. Graphs showing the average of the fEPSP slope for the final 10 minutes (time points 60-70 minutes post high frequency stimulation) as an indication of LTP for each condition at B) 1 month post-injury and D) 3 months post-injury. 1 MPI n= 4 animals and 3-6 slices per condition; 3 MPI n= 3-5 animals and 3-7 slices per condition. One way ANOVA with Bonferroni's post hoc analysis was used to determine statistical significance. Error bars represent standard deviation. *p < 0.05

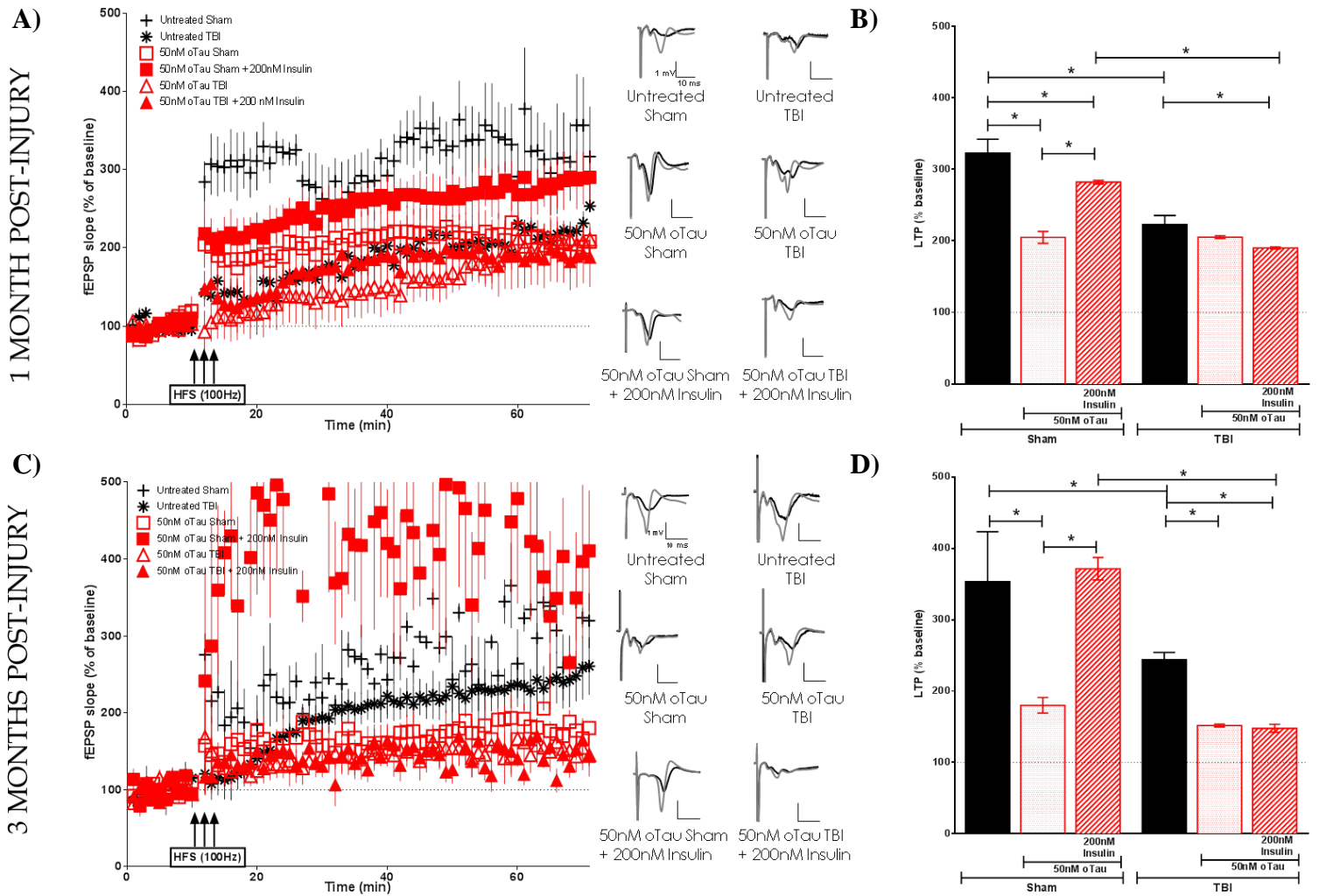


Figure 3.5: Electrophysiological analysis of tau oligomer-treatment in ipsilateral hippocampus.

Schaffer collateral field recordings were performed to determine oligomer-induced LTP impairment in slices from sham and TBI animals. Graphs of fEPSP's slopes as a percentage of the baseline with representative traces for each condition at A) 1 month post-injury and C) 3 months post-injury. Graphs showing the average of the fEPSP slope for the final 10 minutes (time points 60-70 minutes post high frequency stimulation) as an indication of LTP for each condition at B) 1 month post-injury and D) 3 months post-injury. 1 MPI n= 4 animals and 3-6 slices per condition; 3 MPI n= 3-5 animals and 3-7 slices per condition. One way ANOVA with Bonferroni's post hoc analysis was used to determine statistical significance. Error bars represent standard deviation. *p < 0.05

1 MONTH POST-INJURY

3 MONTHS POST-INJURY

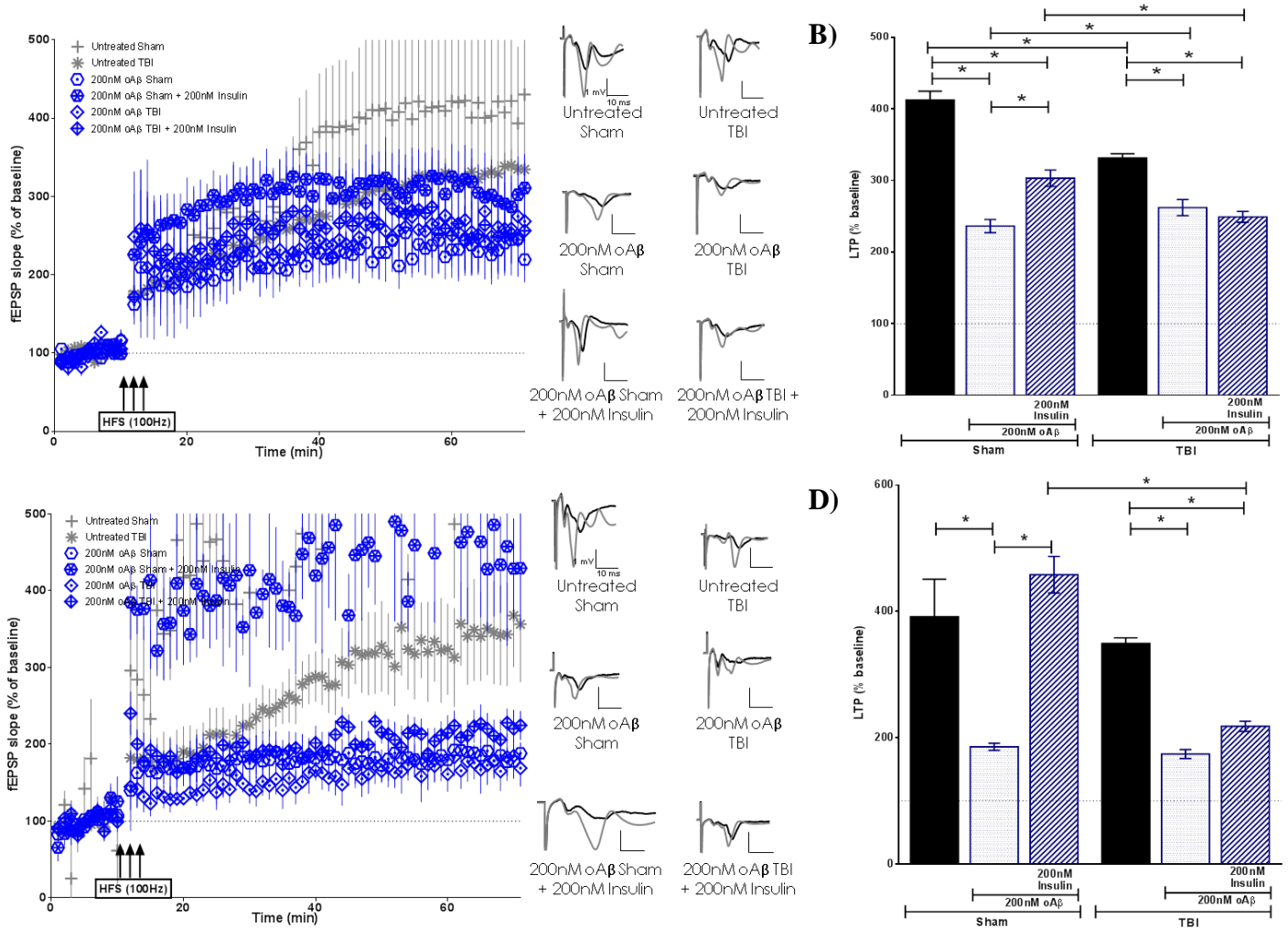


Figure 3.6: Electrophysiological analysis of Aβ oligomer-treatment in contralateral hippocampus.

Schaffer collateral field recordings were performed to determine oligomer-induced LTP impairment in slices from sham and TBI animals. Graphs of fEPSP's slopes as a percentage of the baseline with representative traces for each condition at A) 1 month post-injury and C) 3 months post-injury. Graphs showing the average of the fEPSP slope for the final 10 minutes (time points 60-70 minutes post high frequency stimulation) as an indication of LTP for each condition at B) 1 month post-injury and D) 3 months post-injury. 1 MPI n= 4 animals and 3-6 slices per condition; 3 MPI n= 3-5 animals and 3-7 slices per condition. One way ANOVA with Bonferroni's post hoc analysis was used to determine statistical significance. Error bars represent standard deviation. *p < 0.05

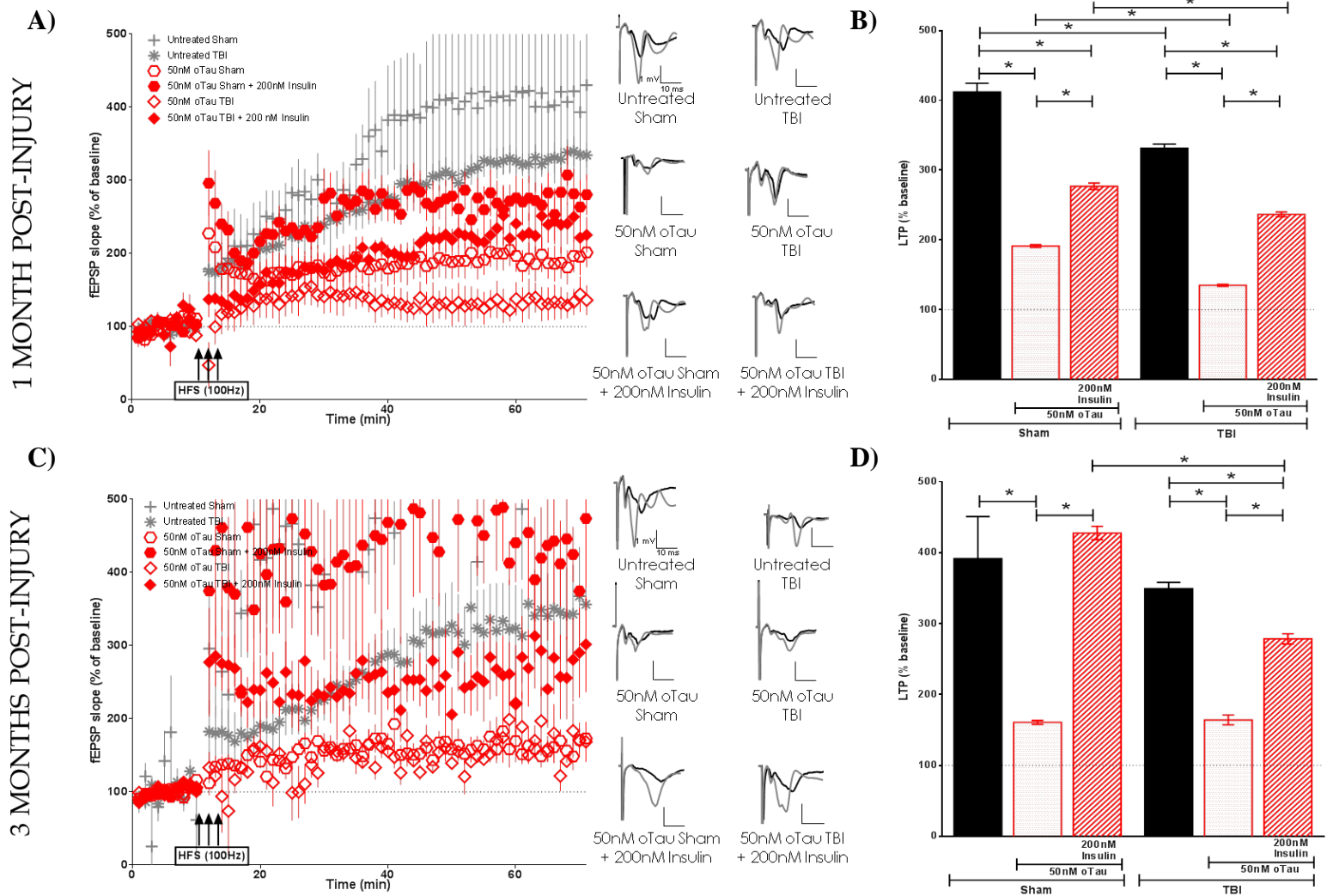


Figure 3.7: Electrophysiological analysis of tau oligomer-treatment in contralateral hippocampus.

Schaffer collateral field recordings were performed to determine oligomer-induced LTP impairment in slices from sham and TBI animals. Graphs of fEPSP's slopes as a percentage of the baseline with representative traces for each condition at A) 1 month post-injury and C) 3 months post-injury. Graphs showing the average of the fEPSP slope for the final 10 minutes (time points 60-70 minutes post high frequency stimulation) as an indication of LTP for each condition at B) 1 month post-injury and D) 3 months post-injury. 1 MPI n= 4 animals and 3-6 slices per condition; 3 MPI n= 3-5 animals and 3-7 slices per condition. One way ANOVA with Bonferroni's post hoc analysis was used to determine statistical significance. Error bars represent standard deviation. *p < 0.05

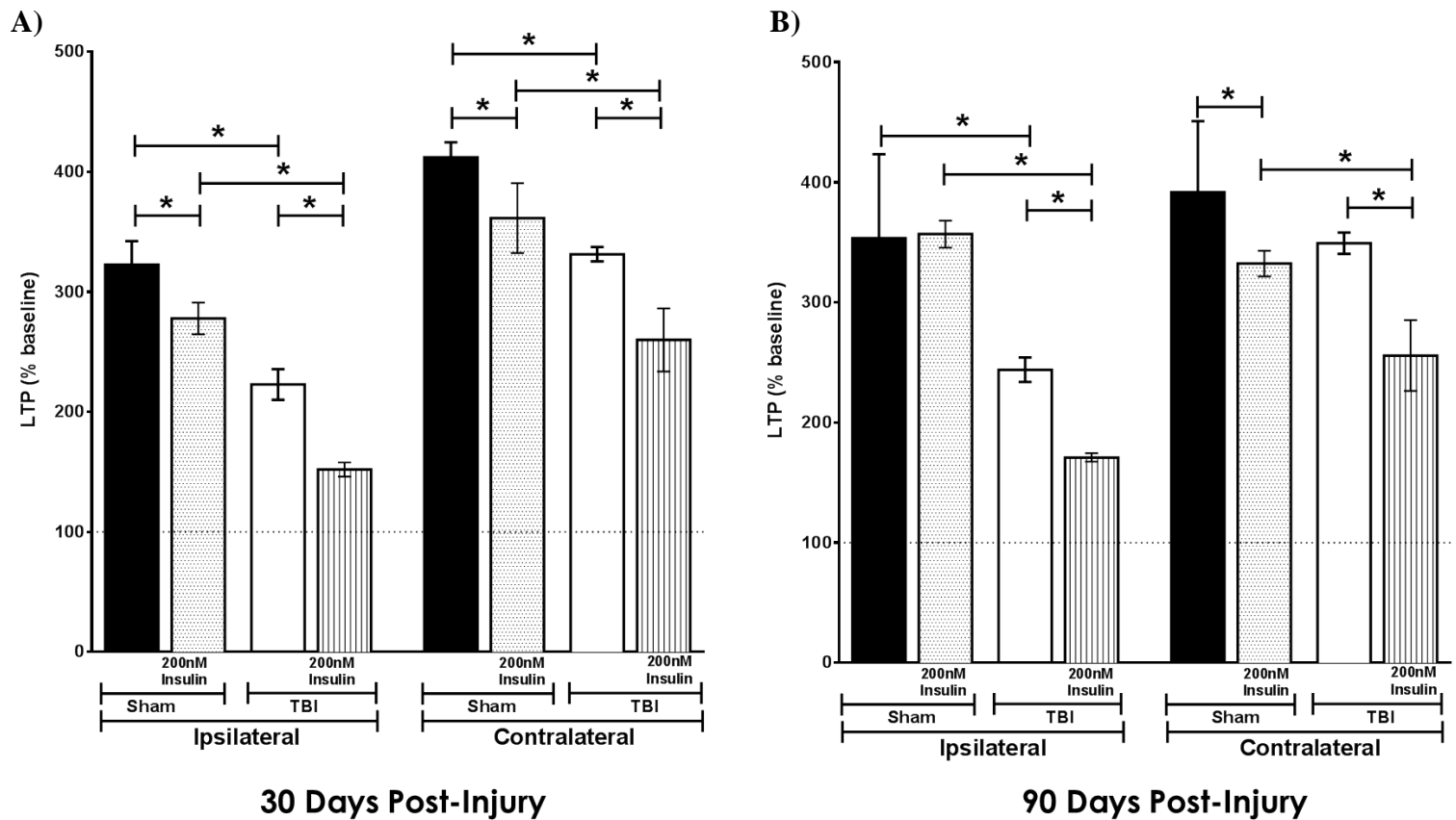


Figure 3.8: Electrophysiological analysis of insulin-treatment alone in ipsilateral and contralateral hippocampi.

Schaffer collateral field recordings were performed to determine the effect of a 200nM insulin treatment on LTP in slices from sham and TBI animals. Graphs showing the average of the fEPSP slope for the final 10 minutes (time points 60-70 minutes post high frequency stimulation) as an indication of LTP at A) 1 month post-injury and B) 3 months post-injury. 1 MPI n= 4 animals and 3-6 slices per condition; 3 MPI n= 3-5 animals and 3-7 slices per condition. One way ANOVA with Bonferroni's post hoc analysis was used to determine statistical significance. Error bars represent standard deviation. *p < 0.05

WHAT COULD BE CAUSING THE BENEFIT IN LTP BY INSULIN IN THE PRESENCE OF OLIGOMERS?

Although my *ex vivo* binding studies as well as the electrophysiology results did not suggest that there is an increase in oligomer binding after TBI, to try and determine why insulin treatment was not able to provide a protection against the A β -induced LTP

depression in TBI animals, I wanted to determine if this insulin treatment is capable of decreasing the amount of A β binding in non-insulin resistant animals (in normal/healthy physiology) using similar conditions as those used for my electrophysiological experiments. To accomplish this, I used brain slices from naïve, wild-type rats and challenged with 2.5 μ M A β -oligomers with or without 200nM insulin for 1 hour at 37°C in an aerated tissue incubator, and I assessed A β -binding using flow cytometry on synaptosomes isolated from these slices (Figure 3.9). I did not detect any change in A β -binding using insulin treatment with this paradigm. Thus, the insulin phenomenon of blocking an A β -induced deficit in LTP in sham animals but not TBI animals cannot be explained by a decrease in A β -binding. Rather, this phenomenon may just be due to a more functionally resilient synapse of uninjured animals.

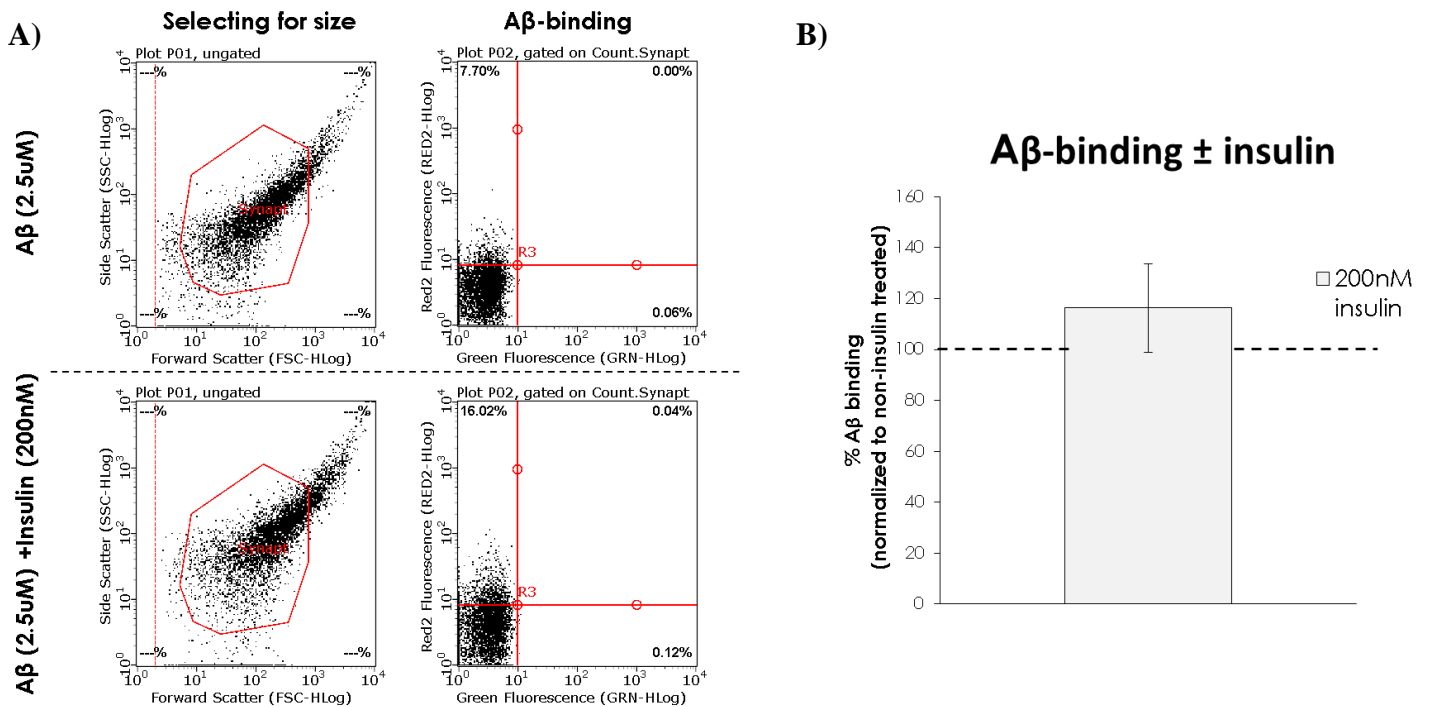


Figure 3.9: Insulin’s effect on A β binding.

Brain slices from naïve, wild-type rats were challenged with 2.5 μ M A β -oligomers \pm 200nM insulin for 1 hour to mimic the insulin stimulation used for the electrophysiology paradigm. A) Representative flow cytometry size gating and fluorescence of the A β -binding analysis performed on synaptosomes isolated from these slices. B) Quantification revealed no changes in A β -binding using insulin treatment with this paradigm. Graph representing mean \pm SEM. N=4 animals total, 11 slices per condition.

In a second attempt to investigate the mechanism through which insulin is acting on oligomer toxicity that is then failing in the case of TBI animals, I wanted to determine if insulin is able to change or enhance synaptic mitochondrial function and/or number using the same electrophysiological paradigm. I performed this experiment on brain slices from naïve, wild-type rats and stimulated slices for 1 hour at 37°C in an aerated tissue incubator with 200nM or 2.5µM insulin. I then isolated synaptosomes, labeled mitochondria, and analyzed mitochondrial membrane potential (Mitosense) and mitochondrial count (Mitotracker) using flow cytometry (Figure 3.10). Neither insulin treatment condition resulted in any changes in mitochondrial membrane potential or mitochondrial number versus insulin unstimulated slices; therefore, mitochondrial stimulation from insulin is not a mechanism that would be able to explain insulin’s ability to block oligomer-induced LTP suppression in sham but not TBI animals.

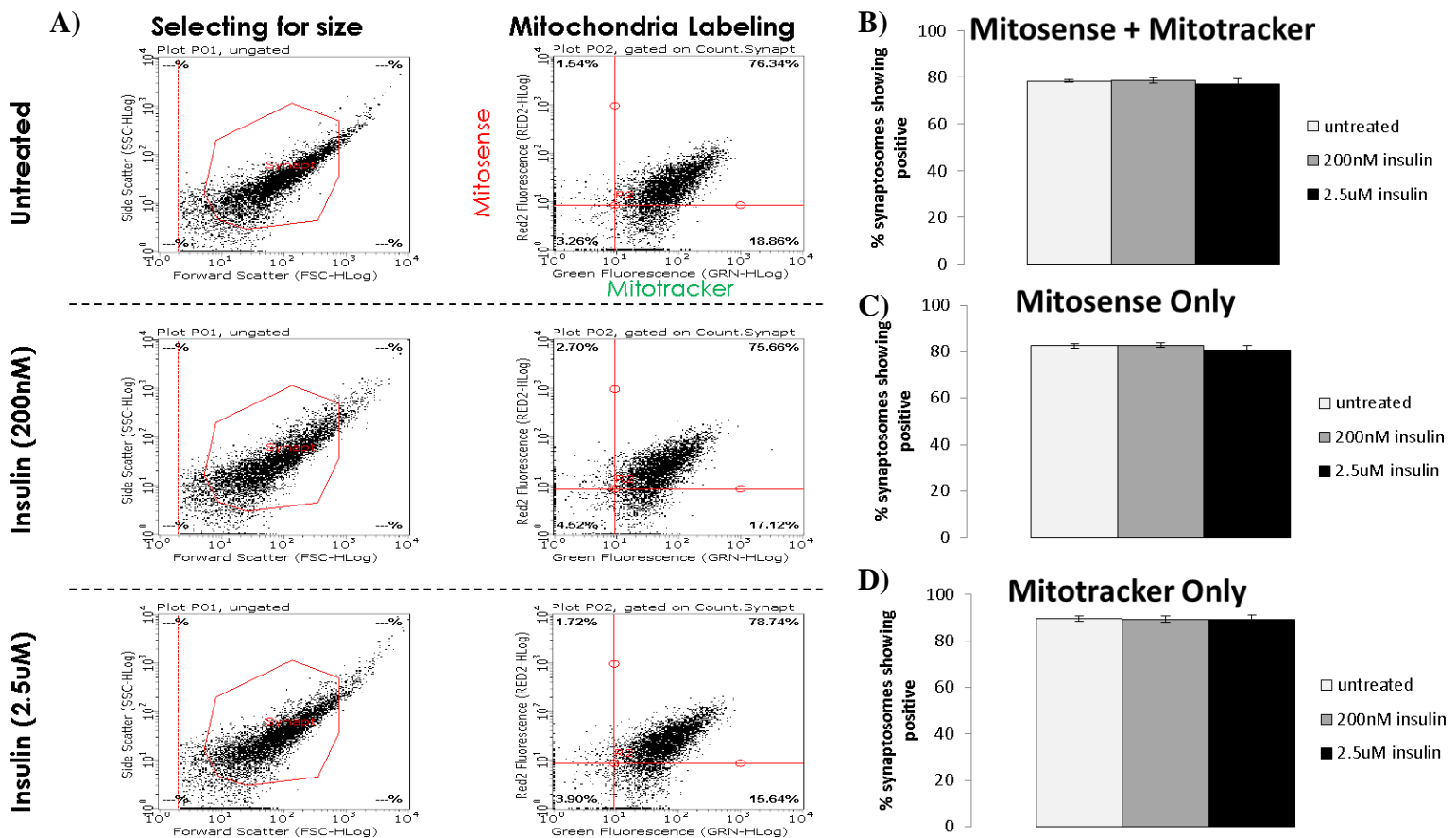


Figure 3.10: Mitochondria analysis after insulin stimulation.

Brain slices from naïve, wild-type rats were treated with either 200nM or 2.5 μ M of insulin for 1 hour to mimic the insulin stimulation used for the electrophysiology paradigm. A) Representative flow cytometry size gating and fluorescence of mitochondrial dyes on synaptosomes isolated from these slices. Quantification revealed no changes in B) mitochondria double labeled for Mitosense and Mitotracker, C) mitochondria analyzed for Mitosense alone, or D) mitochondria analyzed for Mitotracker alone indicating that neither insulin concentration altered mitochondria potential or mitochondria number using this paradigm. Graphs representing mean \pm SEM. Untreated n=10 slices, 200nM insulin n=10 slices, 2.5 μ M insulin n=9 slices. N=3 animals total.

Conclusions

Synaptic dysfunction caused by toxic A β and tau oligomeric species binding to the synapse and disrupting LTP properties is one of the initial events in AD leading to the cognitive decline that is associated with this disease [19,20]. Moreover, insulin signaling plays a role in synaptic health and function [45], and disruption of this normal functioning through insulin resistance at the synapse has been shown to contribute to A β -induced spine loss in AD [46,52]. While I previously found synaptic insulin resistance at 1 month and 3 months after injury, I found that this did not result in a difference in binding nor in LTP functional impairment by either A β or tau oligomers at either of these time points.

For my electrophysiology experiments, my results are consistent with those demonstrated by multiple groups showing that TBI results in impaired LTP, specifically in the hemisphere of injury (ipsilateral). Collectively, my results suggest that TBI does not generally affect vulnerability of synapses to A β or tau oligomer-induced LTP impairments to a higher degree from that seen in sham animals at 1 or 3 months after injury. Importantly though, the concurrence of insulin treatment with either of the oligomer challenges on hippocampal slices blocked the LTP impairment in both ipsilateral and contralateral slices from sham animals. This beneficial effect was not seen

for either A β or tau in the ipsilateral hippocampus of TBI animals at either time point as well as for A β impairment at either time point in the contralateral hippocampus. This data further corroborates the insulin resistance in the hippocampus after TBI shown by the *ex vivo* insulin stimulation analysis previously described and provides a valuable demonstration that even a significant administration of insulin cannot overcome this phenomenon to provide a protection that is normally afforded by insulin.

Additional experiments to investigate the possible mechanism through which insulin provides a benefit on oligomer-induced LTP impairment in healthy brain slices were unsuccessful. I found that insulin treatment using the electrophysiology paradigm did not decrease A β binding nor did the insulin treatment stimulate mitochondria to provide a functional benefit to synaptic health.

CHAPTER 4. GENERAL DISCUSSION AND CONCLUDING REMARKS

Alzheimer's disease (AD) is a devastating neurodegenerative disorder for which there is no resolving therapeutic intervention. While the initial cause of this disease is still unknown, there are many innate and event-triggered factors that increase the risk of developing AD. For example, type 2 diabetes (T2DM) [35–37], central insulin resistance [38], traumatic brain injury (TBI) [39–41], mitochondrial dysfunction [42,43], and neuroinflammation [44] are all known risk factors. In general, it is believed that synaptic dysfunction underlies the initiation and progression of AD [31,32]. It has become increasingly evident that oligomeric aggregates of both amyloid beta ($A\beta$) and tau contribute to this synaptic dysfunction that precedes the cognitive decline seen in AD [19,20]. Notably, decreased insulin receptor function increases synaptic sensitivity to the binding of and dysfunction caused by $A\beta$ [52], and insulin and insulin-sensitizing therapy has been shown to be effective for cognition in mouse models of AD as well as in patients with mild cognitive impairment (MCI) or early AD [52–55]. Furthermore, AD patients exhibit insulin resistance and decreased insulin signaling response in the hippocampus [51]. This multitude of evidence strongly indicates the existence of an intimate relationship between synaptic insulin responsiveness and neuronal sensitivity to AD neuropathology. Several groups have reported hyperglycemia after TBI and found that uncontrolled blood glucose levels lead to a poorer outcome and recovery [71,72]. Previous reports have also found an increased mortality after head injury in people with T2DM [73]. While one group has reported acute decreased insulin signaling in the CNS after TBI [74], no studies have investigated TBI-driven insulin resistance at the synapses, particularly in relation to synaptic vulnerability to $A\beta$ and tau.

Given these premises, the main goal of the present work was 1) to determine whether synaptic insulin responsiveness after TBI is dysregulated/decreased and 2) to

investigate related changes in synaptic vulnerability (including association to and functional disruption of synapses) to A β and tau oligomers.

In chapter 2, I used a moderate fluid-percussion injury (FPI) TBI model in rats to first determine if there were alterations in synaptic insulin responsiveness in the hippocampus at 2 days post-injury (DPI), 7 DPI, 1-month post-injury (MPI), and 3 MPI. I employed an *ex vivo* insulin stimulation method on isolated synaptosomes to directly assess insulin responsiveness of the insulin receptor (IR). I found the synaptic IR to have significantly decreased responsiveness as early as 7 DPI after lateral FPI. This injury-promoted insulin resistance of hippocampal synapses became chronic as deficits were observed up to 3 MPI in hippocampi from both hemispheres. While decreased insulin signaling in the CNS after acute mild TBI has previously been reported [74], this is the first demonstration that insulin signaling is chronically impaired after a moderate TBI. Additionally, direct evaluation of the synaptic IR, as performed here, bypasses assessment of the overall insulin signaling pathway and reveals that there is a chronic impairment at the level of the receptor.

In the ipsilateral hippocampus, my results revealed a significant increase in IR level at 3 MPI at the synapse which could be indicative of an attempted compensatory mechanism for the decreased insulin signaling here. However, these possible efforts were shown to be futile as I found that there is still a significantly decreased synaptic insulin response as well as decreased basal phosphorylation levels at this time point indicating that there is a chronic alteration in the response of the receptor that cannot be overcome by upregulation of the receptor itself. On the other hand, I did not observe any changes in synaptic IR level at any of the time points for the contralateral hemisphere, possibly suggesting that any attempt to compensate TBI-related synaptic insulin resistance is limited to the ipsilateral hemisphere.

In order to begin delving into the mechanisms responsible for driving the synaptic insulin resistance in TBI animals observed in my study, I determined levels of SOCS3.

SOCS3 is a member of the suppressor of cytokine signaling (SOCS) family that act as negative regulators of cytokine and growth factor signaling. SOCS3 protein expression can be induced by IL6 as well as IL10 and has been shown to negatively regulate insulin signaling [81]. Notably, SOCS3 expression has been found to be upregulated in the CNS of AD patients [89]. To investigate whether this protein could be playing a role in the synaptic insulin resistance I saw in my TBI model, I evaluated the levels of this protein in isolated synaptosomes from the ipsilateral and contralateral hippocampi at the 2 DPI, 7 DPI, 1 MPI, and 3 MPI time points.

In the ipsilateral hippocampus, I found a significantly increased level of SOCS3 at the synapse in TBI animals versus sham animals at 2 DPI, 7 DPI, and 1 MPI as well as a trend toward increased levels at 3 MPI. Since increased levels of SOCS3 occur as early as 2 DPI, prior to onset of synaptic insulin resistance that was observed starting only at 7DPI, increased SOCS3 levels could potentially be a driving factor in initiating the dysregulation and insulin resistance ensuing at the synapses after TBI. This upregulation could be a link between the chronic inflammation seen after TBI [61,90] and the insulin resistance that I have reported here in hippocampal synapses after injury.

In the contralateral hemisphere, however, I did not find altered levels of SOCS3 at the synapse at any of the time points. Since I still found synaptic insulin resistance beginning at 7DPI in this hemisphere too, it is possible that the two hemispheres suffer insulin resistance after TBI driven by different mechanisms, with SOCS3 playing a significant role only in the ipsilateral hemisphere. This hypothesis is supported by previous findings that gene expression level of IL-6 signal transducer (IL6ST), a protein involved in the complex for IL-6 signaling, was increased at an acute time point in the ipsilateral hemisphere and decreased in the contralateral hemisphere after a lateral, moderate TBI [91]. Although further studies are needed to establish the exact mechanisms of insulin resistance induction, this scenario would be consistent with prior reports describing opposing bilateral changes in proteins involved in TBI-related

secondary injuries after a unilateral TBI, specifically in pathways involved in cell death, survival, and inflammatory response [91,92]. Future studies could investigate alternative proteins that directly bind to the insulin receptor that I did not investigate in this study to determine whether they may be involved in the contralateral hemisphere's insulin resistance including alternative SOCS proteins, PTP1B, and Grb10/Grb14 adaptor proteins [81].

In chapter 3, I aimed to determine whether reduced synaptic insulin responsiveness in TBI animals was associated with altered synaptic vulnerability to extracellular A β and tau oligomers as well as oligomer-induced synaptic dysfunction. I used *ex vivo* binding methodologies to assess synaptic resistance/vulnerability to extracellular A β and tau oligomer binding. My data indicates that hippocampal synapses are not more susceptible to A β oligomer binding at the chronic time points of 1 month or 3 months after moderate FPI. Similar results were obtained using tau oligomers, whereby synapses were not more susceptible to tau oligomer binding at the chronic time points of 1 month or 3 months after TBI in either hemisphere after moderate FPI.

I further investigated synaptic vulnerability to oligomers by determining functional vulnerability through oligomer-induced LTP inhibition. Consistent with previous reports [93], I found basal LTP levels to be chronically impaired in the side of injury after lateral, moderate FPI through 3 MPI. My electrophysiological results are also consistent with my *ex vivo* binding experiments, suggesting that synaptic vulnerability to A β and tau oligomers is not increased after TBI as I did not find an increase in oligomer-induced LTP impairments compared to sham animals at 1 or 3 MPI.

To explore the relationship between synaptic dysfunction due to the oligomers and the hippocampal synaptic insulin resistance I found in my previous data, I additionally evaluated oligomer-induced LTP suppression with a concurrent insulin treatment. I found that insulin treatment provides protection against A β and tau-induced LTP functional impairments from both the ipsilateral and contralateral hemispheres from

sham animals. This is consistent with the literature showing that insulin inhibits A β -induced impairment of LTP using the same concentrations, animal species, and electrophysiological set-up used here [94]. This group suggested that this beneficial effect of insulin was due to a direct interaction of A β and insulin whereby insulin inhibits the formation of soluble A β oligomers thus preventing oligomer-induced LTP impairment in a manner that is independent of insulin receptor activation. While these two proteins may indeed interact to hinder A β oligomer formation, my results would argue against this conclusion since the beneficial effect of insulin that I observed in slices from sham animals was not seen against either A β or tau in ipsilateral hippocampal slices from TBI animals at both 1 and 3 MPI. Insulin treatment also did not block A β impairment at either time point in the contralateral hippocampus. I did find that insulin treatment partially blocked LTP reduction due to tau oligomers in the contralateral hippocampus at both chronic time points, yet I do not have an explanation for this phenomenon. This differential finding of insulin treatment in slices from sham and TBI animals suggests that activation of the insulin receptor does, in fact, contribute to the functional protection afforded by insulin against oligomer toxicity.

In an attempt to explain how insulin is able to alleviate oligomer-induced LTP suppression in the sham animals, a couple of mechanistic experiments were performed in hope that this would lead me to investigate if these mechanisms were impaired in TBI animals. However, even under standard conditions (using naïve rats), I did not find that insulin was able to block or reduce A β oligomer binding in hippocampal slices with this paradigm. While the work published under Dr. De Felice has demonstrated that insulin can block A β binding in primary hippocampal neuronal cultures, I have not been able to find this demonstration using either *ex vivo* slices or *in vivo*. My second attempt at an explanation evaluated whether insulin could stimulate mitochondria which could possibly cause a functional increase in cell health, thus providing a phenomenon to investigate in TBI animals. This attempt also proved unsuccessful as I did not find any mitochondrial

changes after an insulin treatment in naïve hippocampal slices using this paradigm. A third possibility involves the property of insulin to enhance NMDA receptor activity that has previously been described [49]. For this scenario, rather than blocking the LTP-suppression by oligomers, insulin could be involved in a compensatory mechanism that I am seeing as an increase in LTP. However, my electrophysiology data on insulin treatment alone on sham hippocampal slices suggests otherwise since insulin treatment either did not affect or, in some cases, even significantly decreased LTP. Therefore, a mechanism underscoring this beneficial effect seen by insulin on the LTP suppression by oligomers is still unknown. Further hypothesis and experiments need to be performed to give insight into this mechanism.

Overall, my results demonstrate that the insulin-resistant induced state after TBI is now unresponsive to the beneficial effect of insulin therapy as a treatment against impairments due to AD-pathology. This work demonstrates the importance of having refined treatments for AD based on a history of risk factors and demonstrates how these risk factors may impact the efficacy of particular treatments that are being investigated for AD in the general population.

Concluding Remarks

There are a multitude of future directions that can be taken from here to try to understand the complexity of the lateralization seen in the results and what this would mean for the susceptibility to neurodegeneration and compensation after TBI. Additionally, studies should investigate mechanisms and additional proteins to SOCS3 that may be acting upstream of the synaptic insulin resistance seen here. These could provide lucrative data on determining whether these upstream elements can be targeted acutely to prevent the resulting chronic insulin resistance. Further work is also needed to

determine the mechanism through which insulin can provide a protection against oligomer-induced toxicity (LTP suppression).

While there is consensus that intranasal insulin treatment benefits cognition by acting on neuronal insulin receptors to overcome resistance [95], some have pointed out that indirect pathways may influence cognition, and, thus, neuronal insulin signaling may not be needed for cognitive enhancement via insulin therapy [95]. Evidence such as increased regional cerebral blood flow and enhanced cognition in the insulin-resistant type 2 diabetes patients [96] supports this notion. In an opposing conclusion from animal models of type 2 diabetes where brain insulin resistance has been confirmed, insulin therapy acting on the hippocampus was found to be unsuccessful in improving cognition [97]. This could suggest that once brain insulin resistance has developed, insulin treatment may not be sufficient to overcome resistance at the cellular level [95]. My results would support this overall conclusion using a TBI model showing that brain insulin resistance would negate the efficacy of insulin as a therapy to provide protection against oligomer-induced synaptic dysfunction in injured animals as well as in AD patients with a history of TBI.

References

- [1] Alzheimer's Association (2019) *2019 ALZHEIMER'S DISEASE FACTS AND FIGURES Includes a Special Report on Alzheimer's Detection in the Primary Care Setting: Connecting Patients and Physicians*.
- [2] Strassnig M, Ganguli M (2005) About a Peculiar Disease of the Cerebral Cortex: Alzheimer's Original Case Revisited. *Psychiatry* **September**, 30–33.
- [3] Selkoe DJ, Hardy J (2016) The amyloid hypothesis of Alzheimer's disease at 25 years. *EMBO Mol. Med.* **8**, 595–608.
- [4] Baumgart M, Snyder HM, Carrillo MC, Fazio S, Kim H, Johns H (2015) Summary of the evidence on modifiable risk factors for cognitive decline and dementia: A population-based perspective. *Alzheimer's Dement.* **11**, 718–726.
- [5] Dorszewska J, Prendecki M, Oczkowska A, Dezor M, Kozubski W (2016) Molecular Basis of Familial and Sporadic Alzheimer's Disease. *Curr. Alzheimer Res.* **13**, 1–12.
- [6] Schmidt V, Carlo A-S, Willnow TE (2014) Apolipoprotein E receptor pathways in Alzheimer disease. *WIREs Syst. Biol. Med.* **6**, 255–270.
- [7] Kim DH, Gim J-A, Yeo SH, Kim H-S (2017) Integrated late onset Alzheimer's disease (LOAD) susceptibility genes: Cholesterol metabolism and trafficking perspectives. *Gene* **597**, 10–16.
- [8] Querfurth HW, Laferla FM (2010) Alzheimer's disease. *N Engl J Med* **362**, 329–344.
- [9] Sachdev PS, Blacker D, Blazer DG, Ganguli M, Jeste D V., Paulsen JS, Petersen RC (2014) Classifying neurocognitive disorders: The DSM-5 approach. *Nat. Rev. Neurol.* **10**, 634–642.
- [10] Masters CL, Bateman R, Blennow K, Rowe CC, Sperling RA, Cummings JL (2015) Alzheimer's disease. *Nat. Rev. Dis. Prim.* **1**, 15056.

- [11] Yaari R, Corey-Bloom J (2007) Alzheimer's Disease. *Semin. Neurol.* **27**, 32–41.
- [12] Selkoe DJ (2001) Alzheimer's Disease: Genes, Proteins, and Therapy. *Physiol. Rev.* **81**, 741–766.
- [13] Haass C, Kaether C, Thinakaran G, Sisodia S (2012) Trafficking and proteolytic processing of APP. *Cold Spring Harb. Perspect. Med.* **2**, a006270.
- [14] Kang J, Lemaire HG, Unterbeck A, Salbaum JM, Masters CL, Grzeschik KH, Multhaup G, Beyreuther K, Müller-Hill B (1987) The precursor of Alzheimer's disease amyloid A4 protein resembles a cell-surface receptor. *Nature* **325**, 733–736.
- [15] Wang Y, Mandelkow E (2016) Tau in physiology and pathology. *Nat. Rev. Neurosci.* **17**, 5–21.
- [16] Ross CA, Poirier MA (2005) What is the role of protein aggregation in neurodegeneration? *Nat. Rev. Mol. Cell Biol.* **6**, 891–898.
- [17] Buée L, Bussièrè T, Buée-Scherrer V, Delacourte A, Hof PR (2000) Tau protein isoforms, phosphorylation and role in neurodegenerative disorders. *Brain Res. Rev.* **33**, 95–130.
- [18] Kotler SA, Walsh P, Brender JR, Ramamoorthy A (2014) Differences between amyloid- β aggregation in solution and on the membrane: Insights into elucidation of the mechanistic details of Alzheimer's disease. *Chem. Soc. Rev.* **43**, 6692–6700.
- [19] Fa M, Puzzo D, Piacentini R, Staniszewski A, Zhang H, Baltrons MA, Li Puma DD, Chatterjee I, Li J, Saeed F, Berman HL, Ripoli C, Gulisano W, Gonzalez J, Tian H, Costa JA, Lopez P, Davidowitz E, Yu WH, Haroutunian V, Brown LM, Palmeri A, Sigurdsson EM, Duff KE, Teich AF, Honig LS, Sierks M, Moe JG, D'Adamio L, Grassi C, Kanaan NM, Fraser PE, Arancio O (2016) Extracellular Tau Oligomers Produce An Immediate Impairment of LTP and Memory. *Sci. Rep.* **6**,.
- [20] Puzzo D, Piacentini R, Fa M, Gulisano W, Li Puma DD, Staniszewski A, Zhang H, Tropea MR, Cocco S, Palmeri A, Fraser P, D'Adamio L, Grassi C, Arancio O (2017) LTP and memory impairment caused by extracellular A β and tau oligomers is APP- dependent. *Elife* **6**,.

- [21] Kaye R, Head E, Thompson JL, McIntire TM, Milton SC, Cotman CW, Glabe CG (2003) Common Structure of Soluble Amyloid Oligomers Implies Common Mechanism of Pathogenesis. *Science* (80-.). **300**, 486–489.
- [22] Knowles TPJ, Vendruscolo M, Dobson CM (2014) The amyloid state and its association with protein misfolding diseases. *Nat Rev Mol Cell Biol.* **15**, 384–396.
- [23] Spires-Jones TL, Attems J, Thal DR (2017) Interactions of pathological proteins in neurodegenerative diseases. *Acta Neuropathol.* **134**, 187–205.
- [24] Lacor PN, Buniel MC, Chang L, Fernandez SJ, Gong Y, Viola KL, Lambert MP, Velasco PT, Bigio EH, Finch CE, Krafft GA, Klein WL (2004) Synaptic Targeting by Alzheimer's-Related Amyloid beta Oligomers. *Neurobiol. Dis.* **24**, 10191–10200.
- [25] Lacor PN, Buniel MC, Furlow PW, Clemente AS, Velasco PT, Wood M, Viola KL, Klein WL (2007) Amyloid beta Oligomer-Induced Aberrations in Synapse Composition, Shape, and Density Provide a Molecular Basis for Loss of Connectivity in Alzheimer's Disease. *Neurobiol. Dis.* **27**, 796–807.
- [26] Spires TL, Meyer-Luehmann M, Stern EA, Mclean PJ, Skoch J, Nguyen PT, Bacskai BJ, Hyman BT (2005) Neurobiology of Disease Dendritic Spine Abnormalities in Amyloid Precursor Protein Transgenic Mice Demonstrated by Gene Transfer and Intravital Multiphoton Microscopy. *J. Neurosci.* **25**, 7278–7287.
- [27] Zhao D, Watson JB, Xie C-W, Xie Amyloid C-W (2004) Amyloid Prevents Activation of Calcium/Calmodulin-Dependent Protein Kinase II and AMPA Receptor Phosphorylation During Hippocampal Long-Term Potentiation. *J Neurophysiol* **92**, 2853–2858.
- [28] Dineley KT, Kaye R, Neugebauer V, Fu Y, Zhang W, Reese LC, Tagliavola G (2010) Amyloid- β oligomers impair fear conditioned memory in a calcineurin-dependent fashion in mice. *J. Neurosci. Res.* **88**, 2923–2932.
- [29] Wu H-Y, Hudry E, Hashimoto T, Kuchibhotla K, Rozkalne A, Fan Z, Spires-Jones T, Xie H, Arbel-Ornath M, Grosskreutz CL, Bacskai BJ, Hyman BT (2010) Amyloid Induces the Morphological Neurodegenerative Triad of Spine Loss, Dendritic Simplification, and Neuritic Dystrophies through Calcineurin Activation. *J. Neurosci.* **30**, 2636–2649.

- [30] Mohmmad Abdul H, Baig I, LeVine H, Guttmann RP, Norris CM (2011) Proteolysis of calcineurin is increased in human hippocampus during mild cognitive impairment and is stimulated by oligomeric Abeta in primary cell culture. *Aging Cell* **10**, 103–113.
- [31] Terry RD, Masliah E, Salmon DP, Butters N, DeTeresa R, Hill R, Hansen LA, Katzman R (1991) Physical basis of cognitive alterations in alzheimer's disease: Synapse loss is the major correlate of cognitive impairment. *Ann. Neurol.* **30**, 572–580.
- [32] Spires-Jones TL, Hyman BT (2014) The intersection of amyloid beta and tau at synapses in Alzheimer's disease. *Neuron* **82**, 756–771.
- [33] Golde TE, DeKosky ST, Galasko D (2018) Alzheimer's disease: The right drug, the right time. *Science* (80-.). **362**, 1250–1251.
- [34] Molinuevo JL, Ayton S, Batrla R, Bednar MM, Bittner T, Cummings J, Fagan AM, Hampel H, Mielke MM, Mikulskis A, O'Bryant S, Scheltens P, Sevigny J, Shaw LM, Soares HD, Tong G, Trojanowski JQ, Zetterberg H, Blennow K (2018) Current state of Alzheimer's fluid biomarkers. *Acta Neuropathol.* **136**, 821–853.
- [35] Veitch D, Friedl K, Weiner M (2013) Military Risk Factors for Cognitive Decline, Dementia and Alzheimer's Disease. *Curr. Alzheimer Res.* **10**, 907–930.
- [36] Campdelacreu J (2014) Parkinson's disease and Alzheimer disease: environmental risk factors. *Neurol. (English Ed.)* **29**, 541–549.
- [37] Blázquez E, Velázquez E, Hurtado-Carneiro V, Ruiz-Albusac JM (2014) Insulin in the brain: Its pathophysiological implications for states related with central insulin resistance, type 2 diabetes and alzheimer's disease. *Front. Endocrinol. (Lausanne)*. **5**,.
- [38] De La Monte SM (2012) *Brain Insulin Resistance and Deficiency as Therapeutic Targets in Alzheimer's Disease*.
- [39] Fleminger S, Oliver DL, Lovestone S, Rabe-Hesketh S, Giora A (2003) Head injury as a risk factor for Alzheimer's disease: The evidence 10 years on; a partial replication. *J. Neurol. Neurosurg. Psychiatry* **74**, 857–862.

- [40] Tran HT, LaFerla FM, Holtzman DM, Brody DL (2011) Controlled Cortical Impact Traumatic Brain Injury in 3xTg-AD Mice Causes Acute Intra-Axonal Amyloid- Accumulation and Independently Accelerates the Development of Tau Abnormalities. *J. Neurosci.* **31**, 9513–9525.
- [41] Washington PM, Villapol S, Burns MP (2016) Polypathology and dementia after brain trauma: Does brain injury trigger distinct neurodegenerative diseases, or should they be classified together as traumatic encephalopathy? *Exp. Neurol.* **275**, 381–388.
- [42] Swerdlow RH, Khan SM (2009) The Alzheimer ' s disease mitochondrial cascade hypothesis : An update. *Exp. Neurol.* **218**, 308–315.
- [43] Reddy PH, Manczak M, Mao P, Calkins MJ, Reddy AP, Shirendeb U (2010) Amyloid- β and mitochondria in aging and Alzheimer's disease: Implications for synaptic damage and cognitive decline. *J. Alzheimer's Dis.* **20**,.
- [44] Breunig JJ, Guillot-Sestier MV, Town T (2013) Brain injury, neuroinflammation and Alzheimer's disease. *Front. Aging Neurosci.* **5**,.
- [45] Zhao WQ, Alkon DL (2001) Role of insulin and insulin receptor in learning and memory. *Mol. Cell. Endocrinol.* **177**, 125–134.
- [46] Zhao W-Q, De Felice FG, Fernandez S, Chen H, Lambert MP, Quon MJ, Krafft GA, Klein WL (2008) Amyloid beta oligomers induce impairment of neuronal insulin receptors. *FASEB J.* **22**, 246–260.
- [47] Gray SM, Meijer RI, Barrett EJ (2014) Insulin regulates brain function, but how does it get there? *Diabetes* **63**, 3992–7.
- [48] Craft S, Baker LD, Montine TJ, Minoshima S, Watson GS, Claxton A, Arbuckle M, Callaghan M, Tsai E, Plymate SR, Green PS, Leverenz J, Cross D, Gerton B (2012) Intranasal Insulin Therapy for Alzheimer Disease and Amnesic Mild Cognitive Impairment. *Arch. Neurol.* **69**, 29–38.
- [49] Christie JM, Wenthold RJ, Monaghan DT (1999) Insulin Causes a Transient Tyrosine Phosphorylation of NR2A and NR2B NMDA Receptor Subunits in Rat Hippocampus. *J. Neurochem.* **72**, 1523–1528.

- [50] Wan Q, Xiong ZG, Man HY, Ackerley CA, Braunton J, Lu WY, Becker LE, MacDonald JF, Wang YT (1997) Recruitment of functional GABAA receptors to postsynaptic domains by insulin. *Nature* **388**, 686–690.
- [51] Talbot K, Wang HY, Kazi H, Han LY, Bakshi KP, Stucky A, Fuino RL, Kawaguchi KR, Samoyedny AJ, Wilson RS, Arvanitakis Z, Schneider JA, Wolf BA, Bennett DA, Trojanowski JQ, Arnold SE (2012) Demonstrated brain insulin resistance in Alzheimer’s disease patients is associated with IGF-1 resistance, IRS-1 dysregulation, and cognitive decline. *J. Clin. Invest.* **122**, 1316–1338.
- [52] De Felice FG, Vieira MNN, Bomfim TR, Decker H, Velasco PT, Lambert MP, Viola KL, Zhao W-Q, Ferreira ST, Klein WL (2009) Protection of synapses against Alzheimer’s-linked toxins: Insulin signaling prevents the pathogenic binding of A β oligomers. *Proc. Natl. Acad. Sci.* **106**, 1971–1976.
- [53] Reger MA, Watson GS, Green PS, Wilkinson CW, Baker LD, Cholerton B, Fishel MA, Plymate SR, Breitner JCS, DeGroot W, Mehta P, Craft S (2008) Intranasal insulin improves cognition and modulates β -amyloid in early AD. *Neurology* **70**, 440–448.
- [54] Rodriguez-Rivera J, Denner L, Dineley KT (2011) Rosiglitazone reversal of Tg2576 cognitive deficits is independent of peripheral gluco-regulatory status. *Behav. Brain Res.* **216**, 255–261.
- [55] Bedse G, Di Domenico F, Serviddio G, Cassano T (2015) Aberrant insulin signaling in Alzheimer’s disease: Current knowledge. *Front. Neurosci.* **9**, 204.
- [56] Taylor CA, Bell JM, Breiding MJ, Xu L (2017) Traumatic Brain Injury–Related Emergency Department Visits, Hospitalizations, and Deaths — United States, 2007 and 2013. *MMWR. Surveill. Summ.* **66**, 1–16.
- [57] Traumatic Brain Injury and Concussion.
- [58] National Institute of Neurological Disorders and Stroke, National Institutes of Health (2015) *Traumatic Brain Injury - Hope through Research*.
- [59] What are the treatments for TBI?, Last updated 2016, Accessed on 2016.
- [60] Chauhan NB (2014) Chronic neurodegenerative consequences of traumatic brain

injury. *Restor. Neurol. Neurosci.* **32**, 337–365.

- [61] Walker KR, Tesco G (2013) Molecular mechanisms of cognitive dysfunction following traumatic brain injury. *Front. Aging Neurosci.* **5**, 29.
- [62] Gentleman SM, Greenberg BD, Savage MJ, Noori M, Newman SJ, Roberts GW, Griffin WS, Graham DI (1997) A beta 42 is the predominant form of amyloid beta-protein in the brains of short-term survivors of head injury. *Neuroreport* **8**, 1519–22.
- [63] DeKosky ST, Abrahamson EE, Ciallella JR, Paljug WR, Wisniewski SR, Clark RSB, Ikonovic MD (2007) Association of Increased Cortical Soluble A β 42 Levels With Diffuse Plaques After Severe Brain Injury in Humans. *Arch. Neurol.* **64**, 541.
- [64] Uryu K, Chen X-H, Martinez D, Browne KD, Johnson VE, Graham DI, M-Y Lee V, QTrojanowski J, Smith DH (2007) Multiple Proteins Implicated in Neurodegenerative Diseases Accumulate in Axons After Brain Trauma in Humans. *Exp Neurol* **208**, 185–192.
- [65] Washington PM, Morffy N, Parsadanian M, Zapple DN, Burns MP (2014) Experimental Traumatic Brain Injury Induces Rapid Aggregation and Oligomerization of Amyloid-Beta in an Alzheimer's Disease Mouse Model. *J. Neurotrauma* **31**, 125–134.
- [66] Graham DI, Gentleman SM, Nicoll JA, Royston MC, McKenzie JE, Roberts GW, Griffin WS (1996) Altered beta-APP metabolism after head injury and its relationship to the aetiology of Alzheimer's disease. *Acta Neurochir. Suppl.* **66**, 96–102.
- [67] Blasko I, Beer R, Bigl M, Apelt J, Franz G, Rudzki D, Ransmayr G, Kampfl A, Schliebs R (2004) Experimental traumatic brain injury in rats stimulates the expression, production and activity of Alzheimer's disease b-secretase (BACE-1). *J Neural Transm* **111**, 523–536.
- [68] Chen X-H, Siman R, Iwata A, Meaney DF, Trojanowski JQ, Smith DH (2004) Long-term accumulation of amyloid-beta, beta-secretase, presenilin-1, and caspase-3 in damaged axons following brain trauma. *Am. J. Pathol.* **165**, 357–71.
- [69] Yu F, Zhang Y, Chuang D-M (2012) Lithium reduces BACE1 overexpression, β

amyloid accumulation, and spatial learning deficits in mice with traumatic brain injury. *J. Neurotrauma* **29**, 2342–51.

- [70] Kochanek PM, Bramlett HM, Shear DA, Dixon CE, Mondello S, Dietrich WD, Hayes RL, Wang KKW, Poloyac SM, Empey PE, Povlishock JT, Mountney A, Browning M, Deng-Bryant Y, Yan HQ, Jackson TC, Catania M, Glushakova O, Richieri SP, Tortella FC (2016) Synthesis of Findings, Current Investigations, and Future Directions: Operation Brain Trauma Therapy. *J. Neurotrauma* **33**, 606–614.
- [71] Cerecedo-López CD, Kim-Lee JH, Hernandez D, Acosta SA, Borlongan C V. (2014) Insulin-associated neuroinflammatory pathways as therapeutic targets for traumatic brain injury. *Med. Hypotheses* **82**, 171–174.
- [72] Shi J, Dong B, Mao Y, Guan W, Cao J, Zhu R, Wang S (2015) Review: Traumatic brain injury and hyperglycemia, a potentially modifiable risk factor. *Oncotarget* **7**, 71052–71061.
- [73] Ley EJ, Srour MK, Clond MA, Barnajian M, Tillou A, Mirocha J, Salim A (2011) Diabetic Patients With Traumatic Brain Injury: Insulin Deficiency Is Associated With Increased Mortality. *J. Trauma Inj. Infect. Crit. Care* **70**, 1141–1144.
- [74] Karelina K, Sarac B, Freeman LM, Gaier KR, Weil ZM (2016) Traumatic brain injury and obesity induce persistent central insulin resistance. *Eur. J. Neurosci.* **43**, 1034–1043.
- [75] Verdile G, Fuller SJ, Martins RN (2015) The role of type 2 diabetes in neurodegeneration. *Neurobiol. Dis.* **84**, 22–38.
- [76] Sallam HS, Tumurbaatar B, Zhang WR, Tuvdendorj D, Chandalia M, Tempia F, Laezza F, Taglialatela G, Abate N (2015) Peripheral adipose tissue insulin resistance alters lipid composition and function of hippocampal synapses. *J. Neurochem.* **133**, 125–133.
- [77] Kabadi S V., Hilton GD, Stoica BA, Zapple DN, Faden AI (2010) Fluid-percussion-induced traumatic brain injury model in rats. *Nat. Protoc.* **5**, 1552–1563.
- [78] Franklin W, Taglialatela G (2016) A method to determine insulin responsiveness in synaptosomes isolated from frozen brain tissue. *J. Neurosci. Methods* **261**, 128–134.

- [79] Puig KL, Kulas JA, Franklin W, Rakoczy SG, Taglialatela G, Brown-Borg HM, Combs CK (2016) The Ames dwarf mutation attenuates Alzheimer's disease phenotype of APP/PS1 mice. *Neurobiol. Aging* **40**, 22–40.
- [80] Hsu WCJ, Wildburger NC, Haidacher SJ, Nenov MN, Folorunso O, Singh AK, Chesson BC, Franklin WF, Cortez I, Sadygov RG, Dineley KT, Rudra JS, Taglialatela G, Lichti CF, Denner L, Laezza F (2017) PPARgamma agonists rescue increased phosphorylation of FGF14 at S226 in the Tg2576 mouse model of Alzheimer's disease. *Exp. Neurol.* **295**, 1–17.
- [81] Boucher J, Kleinridders A, Ronald Kahn C (2014) Insulin receptor signaling in normal and insulin-resistant states. *Cold Spring Harb. Perspect. Biol.* **6**,.
- [82] Reese LC, Zhang WR, Dineley KT, Kaye R, Taglialatela G (2008) Selective induction of calcineurin activity and signaling by oligomeric amyloid beta. *Aging Cell* **7**, 824–835.
- [83] Comerota MM, Krishnan B, Taglialatela G (2017) Near infrared light decreases synaptic vulnerability to amyloid beta oligomers. *Sci. Rep.* **7**,.
- [84] Lasagna-Reeves CA, Castillo-Carranza DL, Guerrero-Muñoz MJ, Jackson GR, Kaye R (2010) Preparation and characterization of neurotoxic tau oligomers. *Biochemistry* **49**, 10039–10041.
- [85] Comerota MM, Tumurbaatar B, Krishnan B, Kaye R, Taglialatela G (2018) Near Infrared Light Treatment Reduces Synaptic Levels of Toxic Tau Oligomers in Two Transgenic Mouse Models of Human Tauopathies. *Mol. Neurobiol.*
- [86] Krishnan B, Kaye R, Taglialatela G (2018) Elevated phospholipase D isoform 1 in Alzheimer's disease patients' hippocampus: Relevance to synaptic dysfunction and memory deficits. *Alzheimer's Dement. Transl. Res. Clin. Interv.* **4**, 89–102.
- [87] Presley AD, Fuller KM, Arriaga EA (2003) MitoTracker Green labeling of mitochondrial proteins and their subsequent analysis by capillary electrophoresis with laser-induced fluorescence detection. *J Chromatogr B Anal. Technol Biomed Life Sci* **793**, 141–150.
- [88] Mattiasson G, Friberg H, Hansson M, Elmér E, Wieloch T (2003) Flow cytometric analysis of mitochondria from CA1 and CA3 regions of rat hippocampus reveals differences in permeability transition pore activation. *J. Neurochem.* **87**, 532–544.

- [89] Cao L, Wang Z, Wan W (2018) Suppressor of cytokine signaling 3: Emerging role linking central insulin resistance and Alzheimer's disease. *Front. Neurosci.* **12**, 417.
- [90] Ramlackhansingh AF, Brooks DJ, Greenwood RJ, Bose SK, Turkheimer FE, Kinnunen KM, Gentleman S, Heckemann RA, Gunanayagam K, Gelosa G, Sharp DJ (2011) Inflammation after trauma: Microglial activation and traumatic brain injury. *Ann. Neurol.* **70**, 374–383.
- [91] White TE, Ford GD, Surles-Zeigler MC, Gates AS, Laplaca MC, Ford BD (2013) Gene expression patterns following unilateral traumatic brain injury reveals a local pro-inflammatory and remote anti-inflammatory response. *BMC Genomics* **14**, 282.
- [92] White TE, Surles-Zeigler MC, Ford GD, Gates AS, Davids B, Distel T, LaPlaca MC, Ford BD (2016) Bilateral gene interaction hierarchy analysis of the cell death gene response emphasizes the significance of cell cycle genes following unilateral traumatic brain injury. *BMC Genomics* **17**, 130.
- [93] Titus DJ, Wilson NM, Freund JE, Carballosa MM, Sikah KE, Furones C, Dietrich WD, Gurney ME, Atkins CM (2016) Chronic Cognitive Dysfunction after Traumatic Brain Injury Is Improved with a Phosphodiesterase 4B Inhibitor. *J Neurosci* **36**, 7095–108.
- [94] Lee CC, Kuo YM, Huang CC, Hsu K Sen (2009) Insulin rescues amyloid β -induced impairment of hippocampal long-term potentiation. *Neurobiol. Aging* **30**, 377–387.
- [95] Stanley M, Macauley SL, Holtzman DM (2016) Changes in insulin and insulin signaling in Alzheimer's disease: cause or consequence? *J. Exp. Med.* **213**, 1375–1385.
- [96] Novak V, Milberg W, Hao Y, Munshi M, Novak P, Galica A, Manor B, Roberson P, Craft S, Abduljalil A (2014) Enhancement of vasoreactivity and cognition by intranasal insulin in type 2 diabetes. *Diabetes Care* **37**, 751–759.
- [97] McNay EC, Ong CT, McCrimmon RJ, Cresswell J, Bogan JS, Sherwin RS (2010) Hippocampal memory processes are modulated by insulin and high-fat-induced insulin resistance. *Neurobiol. Learn. Mem.* **93**, 546–553.

Vita

PRESENT POSITION AND ADDRESS:

Graduate Assistant
Univ. of Texas Medical Branch at Galveston 10.150 Medical Research Bldg.
301 University Blvd., Galveston, Texas, 77555

BIOGRAPHICAL:

Date and Place of Birth: June 12, 1991. Houston, Texas
Tel.: (832) 338-8849
E-mail: whfrankl@utmb.edu

EDUCATION:

- 11/2015 to present: Predoctoral Research Fellow
Combined Graduate Program with the University of Palermo, IT
Department of Neuroscience and Cell Biology and Biomedicina e
Neuroscienze
The University of Texas Medical Branch, Galveston, Texas
- 08/2013 to present: Predoctoral Research Fellow
Neuroscience Graduate Program
Department of Neuroscience and Cell Biology
The University of Texas Medical Branch, Galveston, Texas
- 08/2009-08/2013: Bachelors of Arts in Biochemistry, Minor equivalent in French The
University of Texas, Austin, Texas

PROFESSIONAL AND TEACHING EXPERIENCE:

Professional Experience:

- 08/2013 to present: Predoctoral Research Fellow, Dept. of Neuroscience
The University of Texas Medical Branch, Galveston, Texas
Mentor: Giulio Tagliatela
Project: Susceptibility of synapses to AD pathology after traumatic brain injury.
Mechanisms linking Alzheimer's disease and Traumatic Brain Injury.
- 08/2012-12/2012: Undergraduate Teaching Assistant, Research Methods class The University of
Texas, Austin, Texas
- 08/2011-12/2011: Undergraduate Teaching Assistant, Research Methods class The University of
Texas, Austin, Texas
- 01/2011-05/2011: Undergraduate Research Assistant, Nanomaterials for Chemical Catalysis
Laboratory The University of Texas, Austin, Texas

Teaching and Mentoring Experience:

- 01/2017-04/2017: Small-group discussion Facilitator, Molecular Biology and Genetics graduate
class The University of Texas Medical Branch, Galveston, Texas
- 01/2016-04/2016: Small-group discussion Facilitator, Molecular Biology and Genetics graduate
class The University of Texas Medical Branch, Galveston, Texas
- 03/2015-04/2015: Laboratory Teaching Assistant, Neuroscience of Human Behavior medical
school class The University of Texas Medical Branch, Galveston, Texas

- 08/2012-12/2012: Undergraduate Teaching Assistant, Research Methods class The University of Texas, Austin, Texas
- 08/2011-12/2011: Undergraduate Teaching Assistant, Research Methods class The University of Texas, Austin, Texas
- 08/2011-12/2011: Mentor and Tutor for solution-focused high school initiative program Garza High School, Austin, Texas
- 01/2011-05/2011: Mentor for undergraduate students, Nanomaterials for Chemical Catalysis Laboratory The University of Texas, Austin, Texas

MEMBERSHIPS IN SCIENTIFIC SOCIETIES/PROFESSIONAL ORGANIZATIONS:

International:

- 10/2016 to present: Sigma Xi: The Scientific Research Society
- 08/2016 to present: American Association for the Advancement of Science (Member No.: 20345624)
- 05/2014 to present: Society for Neuroscience, (Member No.: 210568137)

Local:

- 08/2013 to present: Society for Neuroscience, UTMB chapter
- 08/2011-05/2013: Women in Medicine, The University of Texas, Austin, Texas

AWARDS AND HONORS:

- 12/2018 Edith and Robert Zinn Presidential Scholarship, UTMB, Galveston, Texas
- 10/2018: Excellence in Basic Science and Neuroscience Research Poster Award in Student Category, 22nd Annual Forum on Aging, Galveston, Texas
- 07/2018: First Place Presentation Award in Pain and Trauma Category, 3rd Annual Neuroscience Graduate Program Student Symposium, Galveston, Texas
- 03/2018: NIH/NIA F31 Ruth L. Kirschstein Predoctoral Fellowship
- 11/2017: Rose and Harry Walk Memorial Award, UTMB, Galveston, Texas
- 2017: Elected Honoree into Who's Who Among Students In American Universities & Colleges, UTMB, Galveston, Texas
- 12/2016: Second Place Poster Presentation Award, Neuroscience and Cell Biology 2016 Annual Research Retreat, Galveston, Texas
- 11/2016: James E. Beall II Memorial Award, UTMB, Galveston, Texas
- 08/2016: American Association for the Advancement of Science (AAAS)/ Science Program for Excellence in Science
- 06/2016: Neuroscience Graduate Program Service Excellence Award, UTMB, Galveston, Texas
- 08/2012-05/2013: University Honors, The University of Texas, Austin, Texas
- 08/2011-12/2011: University Honors, The University of Texas, Austin, Texas
- 01/2010-05/2010: University Honors, The University of Texas, Austin, Texas

LEADERSHIP RESPONSIBILITIES:

UTMB:

10/2015-04/2016: GSBS Senator, Student Government Association
4/2018, 3/2017, 10/2016,
3/2015,10/2014,3/2014:Station leader, Brain Fair hosted by the Society for Neuroscience
Galveston chapter

Departmental:

06/2016: Chair of the “5th year and above” session, Neuroscience Graduate Program
Symposium
09/2015-08/2016: President, Neuroscience Graduate Program Student Organization
09/2014-08/2015: Vice President, Neuroscience Graduate Program Student Organization

Other:

06/2018 to present: Junior Director, St. Vincent’s Student Clinic, Galveston, Texas
01/2015 to present: Establishment of Fluid Percussion Traumatic Brain Injury on rats in Dr.
Tagliatela’s lab (writing and securing IACUC protocol approval in addition to
obtaining surgery room approval)
The University of Texas Medical Branch, Galveston, Texas
08/2010-05/2013: Women’s Gymnastics President, University of Texas at Austin Gymnastics Club
The University of Texas, Austin, Texas
08/2011-12/2011: Committee member for the Hope Africa Fundraiser, Women in Medicine
Organization The University of Texas, Austin, Texas

BIBLIOGRAPHY:

Publications:

1. **Franklin W.**, Tagliatela G. "A method to determine insulin responsiveness in synaptosomes isolated from frozen brain tissue." J Neurosci Methods. 2016 Mar 1; 261:128-34.
2. Puig K.L., Kulas J.A., **Franklin W.**, Rakoczy S.G., Tagliatela G., Brown-Borg H.M., Combs C.K. "The Ames Dwarf Mutation Attenuates Alzheimer's Disease Phenotype of APP/PS1 mice." Neurobiol Aging. 2016 Apr; 40:22-40.
3. Hsu, W.J. Wildburger, N.C. Haidacher, S.J. Nenov, M.N. Folorunso, O. Singh, A.K. Chesson, B.C. **Franklin, W.F.** Cortez, I. Sadygov, R.G. Dineley, K.T. Rudra, J.S. Tagliatela, G. Lichti, C.F. Denner, L. Laezza, F. "PPARgamma agonists rescue increased phosphorylation of FGF14 at S226 in the Tg2576 mouse model of Alzheimer's disease." Exp Neurol. 2017 May 15; 295:1-17.
4. Kulas J.A., **Franklin W.**, Smith N.A., Manochal G.D., Puig K.L., Nagamoto-Combs K., Hendrix R.D., Tagliatela G., Barger S.W., Combs C.K. "Ablation of Amyloid Precursor Protein Increases Insulin Degrading Enzyme Levels and Activity in Brain and Peripheral Tissues." Am J Physiol Endocrinol Metab. 2019 Jan 1; 316(1):E106-E120.
5. **Franklin W.**, Krishnan B., Tagliatela G. "Chronic synaptic insulin resistance after traumatic brain injury abolishes insulin protection from amyloid beta and tau oligomer-induced synaptic dysfunction." Submitted to Scientific Reports. 26 Feb, 2019.

Oral Presentations:

1. **Whitney Franklin**, Balaji Krishnan, Giulio Tagliatela. Decreased synaptic insulin responsiveness in the hippocampus after traumatic brain injury: Relevance to Alzheimer's disease and therapeutic implications. Neurobiology of Brain Disorders Gordon Research Conference. August 2018. Castelldefels, Spain.

Abstracts/ Poster Presentations:

International:

1. **Whitney Franklin**, Balaji Krishnan, Giulio Tagliatela. Decreased synaptic insulin responsiveness in the hippocampus after traumatic brain injury: Relevance to Alzheimer's disease and therapeutic implications. Neurobiology of Brain Disorders Gordon Research Conference. August 2018. Castelldefels, Spain.
2. **Whitney Franklin**, Giulio Tagliatela. Ex vivo synaptosomal insulin responsiveness in the hippocampus of traumatic brain injured rats. Society for Neuroscience 2017 Annual National Conference. November 2017. Washington, D.C.
3. **Whitney Franklin**, Giulio Tagliatela. Ex vivo synaptosomal insulin responsiveness in the hippocampus of traumatic brain injured rats. Society for Neuroscience 2016 Annual National Conference. November 2016. San Diego, California.
4. **Whitney Franklin**, Giulio Tagliatela. A method to determine *Ex Vivo* insulin responsiveness in synaptosomes isolated from frozen brain tissue. Society for Neuroscience 2015 Annual National Conference. October 2015. Chicago, Illinois.
5. **Whitney Franklin**, Margaret Parsley, Maria-Adelaide Micci, Giulio Tagliatela. Increased synaptic sensitivity to A β -oligomer binding after traumatic brain injury in the rat. Society for Neuroscience 2014 Annual National Conference. November 2014. Washington, D.C.

Local:

6. **Whitney Franklin**, Balaji Krishnan, Giulio Tagliatela. Decreased synaptic insulin responsiveness in the hippocampus after traumatic brain injury: Relevance to Alzheimer's disease and therapeutic implications. 22nd Annual Forum on Aging. October 18, 2018. Galveston, Texas.
7. **Whitney Franklin**, Balaji Krishnan, Giulio Tagliatela. Decreased synaptic insulin responsiveness in the hippocampus after traumatic brain injury: Relevance to Alzheimer's disease and therapeutic implications. 2018 Alzheimer's Association Research Symposium. May 2, 2018. Houston, Texas.
8. **Whitney Franklin**, Giulio Tagliatela. Ex Vivo synaptosomal insulin responsiveness in the hippocampus of traumatic brain injured rats. Galveston Symposium on Alzheimer's Disease & Related Disorders: Basic, Translational & Clinical Advances. March 22, 2017. Galveston, Texas.
9. **Whitney Franklin**, Giulio Tagliatela. Ex vivo synaptosomal insulin responsiveness in the hippocampus of traumatic brain injured rats. UTMB

Neuroscience and Cell Biology 2016 Annual Research Retreat. December 13, 2016. Galveston, Texas.

10. **Whitney Franklin**, Giulio Tagliatela. Decreased synaptic insulin responsiveness in the hippocampus of traumatic brain injured rats. 20th Annual Forum on Aging. October 20, 2016. Galveston, Texas.
11. **Whitney Franklin**, Giulio Tagliatela. *Ex vivo* synaptosomal insulin responsiveness in the hippocampus of traumatic brain injured rats. Clinical and Translational Forum. March 21, 2016. Galveston, Texas.
12. **Whitney Franklin**, Giulio Tagliatela. A method to determine *Ex Vivo* insulin responsiveness in synaptosomes isolated from frozen brain tissue. 9th Annual Research Symposium on Alzheimer's disease and Related Dementias. September 16, 2015. Houston, Texas.
13. **Whitney Franklin**, Margaret Parsley, Maria-Adelaide Micci, Giulio Tagliatela. Increased synaptic sensitivity to A β -oligomer binding after traumatic brain injury in the rat. 18th Annual Forum on Aging. December 2, 2014. Galveston, Texas.

Permanent address: 17714 Fife Lane, Webster, Texas 77598

This dissertation was typed by Whitney Franklin.